UNIVERSITY
OF OSLO

Master thesis

Method Development for Detection of Underivatized Oxysterols in Cell Medium

Eva Kvalvik

Thesis submitted for a Master's degree in Chemistry

30 credits

Department of Chemistry

Faculty of Mathematics and Natural Sciences

Method Development for Detection of Underivatized Oxysterols in Cell Medium

Eva Kvalvik

2023

Method Development for Detection of Underivatized Oxysterols in Cell Medium

Eva Kvalvik

http://www.duo.uio.no/

Printing: Grafisk senter, Universitetet i Oslo

Preface

I would like to thank all the great people who have helped and supported me throughout the work on my Master's thesis. Without their support, this achievement would not have been possible.

First and foremost, I would like to express my gratitude to Assoc. Prof Hanne Røberg-Larsen and Prof Steven Wilson for welcoming me into their research group. The opportunity to pursue a Master's degree in the field of bioanalytical chemistry made me find my place at UiO.

I want to thank my supervisors, Hanne and Stian. Your guidance and expertise have been invaluable. Hanne, I appreciate your continuous support and active involvement throughout the process. You were always there to answer my questions and to provide feedback, which has helped me grow. Stian, I am grateful for your unwavering support through both the ups and downs. The countless hours we spent together in the lab have been incredibly important to me. Thank you for always being available to help me.

I also want to express my appreciation to Kristina for sharing extensive knowledge about NAFLD and oxysterols, and for meaningful conversations and enjoyable car rides. Christine, your input has contributed greatly. Thank you for the engaging discussions in the lab. Furthermore, I would like to thank Inge, for resolving the technical issues that arose, ensuring the progress of the project.

Thank you to my co-students, Gustav, Lise, Jon Erlend, Silje, and Marius for all the support and fun conversations. I am going to miss spending time with you. Thank you for generously sharing your knowledge, insights, and perspectives during our study sessions.

Finally, I want to express my appreciation to my family and friends for their constant presence and support, even when they may not fully comprehend the specifics of my work. I also want to thank my better half, Martin, for his remarkable patience, care, and love. Your encouragement has been the driving force that keeps me motivated every single day.

Abstract

Non-alcoholic fatty liver disease (NAFLD) is a disease caused by the accumulation of fat in the liver, mainly due to obesity and lifestyle. The disease is a worldwide health issue, with high prevalence and a lack of non-invasive biomarkers. To understand the disease, a model system is needed. The use of organoids, stem cell-derived three-dimensional cultures, is suggested as a model reflecting human physiology better than animal models.

NAFLD can be induced in liver organoids. This enables the use of "Organ-in-a-Column" technology for studying the disease. Previous research has suggested that oxysterols are potential biomarkers of NAFLD. To make detection easier, oxysterols are usually derivatized in advance of analysis. "Organ-in-a-column" is an on-line system, in which organoids are coupled with Liquid Chromatography – Mass Spectrometry. The on-line approach makes sample preparation in the form of derivatization difficult. Therefore, this study has focused on method development for detecting underivatized oxysterols, with the aim of using the method in an "organ-in-a-column"-setup.

Without a derivatization step in the sample preparation, the detection of oxysterols was challenging due to low sensitivity. Attempts of coeluting the groups of hydroxycholesterols and dihydroxycholesterols to establish a steatotic and control fingerprint from organoids with enhanced detection limit were partly successful for the analyte group of dihydroxycholesterols, but not the group of hydroxycholesterols. Sample clean-up was performed on-line using an automated filtration and filter flush solid phase extraction. This ensured robust analysis by the removal of particles before analysis. The optimized experimental parameters included a 5 μL injection volume, a gradient elution utilizing isopropanol (IPA) as the organic modifier (20-65 %), 0.1 % formic acid for pH control in the mobile phase, and the use of a SuperPhenyl hexyl (2.1 mm x 5 cm) column at a temperature of 40 ℃.

The method allowed for detection of underivatized oxysterols in concentrations down to 0.050 μg/mL in 10:90 IPA:Cell medium. The detection limit was too high to detect oxysterols secreted from liver organoids and the method needs further development before the organ-in-a-column approach can be used for disease monitoring. Also, adjustments to reduce the carry-over would be important to achieve a method providing reliable results.

Abbreviations

2D	Two dimensional
3D	Three dimensional
24(*S*)-HC	24S-hydroxycholesterol
25-HC	25-hydroxycholesterol
26-HC	26-hydroxycholesterol
7a, 24(*S*)-diHC	7a, 24S-dihydroxycholesterol
7a, 25-diHC	7a, 25-dihydroxycholesterol
7a, 26-diHC	7a, 26-dihydroxycholesterol
7b, 25-diHC	7b, 25-dihydroxycholesterol
7b, 26-diHC	7b, 26-dihydroxcholesterol
ACN	Acetonitrile
AFFL-SPE	Automated filtration and filter flush solid phase extraction
APCI	Atmospheric pressure chemical ionization
APPI	Atmospheric pressure photo-ionization
DFA	Difluoroacetic acid
diHC	Dihydroxycholesterol
CYP	Cytochrome P450
ESC	Embryonic stem cells

ESI	Electrospray ionization
FA	Formic acid
GC	Gas chromatography
HC	Hydroxycholesterol
HESI	Heated electrospray ionization
HPLC	High performance liquid chromatography
ID	Inner diameter
IPA	Isopropanol
iPSC	Induced pluripotent stem cell
LC	Liquid chromatography
MeOH	Methanol
MRM	Multiple reaction monitoring
MS	Mass spectrometry
m/z	Mass-to-charge ratio
NAFLD	Non-alcoholic fatty liver disease
NASH	Non-alcoholic steatohepatitis
OD	Outer diameter
OiC	Organ-in-a-column
OoC	Organ-on-a-chip
PFA	Perfluoroalkoxy alkane

RP	Reversed phase
SIM	Selected ion monitoring
SPE	Solid phase extraction
SRM	Selected reaction monitoring
SS	Stainless steel
TFA	Trifluoroacetic acid

Table of Contents

1 Introduction

1.1 Drug development and disease monitoring

The process of drug discovery is both time-consuming and highly expensive. Animal models serve as the gold standard for testing due to their ability to reflect the complexity of human physiology better than two-dimensional (2D) cell cultures [1]. However, many human diseases and conditions lack suitable animal models for studies, and there are drawbacks associated with their use, including ethical concerns, high costs, and the genetic and physiological distance between animal models and humans [2, 3].

Similar limitations are encountered when using animal models for disease modeling and biomarker discovery. Animal models often fail to accurately predict the pathophysiology of many human diseases [4, 5]. Humans differ from animals in multiple aspects, including liver metabolism, the immune system, and inflammatory responses.

Therefore, there is a need for alternative approaches to animal models in drug development and disease modeling. These alternatives aim to speed up the development process, reduce costs, and produce safer and more effective drugs [6, p. 28]. The utilization of alternatives to animal models aligns with the 3R principles of animal testing: Refinement, Reduction, and Replacement. One such alternative that is currently being studied is the use of organoids.

1.2 Organoids

Organoids are three-dimensional (3D) cultures derived from stem cells, and they exhibit organ-like features [7]. The use of organoids was recognized by the science journal Nature as the "Method of the Year" in 2017 [8], as they possess a huge potential to positively impact drug development, disease modeling, and personalized medicine.

Organoids self-organize and form structures that resemble organs *in vivo*. This occurs through cell sorting and spatially restricted lineage commitment [9]. Various types of organoids have been successfully generated, including liver, gut, kidney, brain, and retina organoids [9, 10]. Liver organoids have the potential of playing a central role in drug development, as the liver has a unique metabolic profile [9]. Human liver organoids are particularly relevant, because of

the drug metabolism, which differs from animal models [11]. If this approach is successful, it could significantly reduce the reliance on animal models in the drug development process.

Organoids can be generated from two types of stem cells: embryonic stem cells (ESC) and patient-derived induced pluripotent stem cells (iPSCs) [7, 9]. ESCs and iPSCs differ in origin, but both possess the ability to differentiate into all somatic cell types [11, 12]. ESCs are derived from the preimplantation stage of embryos, whereas the iPSCs are derived artificially from adult somatic cells and reprogrammed using transcription factors [12]. Utilizing iPSCs offers the advantage of a renewable tissue resource, as they can be derived from any patient, renew themselves and differentiate into a variety of cell types [12].

Organoids have the capability to model human development and disease. By introducing mutations or utilizing iPSCs, it becomes possible to model diseases in organoids [9, 10, 13]. Some biological principles are specific to humans, and organoids hold the potential to answer developmental questions that remain unanswered using traditional techniques, such as 2D cell cultures and animal models. Organoids can be used for drug testing and may be used in tissue replacement therapy in the future [9]. **Figure 1** illustrates the potential applications of organoids in drug development.

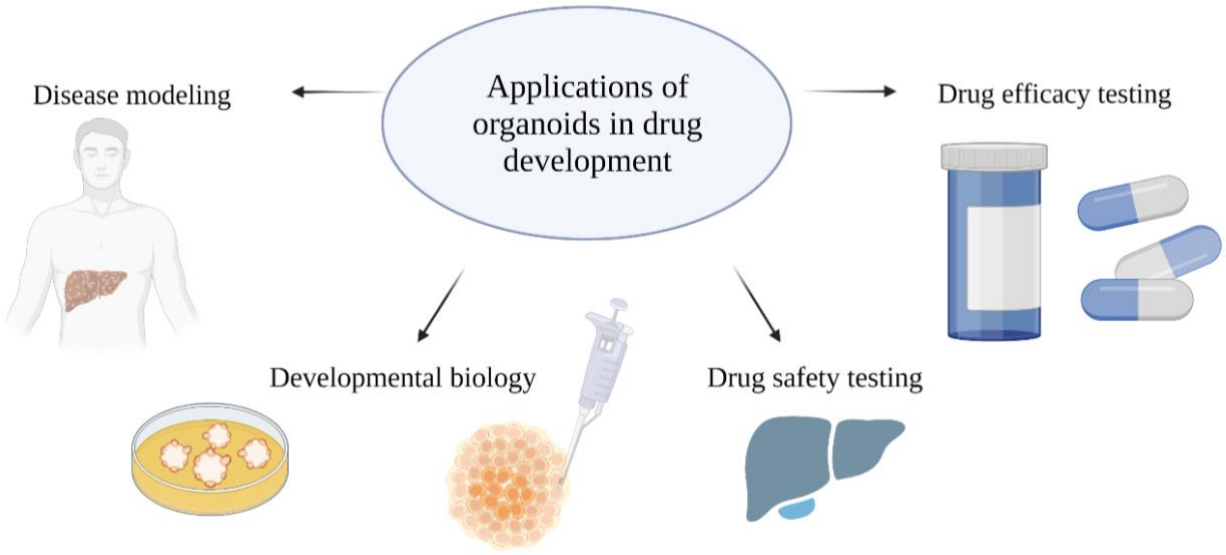

Figure 1. Examples of applications of organoids in drug development include disease modeling, the study of developmental biology, drug safety testing, and drug efficacy testing. Created in BioRender.

The use of organoids has shortcomings, with maturation being one of the key issues [9]. Therefore, future research is required for organoids to become a well-established alternative to animal models, as they are still in the developmental phase. Organoids may exhibit characteristics more like the organs of a newborn than the ones of a matured adult. One factor contributing to this is their limited growth potential, which stems from inadequate nutrient supply due to the absence of vascularization [9]. Despite these shortcomings, 3D models can offer a more accurate representation of human physiology compared to traditional 2D cell cultures and animal models [3].

1.3 Organ-on-a-chip

"Organ-on-a-chip" (OoC) is a microfluidic device with 3D cell cultures integrated [14]. These chips consist of interconnected chambers that are continuously perfused, with the cell cultures arranged in a manner that simulates tissue- and organ-level physiology [10, 13, 14]. An OoC can be a simple system comprising a single microfluidic chamber housing a specific cell type, thereby replicating the functions of a particular tissue [14]. Alternatively, more complex OoC designs involve connected chips with different cell tissues separated by porous membranes [14, 15]. When these chips are connected, they can mimic the physiological behavior of the body [6]. The first reported OoC was a model of lungs by the Ingber group at Harvard Medical School in 2010 [16].

The utilization of fluorescent tags enables high-resolution, real-time imaging, and *in vitro* analysis of tissue and organ activities in OoCs [14]. However, a drawback of using OoC is the inability to simultaneously monitor multiple metabolites or molecules. This would be possible by utilizing advanced analytical instrumentation like Liquid Chromatography – Mass Spectrometry (LC-MS), which is considered the golden standard for bioanalysis. Nonetheless, integrating OoC technology with LC-MS poses a significant challenge due to the lack of standardized couplings [17]. An on-line approach where the organoids are coupled to instrumentation like LC-MS would enable the monitoring of metabolites and non-fluorescence tagged molecules in their native form. Additionally, on-line analysis of organoids makes automation possible, leading to faster and more precise analysis with reduced contamination risks [17]. Even so, it is important to note that automation also introduced additional complexity [13].

1.4 Organ-in-a-column

A new prototype called “Organ-in-a-column” (OiC) has been developed to overcome the limitations of OoC-technology by employing standardized couplings to connect the organoids within a compartment to LC-MS [13, 17]. In OiC, organoids are packed in a liquid chromatography column housing. The column containing organoids is coupled on-line with LC-MS. The on-line analysis of organoids using mass spectrometry enables automation and direct integration of organoids with LC-MS [17]. Consequently, analytes can be selectively monitored and tracked over time. In a proof-of-concept study, OiC was utilized to measure the metabolism of heroin in liver organoids [17]. This demonstrates the potential of OiC in enabling detailed studies of drug metabolism and other processes within organoids.

The OiC consists of 10 cm perfluoroalkoxy alkane (PFA) tubing, nuts, ferrules, and unions with screens to keep the content in the tubing as illustrated in **Figure 2** [17]. The contents are organoids mixed with acid-washed glass beads in an organoid medium. The glass beads are used to prevent the organoids from aggregating during packing and to secure the organoids in the tubing.

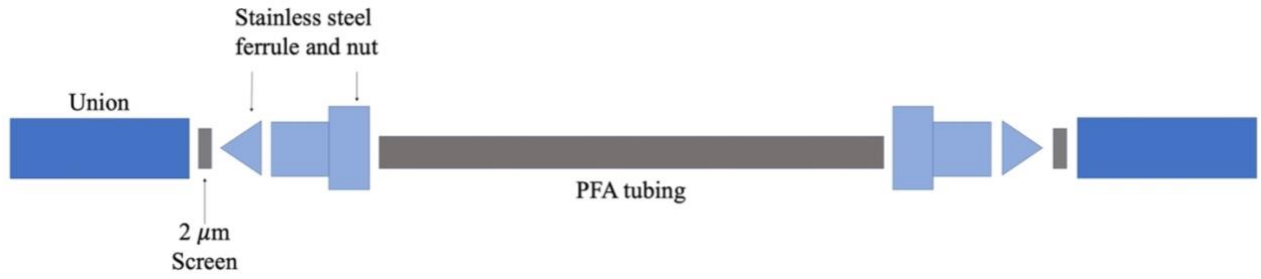

Figure 2. The column housing for Organ-in-a-column (OiC). OiC consists of 10 cm PFA tubing, nuts, ferrules, and a union with a screen to keep the organoids mixed with glass beads in the tubing. Adapted from [17].

The use of standardized couplings makes it easy to couple with LC-MS, as illustrated in **Figure 3** [17]. This makes it possible to examine metabolites, including those derived from endogenous molecules and drugs. However, one limitation of this on-line system is the absence of sample preparation. To address this issue, the implementation of an on-line automated filtration and filter-flush solid phase extraction (AFFL-SPE) could be a potential solution to eliminate potential interferences in the sample. This approach has, to the author’s knowledge, previously not been explored.

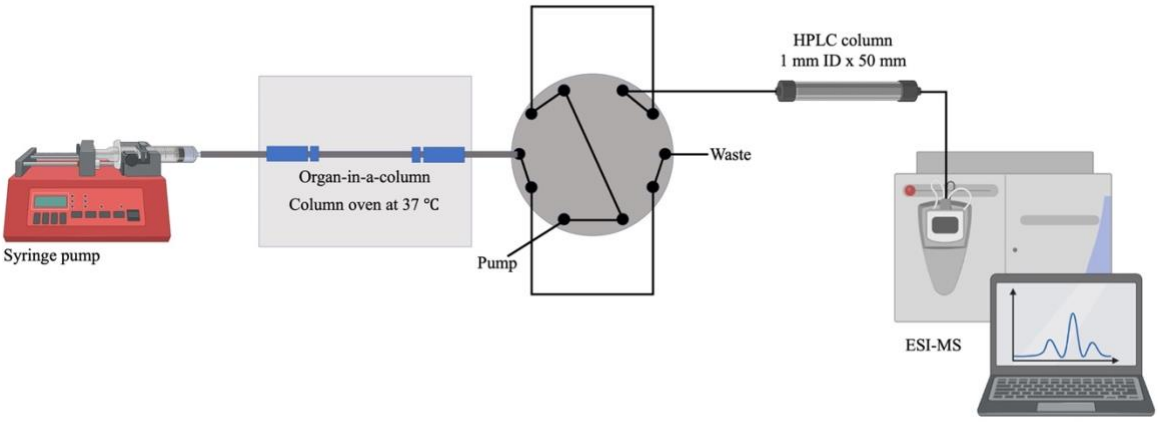

Figure 3. The instrumentation in "Organ-in-a-column" (OiC). Organoid medium is pumped through the system using a syringe pump. The OiC is connected to LC-MS instrumentation by a 10-port valve. Eluate from the organoid column is fractioned in the valve system, consisting of two sample loops that are being filled and injected sequentially prior to LC-MS analysis and detection. Adapted from [17]. Created in BioRender.

1.5 Non-alcoholic fatty liver disease

Non-alcoholic fatty liver disease (NAFLD) is a disease characterized by the accumulation of fat in the liver, mainly due to obesity and lifestyle factors [18, 19]. As the name implies, alcohol consumption does not cause the disease [19]. The most common metabolic risk factors associated with NAFLD development include obesity, type 2 diabetes mellitus, and dyslipidemia [20, 21, 22]. It is estimated that NAFLD affects approximately 30 % of the global population [23]. Recent studies have also revealed a link between exposure to persistent organic pollutants and the development of NAFLD [24].

NAFLD develops in stages, starting from steatosis (simple fatty liver), then advancing to non-alcoholic steatohepatitis (NASH), and in severe cases cirrhosis, as illustrated in **Figure 4** [19]. While the majority of patients remain in the early stages, approximately 25 % of cases progress to NASH and cirrhosis [19, 25]. Cirrhosis may cause liver failure and hepatocellular carcinoma (liver cancer) [26]. When this occurs, a liver transplant becomes necessary for survival. With the increasing prevalence of NAFLD, the disease has become the leading cause of liver transplants among women and the second leading cause among men in the USA [27].

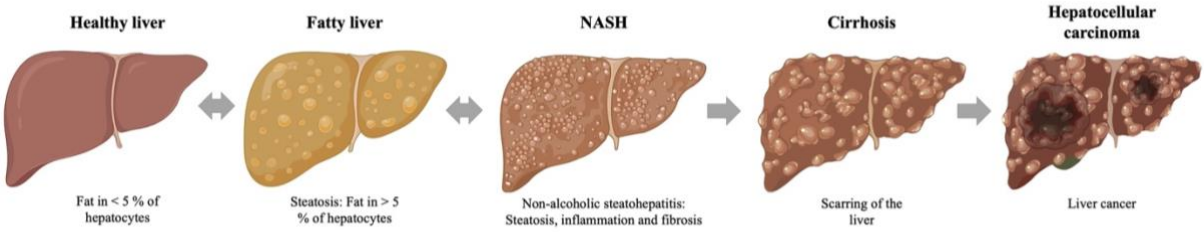

Figure 4. The spectrum of non-alcoholic fatty liver disease (NAFLD). NAFLD develops from steatosis (simple fatty liver) to non-alcoholic steatohepatitis (NASH) and can lead to cirrhosis if not treated. Cirrhosis may cause liver failure and cancer (hepatocellular carcinoma) [26]. Figure adapted from [28]. Created in BioRender.

Diagnosing NAFLD presents challenges due to the lack of non-invasive biomarkers for the disease [29]. Currently, liver ultrasound serves as a non-invasive method [18]. However, this method has limitations in detecting the disease during its early stages: The optimal sensitivity for detecting NAFLD by liver ultrasound is achieved at a liver fat content of 12.5 % [19, 30]. Liver biopsy remains the most accurate diagnostic approach for NAFLD, as it allows for distinguishing simple steatosis from NASH [18, 19, 21, 31]. Nevertheless, liver biopsy is also subject to significant variability as it involves the examination of a relatively small liver fragment [32, 33]. Non-invasive methods would provide economic benefits compared to liver biopsy and would be a better alternative for patient well-being, as complications can arise from the invasive nature of a liver biopsy [29, 34].

Animal models have played a crucial role in studying the physiological mechanisms of NAFLD. However, the translation of findings from animal models to humans has proven to be challenging and unsuccessful multiple times [35]. This can be explained by the complex, and multifaceted nature of the disease's pathophysiology, making it difficult for any animal model to accurately represent the entire spectrum of the disease within a practical timeframe [35]. As an alternative to animal models, organoids have emerged as a promising approach. By exposing liver organoids to fatty acids, they become steatotic and the first stage of NAFLD is induced [36].

One of the characteristics of NAFLD is a disruption in the cholesterol homeostasis and high cholesterol levels [37]. Oxysterols, which play a role in regulating the cholesterol homeostasis, have the potential to serve as non-invasive markers for tracking disease progression [38]. Having an analysis system that can monitor the progression of NAFLD in organoids over time would be highly valuable. In this regard, the potential of OiC comes into play. Although the use of steatotic organoids in OiC is yet to be explored, there are indications that it is feasible, given that NAFLD can be induced in liver organoids and incorporated into the organoid columns.

1.5.1 Oxysterols as biomarkers for non-alcoholic fatty liver disease

Oxysterols are a group of molecules that act as intermediates in the metabolism of cholesterol and the synthesis of bile acids [26, 39]. This was first demonstrated by Kandutsch and colleagues in 1973 [39]. Oxysterols are oxidized cholesterol molecules, formed by the addition of hydroxyl-groups to cholesterol. The formation of oxysterols can occur through enzymatic reactions catalyzed by different cytochrome P450 (CYP) enzymes, as well as through non-enzymatic mechanisms like autoxidation, illustrated in **Figure 5** [36].

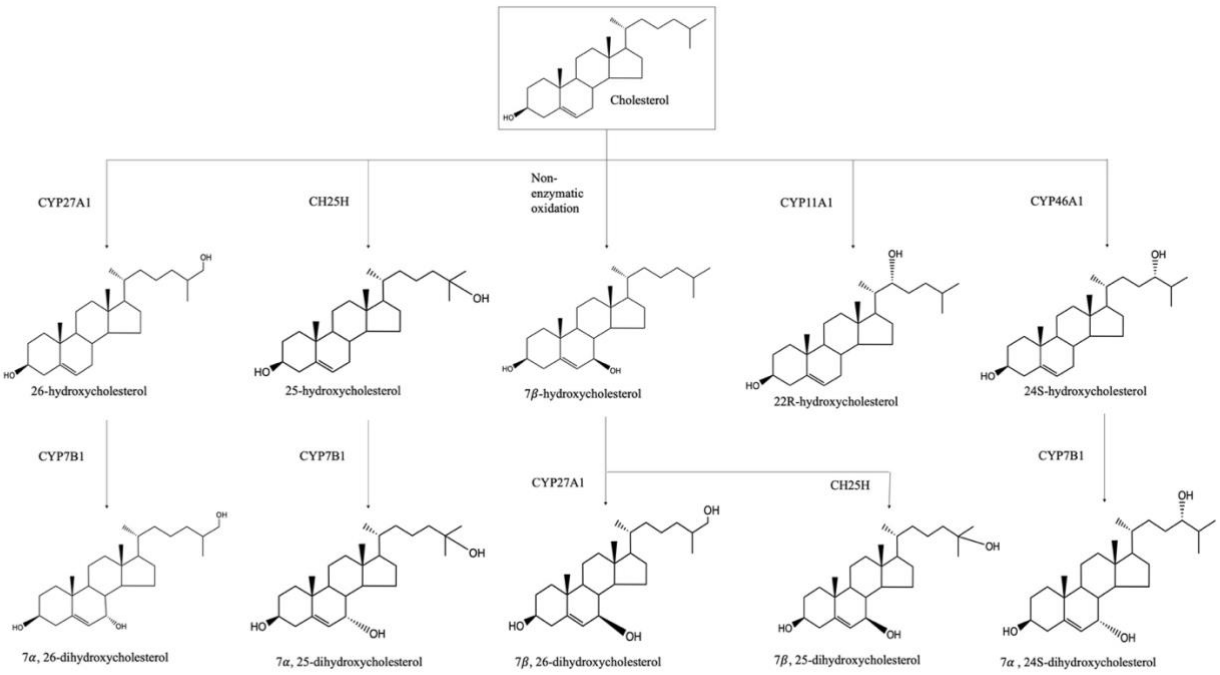

Figure 5. Overview of the formation of oxysterols. The figure shows how cholesterol is oxidized and form oxysterols. Different cytochrome P450 (CYP) enzymes and non-enzymatic oxidation form the oxysterols. Adapted from [36].

Studies has demonstrated elevated levels of certain oxysterols in the livers of human and mice with NAFLD [26]. This is thought to be due to increased bile acid synthesis in steatotic organs. Additionally, research has revealed that oxysterols modulate a receptor in the liver called liver X-receptor, potentially playing a significant role in the development of NAFLD [40]. Elevated levels of oxysterols in the circulation may also serve as an important indicator of the disease [41]. Liver organoids have been found to secrete oxysterols, with steatotic organoids showing higher secretion compared to healthy organoids [36]. This suggests that oxysterols have the potential to be used as a marker of disease progression.

Detecting oxysterols poses a challenge due to their low concentrations in limited sample volumes [42, 43]. Oxysterols are neutral molecules, which makes it difficult to use Electrospray Ionization – Mass Spectrometry (ESI-MS) for their analysis [42, 44]. Including a derivatization step in the sample preparation can enhance the ionization efficiency and lower the limit of detection [36, 42, 45]. However, derivatization is a time-consuming process and would not be feasible in an on-line system like OiC. Although there are LC-MS methods available for native oxysterols, they typically require high sample start volumes (e.g. 200 μL of plasma) [46, 47, 48]. Considering the observation of an increase in multiple oxysterol isomers from liver organoids by Kømurcu et al. (2023), a collective increase might serve as a disease marker [36]. Coeluting the isomeric oxysterols from the column can be a solution to enhance the sensitivity, as this leads to higher signal intensity, and addresses the issue of high limits of detection.

1.6 Analytical method theory

1.6.1 Mass spectrometric detection

Mass spectrometry (MS) can be used for both qualitative and quantitative determination of analytes. It is commonly used for detection as long as the compounds of interest can be ionized and transitioned into the gas phase [49, p. 85]. This process involves ionizing a sample, separating the ions based on their mass-to-charge ratio (*m/z)* and then detecting the ions [50, p. 2]. The main components of a mass spectrometer are (1) the sample inlet, (2) the ion source, (3) the mass analyzer, (4) the detector, and (5) the data system as illustrated in **Figure 6** [51, p. 788].

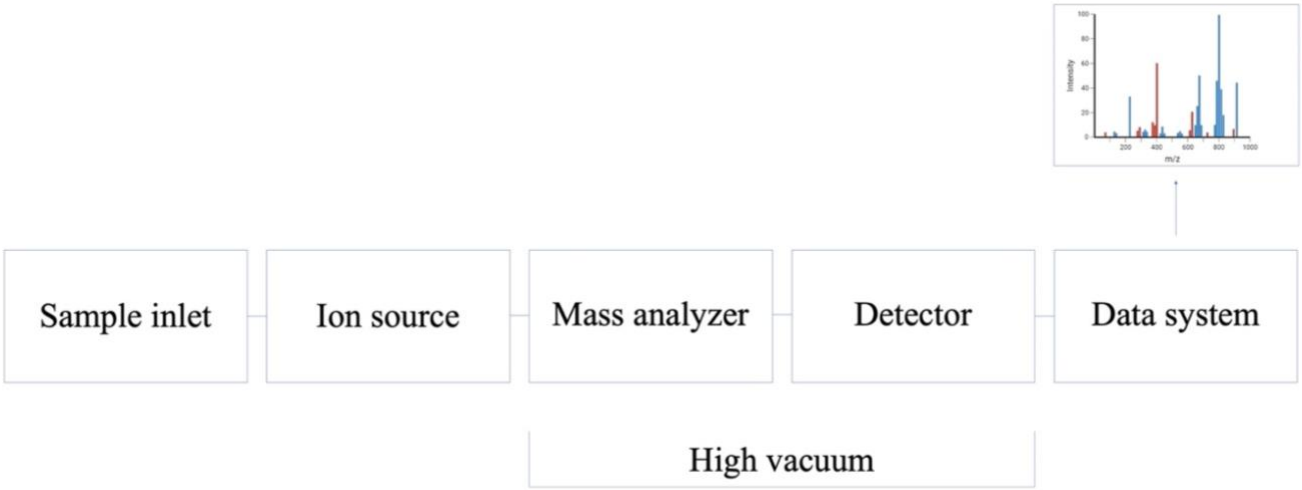

Figure 6. Illustration of the main components of a mass spectrometer: The sample inlet where the sample is introduced, the ion source where the sample is ionized, the mass analyzer which separates the ions of different m/z values, the detector which generates an electric signal in response of the ion abundance of each m/z value and the data system which provides a mass specter presenting the relative abundance of different m/z values. Adapted from [51, p. 722] and [50, p. 3]. Created in BioRender.

The sample is often separated by chromatography prior to mass spectrometric detection. When coupling high-performance liquid chromatography (HPLC) with MS, an interface is required to bridge the gap between the liquid phase of HPLC and the gas phase of the MS, which operates under high vacuum conditions [49, p. 85]. A commonly used interface is electrospray ionization (ESI).

Triple quadrupole mass spectrometer

The quadrupole is a widely used mass analyzer. It consists of four rods which induce an oscillating electric field through the application of an alternating current [49, p. 91-92]. By applying a constant voltage and a radio-frequency oscillating voltage to the four rods, the quadrupole creates electric fields that influence the trajectories of ions [51, p. 572]. Specifically, it permits ions with a specific *m/z* ratio to pass from the ionization chamber to the detector, while ions with other *m/z* ratios collide with the rods and are lost before reaching the detector [51, p. 572]. This selective transmission of ions based on their *m/z* ratio enables targeted analysis. By controlling the electric field, a mass spectrum can be obtained for the desired *m/z* values in a sample [49, p. 91-92]. The process of ion selection and transmission in the quadrupole is illustrated in **Figure 7**.

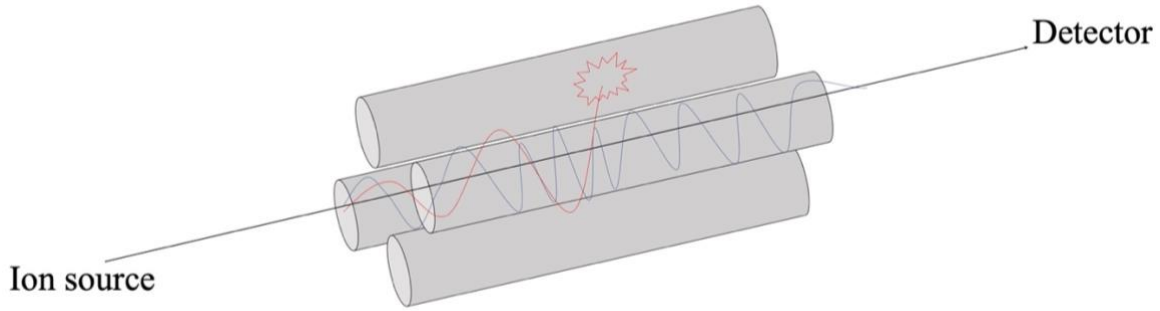

Figure 7. The figure illustrates how the stable oscillating ions goes through the quadrupole to the detector (blue), while the unstable ions collide with the quadrupole (red) and does not reach the detector. Adapted from [49, p. 92].

Selected ion monitoring (SIM) is a mode of operation that is employed when there is detailed information about the analytes ahead of the analysis [52, p. 165]. In SIM mode, only predefined *m/z* values corresponding to the target analytes are monitored, while the other ions are ignored. This will allow for lower detection limits as the noise is reduced by focusing on the specific *m/z* values of interest, and is useful for quantitative purposes [53, p. 849].

Mass spectrometers can be coupled in tandem to enhance the reliability and accuracy of the analyte identification [49, p. 94]. One commonly used configuration is the triple quadrupole, which consists of three quadrupoles in a row. The first and third quadrupole, denoted as Q1 and Q3, functions as mass analyzers, while the second quadrupole, referred to as q2, acts as a collision cell made up of a quadrupole applying only radio frequency to the ions [53, p. 566].

The triple quadrupole MS can be used in several measuring modes, such as selected reaction monitoring (SRM) and multiple reaction monitoring (MRM) [52, p. 165]. In SRM mode, only fragments originating from a selected precursor ion are detected. The first quadrupole is used to select a particular *m/z* value corresponding to the precursor ion of interest [52, p. 165]. The second quadrupole, acting as a collision cell, induces fragmentation of the selected ion through collision induced dissociation. In the third quadrupole, the signal from one or multiple selected *m/z* values representing the fragments are measured [52, p. 165]. This process is illustrated in **Figure 8**. MRM operates similar to SRM but involves the selection of multiple precursor ions for analysis. Both SRM and MRM enables selective operation of the MS, resulting in low detection limits and increased sensitivity [52, p. 165].

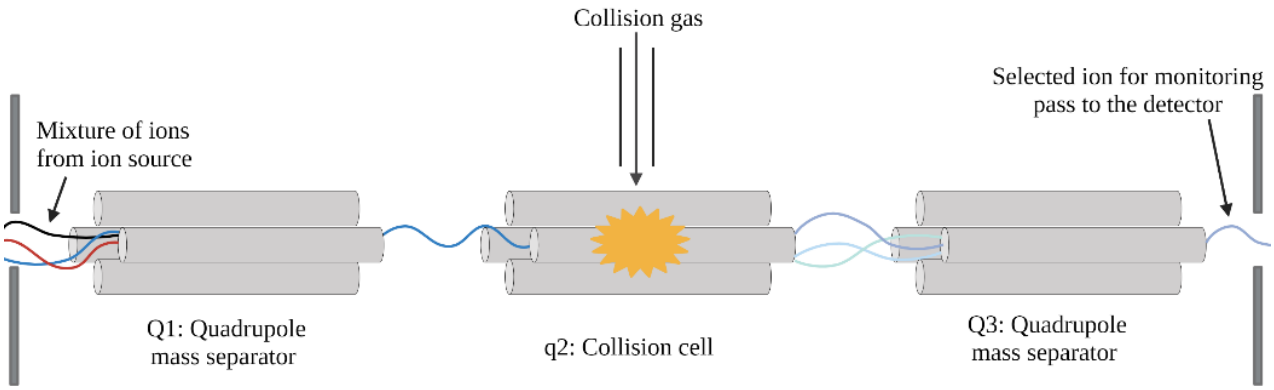

Figure 8. The figure illustrates selected reaction monitoring where the first quadrupole (Q1) functions as a mass analyzer and an m/z value for the ion of interest is chosen. The second quadrupole (q2) functions as a collision cell, fragmenting the ion of interest. The third quadrupole (Q3) functions as a mass analyzer, and the fragment ion with the chosen m/z value proceed through to the detector. Adapted from [51, p. 585]. Created in BioRender.

Electrospray ionization

Electrospray ionization (ESI) is a technique used to ionize analytes and transfer them from liquid phase to the gas phase [49, p. 86-87]. The ionization process occurs mainly in the mobile phase by pH adjustment, which can protonate or deprotonate the analytes. Typically, a potential of $\pm$ 2-5 kV is applied to the capillary where the mobile phase and solutes are introduced [49, p. 86, 54, p. 728]. Positive ions are generated by using a positive potential. At the outlet of the capillary, a nebulizing gas, often nitrogen, is mixed with the mobile phase and analytes [54, p. 728]. Simultaneously, a dry gas is introduced in the opposite direction to aid droplet formation. The high voltage applied leads to accumulation of ions, resulting in highly charged droplets leaving the capillary [54, p. 728].

As the mobile phase evaporates from the droplets, the droplet size decreases, leading to an increase in the intrinsic repulsion between ions with the same charge inside the droplets [52, p. 146]. When the repulsive forces exceed the surface tension (reaching the Rayleigh limit), the droplets disintegrate into smaller droplets [52, p. 146]. This process is repeated, resulting in ions in the gas phase through ion evaporation or as a charge residue where the solvent is evaporated and ions are left [52, p. 146]. The process of ESI is illustrated in **Figure 9**.

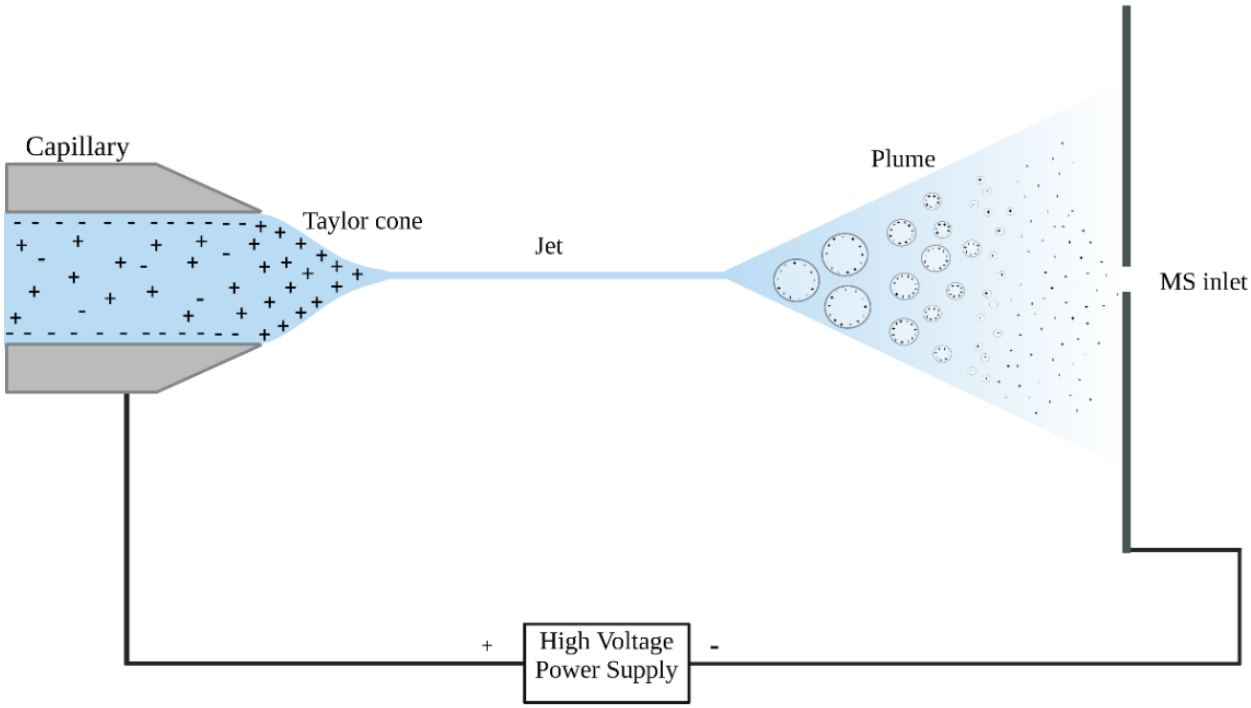

Figure 9. The figure illustrates electrospray ionization. A high voltage is applied to the capillary where the mobile phase with analytes is introduced. A nebulizing gas is mixed with the mobile phase at the outlet of the capillary to facilitate droplet formation. A dry gas is introduced in the opposite direction. The droplets leaving the capillary are highly charged, and as the mobile phase evaporates the repulsion between the charge will increase. This causes the droplets to explode in smaller droplets, and yield ions in gas phase either through ion evaporation from the droplets or charge residue where the solvent evaporates and the ions are left [52, p. 146]. Adapted from [49, p. 87] and [55, p. 9]. Created in BioRender.

After the ionized analytes transition to the gas phase, they enter the mass analyzer through lenses and skimmers, which help in forming a focused ion beam [49, p. 91]. Within the mass analyzer, the ions undergo separation based on their *m/z*-ratio and are subsequently monitored by a detector. This process results in the production of a mass spectrum, revealing the relative abundance of the ions generated by ionization of the sample and their separation based on *m/z* ratio [54, p. 761].

Alternative ionization methods

The choice of ionization method depends on both analyte size and polarity, as illustrated in **Figure 10**.

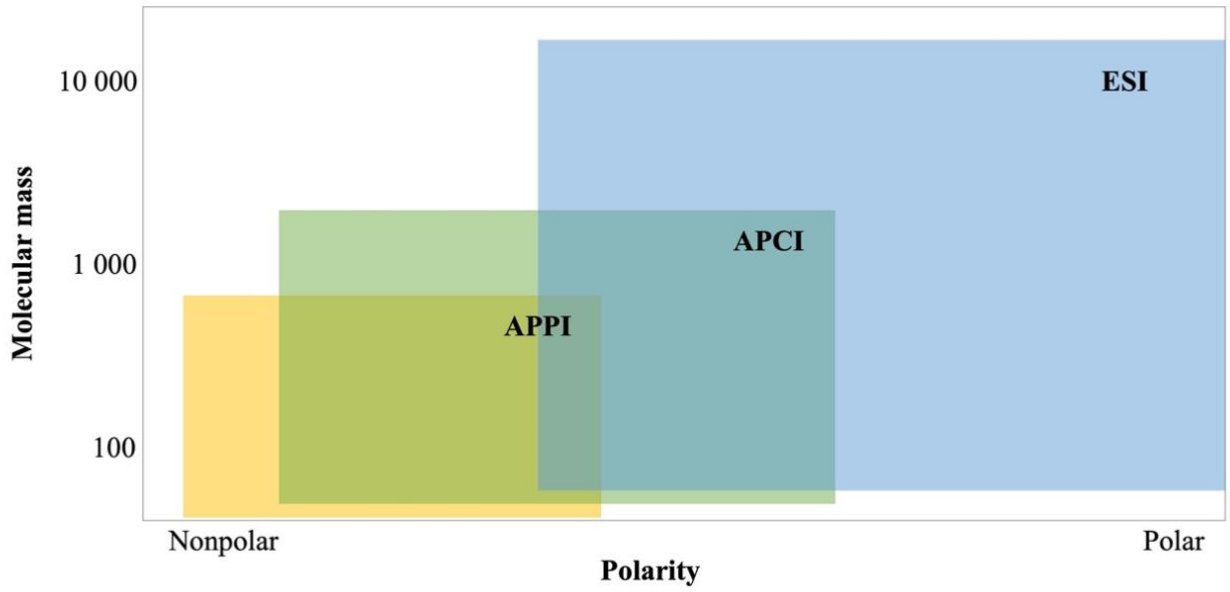

Figure 10. The choice of ionization method depends on both analyte size and polarity of the analyte. The figure illustrates an approximate proper of use of three different interfaces: atmospheric pressure photo-ionization (APPI), atmospheric pressure chemical ionization (APCI) and electrospray ionization (ESI). Adapted from [49, p. 86]. Created in BioRender.

Atmospheric pressure chemical ionization (APCI) is an alternative interface to ESI [51, p. 691]. APCI is particularly useful for ionizing compounds that do not ionize well with ESI such as those more stable, with lower molecular mass and often nonpolar [51, p. 691]. In APCI, the sample undergoes vaporization, and the analytes in gas phase are charged by a corona discharge needle [51, p. 691].

Another alternative ionization method is atmospheric pressure photo-ionization (APPI). This method is similar to APCI, but instead of a corona discharge needle, ultraviolet (UV) light is employed [50, p. 63]. APPI offers the advantage of removing background signals from solvents and gases, due to the low energy provided by UV light [50, p. 63]. The energy level of approximately 10 eV is sufficient for ionizing most organic compounds. However, it falls below the ionization energy required for commonly used solvents in LC, such as water, methanol and acetonitrile and atmospheric gases such as nitrogen [50, p. 63]. While both APCI and APPI would be compatible with the "organ-in-a-column"-system, they were not available in the current laboratory setting.

Matrix effects

Matrix effects in mass spectrometry occur when compounds present in the matrix, distinct from the analytes of interest, cause changes in the signal [51, p. 106, 52, p. 167-168]. These effects can either suppress or enhance the signal intensity, leading to non-representative analyte concentration and poor reproducibility [52, p. 167]. While the MS is highly accurate for determining a single *m/z* value, it faces challenges when multiple molecules are injected simultaneously. ESI as the ion source is particularly associated with matrix effects, and the underlying mechanism are not fully understood [52, p. 167]. Two common explanations are altered ion desorption from the droplet surface during the electrospray process, and competition between the analyte and co-eluting interferences for charges. Both resulting in changes in the analytes signal intensity [52, p. 167]. To overcome matrix effects and separate the analytes from interfering compounds, chromatography is commonly employed [49, p. 161]. Additionally, performing a sample preparation step prior to analysis can minimize the impact of matrix effect.

1.6.2 Chromatography

Chromatography is a collective term used to describe techniques used for separating components in mixtures. Different chromatographic techniques exist, including gas chromatography (GC), high-performance liquid chromatography (HPLC), supercritical fluid chromatography, thin layer chromatography, electrochromatography and micellar electrokinetic chromatography. While many of these techniques are employed for niche applications, the two most widely used techniques are HPLC and GC [49, p. 2]. HPLC is often preferred for analyzing biological samples because it allows for direct analysis of aqueous samples using reversed-phase liquid chromatography [52, p. 32].

In chromatographic techniques such as liquid chromatography, a sample is introduced in a small volume and carried by the mobile phase through a column with a stationary phase [49, p. 2, 52, p. 123]. The compounds in the sample pass through the system and elute from the column at different velocities due to varying degree of interactions with the stationary phase [49, p. 2]. The time between sample injection and the elution of compounds is called the retention time [49, p. 2]. A detector is placed at the outlet of the column to detect the separated compounds [49, p. 3]. The detector generates a chromatogram, which represents the detector response as a function of retention time [51, p. 612].

The retention factor of a compound, denoted as k, can be defined as

$$k = \frac{t_s}{t_m} = \frac{t_R - t_m}{t_m}$$

Where t_s is the time the compound spends in the stationary phase, t_m is the time the compound spends in the mobile phase and t_R is the retention time of the compound of interest [51, p. 612]. A higher retention factor implies a longer retention time for the compound [51, p. 612].

Separation efficiency

In chromatography, it is desirable to achieve narrow and well separated peaks. However, when a sample is injected into the chromatographic system, band broadening occurs [49, p. 5]. Band broadening primarily arises from the three physical processes of eddy dispersion, longitudinal diffusion in the mobile phase and resistance to mass transfer [49, p. 5]. Eddy dispersion occurs due to variations in widths and lengths of channels in porous structures, as well as the presence of inhomogeneous particles, which contribute to significant band broadening as the analyte particles will go through the column at different velocity [49, p. 6]. Longitudinal diffusion takes place within the mobile phase, where compounds in concentrated bands tend to diffuse towards less concentrated regions [49, p. 6]. Lastly, resistance to mass transfer occurs during the transportation of compounds through diffusion and convection, resulting in further band broadening [49, p. 7]. Band broadening can also occur outside the column, e.g. in the injector or in the tubing connecting the injector, the column and the detector [49, p. 9].

The plate number (N) can be used as an expression of the column efficiency [49, p. 9].

$$N = (t_R/\sigma)^2$$

Where t_R is the retention time and σ is the standard deviation of a Gaussian distribution of each band. When measuring the plate number from a chromatogram, the following formula can be used:

$$N = \frac{16t_R^2}{w^2} = \frac{5.55t_R^2}{w_{1/2}^2}$$

Where w is the width at base of the peak and $w_{1/2}$ is the width at half-height [51, p. 621].

Plate height is also used as a measure for band broadening, defined as

$$H = \frac{\sigma^2}{x} = \frac{L}{N}$$

Where σ is the standard deviation of band, x is the distance travelled by center of band, L is the length of the column and N is the number of plates on column [51, p. 621]. Plate heights of 5-10 μm for packed HPLC columns and 0.2-0.25 mm for capillary GC should be obtained [49, p. 11]. A smaller the plate height corresponds to a narrower bandwidth [51, p. 618].

The resolution of two peaks is a measure of how well separated they are from each other. This can be determined by the retention factor (k), the plate number (N) and the separation factor (α) [49, p. 12]. The separation factor is a measure of the selectivity/relative retention, defined as $\alpha = k_2/k_1$ (where $k_2 > k_1$) [49, p. 12].

The resolution for two compounds eluting close to each other, can be described by the following equation:

$$R_S = \frac{1}{4}(\alpha - 1)\sqrt{N}\frac{k}{(1+k)}$$

Where α is the relative retention, N is the plate number and k is the retention factor for the second peak [49, p. 13]. For analysis of quantitative purposes, a baseline separation of the peaks ($R_S \geq 1.5$) is highly desirable [51, p. 616].

1.6.3 Liquid chromatography

High-performance liquid chromatography (HPLC) is the use of smaller particles that generate higher backpressure, and also requires high-pressure mobile phase delivery units [49, p. 47]. The instrumentation consists of one or more pumps, an injector, one or more columns, a detector, and a device for data handling [49, p. 47]. The mobile phases are liquid solvents and are delivered to the system with a given flow by the pumps. An illustration of HPLC instrumentation is shown in **Figure 11**.

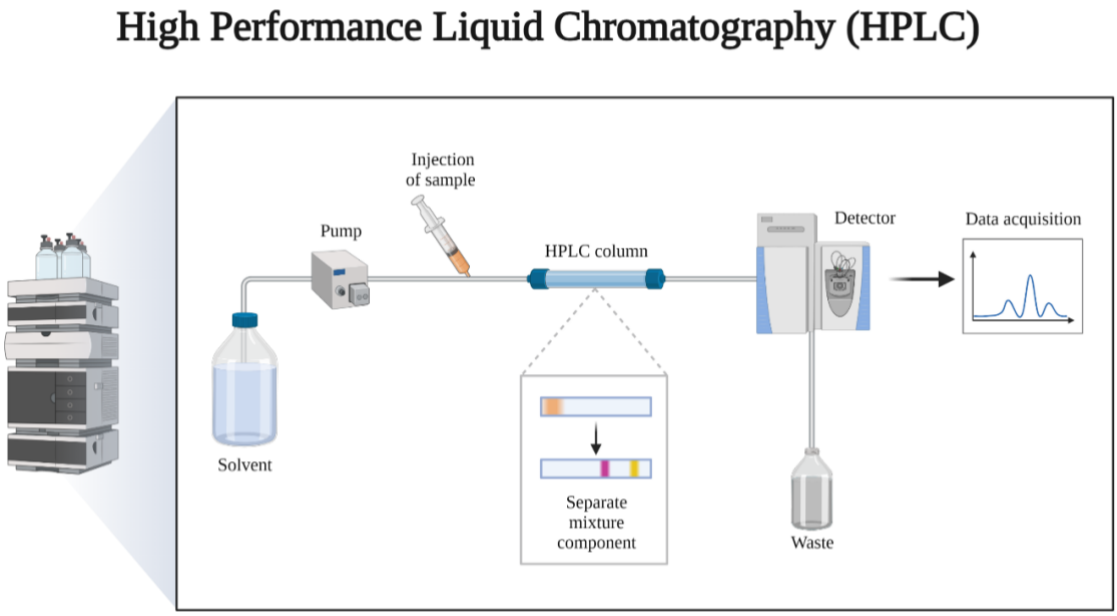

Figure 11. The HPLC instrumentation where the mobile phase is delivered to the system by a pump. The sample is injected to the system before the column, either by manual or automatic injection. Separated compounds from the column reaches the detector, illustrated by a mass spectrometer. Excess solvent goes to waste. Created in BioRender.

Different separation principles (i.e. stationary phases) exist, with reversed phase (RP) chromatography as the most commonly used [51, p. 674]. An RP separation is defined by the use of a polar mobile phase and a relatively nonpolar stationary phase [54, p. 301]. It will cause nonpolar analytes to be more retained than polar analytes.

Stationary phases in reversed phase chromatography

The principle of reversed phase chromatography is based on partition chromatography, where analytes are distributed between the mobile phase and a bonded stationary phase on the silica surface [51, p. 675]. The retention time of an analyte increases with increasing interaction with the stationary phase [51, p. 675].

Reversed phase materials are usually made of hydrophobic chains chemically bonded to silica particles [49, p. 68-69, 52, p. 45-47]. These chains, such as alkyl chains, can vary in length, ranging from a few carbon atoms up to thirty [49, p. 71]. The hydrophobicity of the stationary phase increases with longer alkyl chains. The widely used C18 (octadecylsilane) stationary phase, shown in **Figure 12**, is often preferred due to its relatively hydrophobic properties, enabling retention and separation of nonpolar analytes [49, p. 71]. The primary mechanism of

separation is based on hydrophobic interactions occurring between the hydrocarbon chains in the stationary phase and the hydrophobic parts of the analyte molecule [52, p. 48].

In recent years, alternative materials have been developed, such as those with phenyl groups, which exhibit lower hydrophobicity than the plain alkyl groups. These materials can enhance the resolution for aromatic compounds by facilitating pi-pi interactions between the phenyl group and the aromatic ring structures [49, p. 71]. An example of such a material is phenyl hexyl bounded to silica, illustrated in **Figure 12**.

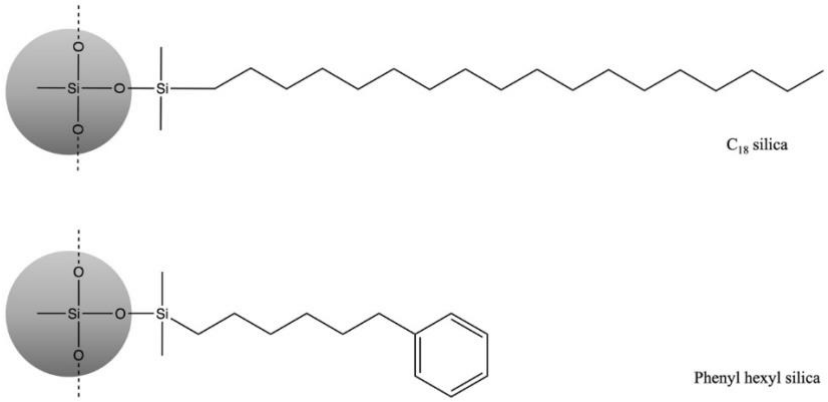

Figure 12. An illustration of the chemical structure of the stationary phase materials C18-bonded silica (top) and phenyl hexyl-bonded silica (bottom). Adapted from [56].

Mobile phases in reversed phase liquid chromatography

The mobile phases in RP-LC consist of water mixed with organic solvents, referred to as organic modifiers. This is because the amount of organic solvent modifies the eluting strength of the mobile phase: Thus, the more organic modifier added to the mobile phase, the less retention of the analytes, as it increases the elution strength of the mobile phase [52, p. 49]. Common organic modifiers in reversed phase chromatography are methanol and acetonitrile, whereas methanol has somewhat lower elution strength than acetonitrile [52, p. 49].

Elution can be performed isocratic, or using a gradient as illustrated in **Figure 13**. Isocratic elution means that the mobile phase consists of a single solvent or a constant ratio of a mixture of solvents [51, p. 676]. Isocratic elution is suited for less retained analytes, providing short analysis time. As the peak width increases with the retention time, it could be more beneficial to use gradient elution in some cases. If the analytes have different retention factors, k, a gradient elution can be used for faster analysis and more narrow peaks. To elute the more

retained analytes, an increased mobile phase strength is required [51, p. 676]. However, more time is needed for re-equilibration to the initial mobile phase conditions before the next injection [52, p. 126].

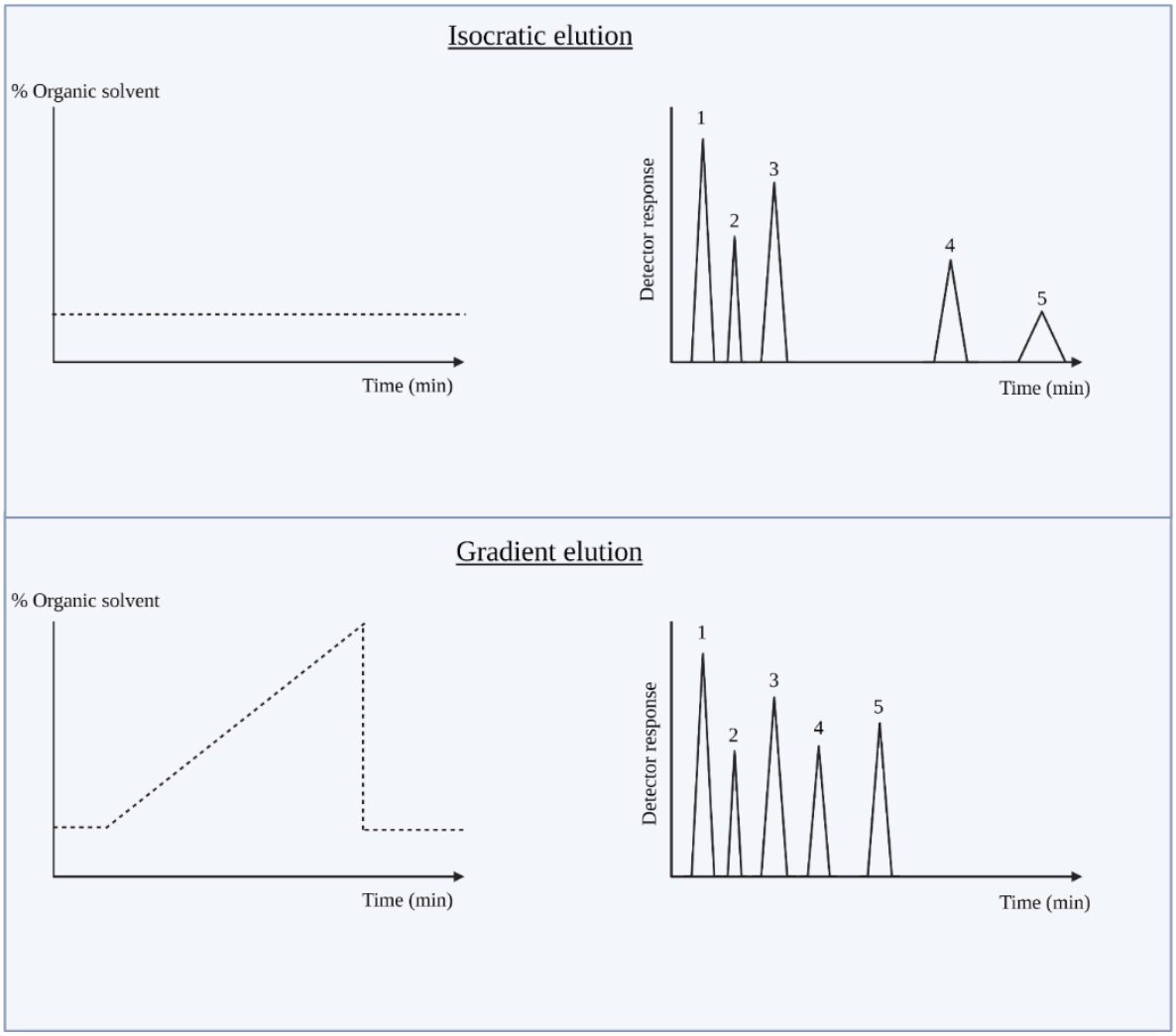

Figure 13. Illustration of the mobile phase composition when performing isocratic elution (top) and gradient elution (bottom) with an example of a chromatogram with five analytes. Created in BioRender.

Another alternative is to perform isocratic elution in multiple steps, called isocratic segments. By using isocratic segments, the elution distance between the peaks can be adjusted and one can control the selectivity and maintain sharp peaks in the chromatography [57]. Fekete et al. (2019) has shown that the sensitivity and resolution are higher using isocratic segments than using linear gradients [57].

pH control for reversed phase liquid chromatography mass spectrometry

Additives control the pH in the mobile phase and are used to achieve good chromatographic performance and adequate sensitivity in the MS [52, p. 49, 58]. It is common to use volatile organic acids, e.g. formic acid and acetic acid, when using mass spectrometric detection [52, p. 50]. However, alternatives exist and can provide increased ionization efficiency.

Trifluoroacetic acid (TFA) is a strong acid, providing good chromatographic performance because of its ion pairing characteristics and is considered the gold standard for analysis of protein biopharmaceuticals even though it suppresses the MS signal [58, 59]. Difluoroacetic acid (DFA) can provide comparable chromatographic behavior as TFA, but with less suppression of the MS signal [58]. Even though these alternatives exist, formic acid (FA), is widely used. FA reduces the chromatographic performance compared to TFA, but is still used due to its abilities in providing MS detection with less ion suppression than the alternatives [58].

The problem with additives is their dependency of the analyte, the experimental conditions and the mass spectrometer [59]. One may argue that the choice of pH control is a compromise concerning the chromatographic performance, the ionization efficiency and MS detection.

The influence of injection volume in liquid chromatography

Typical injection volumes in HPLC ranges from 1 to 100 μL [52, p. 125]. The injection can be performed manually or automatically. Using a syringe, a loop is filled with a sample and then injected into the system [49, p. 50]. By overfilling the loop, the injection volume is determined by the loop size [49, p. 50]. If the injected volume of the sample is smaller than the loop, it will result in dilution of the sample. The maximum volume of injection without encountering issues of extra band broadening is dependent on the elution strength of the sample solvent compared to the elution strength of the mobile phase [49, p. 52]. Injecting the sample in a solvent with lower elution strength than the mobile phase can lead to a refocusing of the sample at the column inlet [49, p. 52]. In contrast, injecting a solvent with higher elution strength will dilute the sample [49, p. 52].

When the injected volume of the sample is much smaller than the volume of the mobile phase carrying the peak out of the column, the volume of the sample injected affects the peak height linearly [60]. But it has no effect on the peak width. To counter high limits of detection, one

may inject a larger sample volume. A large-volume injection will possibly result in a refocusing of the analytes on the column. However, this can lead to volume overload and result in a broadened eluting peak [60].

1.6.4 Sample preparation by solid phase extraction

The goal of the sample preparation is to remove compounds that interfere with the analytes or compounds that can be harmful to the separation system, to enrich the analytes or to derivatize the analytes to improve the ability to separate and detect those [49, p. 161].

A commonly used sample preparation technique is solid phase extraction (SPE). In SPE, a small volume of a stationary phase, called a sorbent, is used to isolate compounds of interest from the sample matrix [51, p. 785], as illustrated in **Figure 14**. Reversed phase sorbents are used for extraction of relatively nonpolar analytes from a polar sample matrix [49, p. 172]. The SPE removes potential interferences in the sample matrix and simplifies the analysis [51, p. 785].

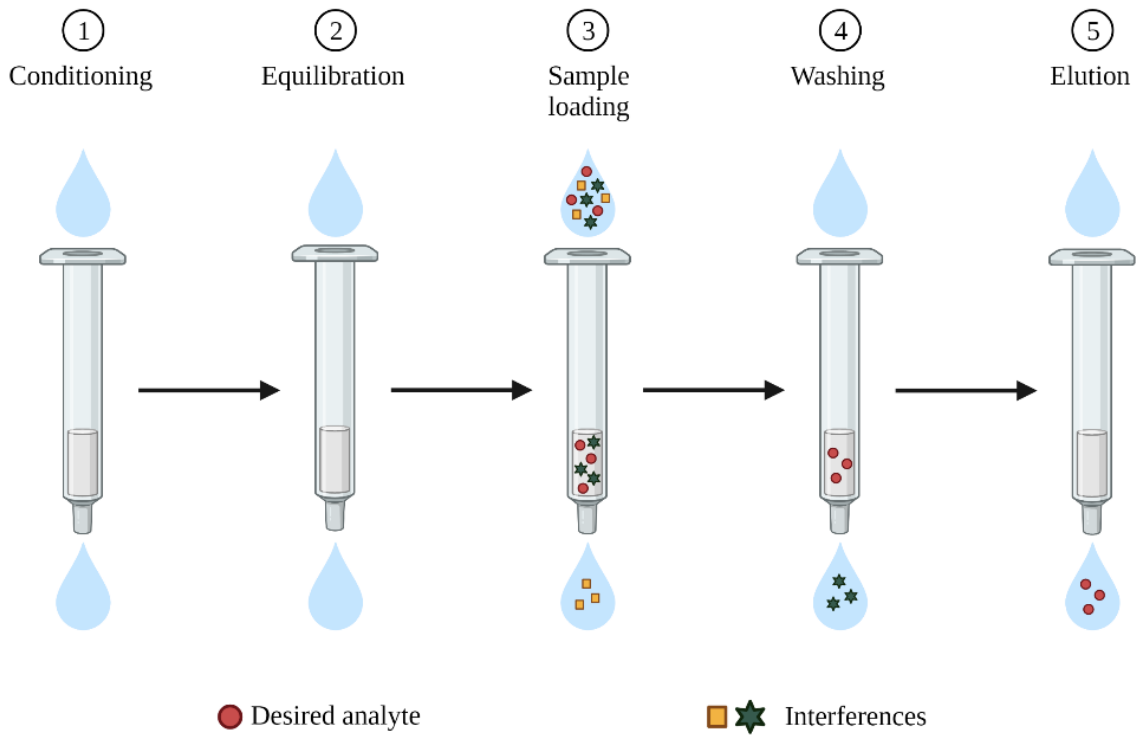

Figure 14. Illustration of solid phase extraction. The sorbent is first conditioned and equilibrated before the sample is loaded. Potential interferences are removed by washing, before the desired analytes are eluted. Adapted from [49, p. 169]. Created in BioRender.

With the use of a column-switching system, SPE can be done on-line by the use of a HPLC instrument [49, p. 170]. This allows for automation and rapid analysis. On-line SPE could be useful for the OiC-system, as the sample matrix may contain potential interferences. However, the SPE can be clogged over time and be prone to backpressure build-up [61]. A filtration step in advance to the SPE-LC can be performed to protect the on-line system, but can lead to contamination of the sample or potentially sample loss when performed off-line [61].

Automated filtration and filter flush solid phase extraction

A system that could be used to prevent clogging of online SPE columns, is an automated filtration and filter flush solid phase extraction (AFFL-SPE) [61]. This system will secure robust SPE-LC analysis through the removal of particles by filtration prior to the SPE. Back-flushing the filter flushes the particles off the filter. As the filtration is placed upstream to the SPE, it will not affect the chromatographic performance [61]. The AFFL-SPE-system is illustrated in **Figure 15**, and **Figure 16** illustrates how two 10-port valves can be used to connect OiC to the AFFL-SPE-LC-MS-system.

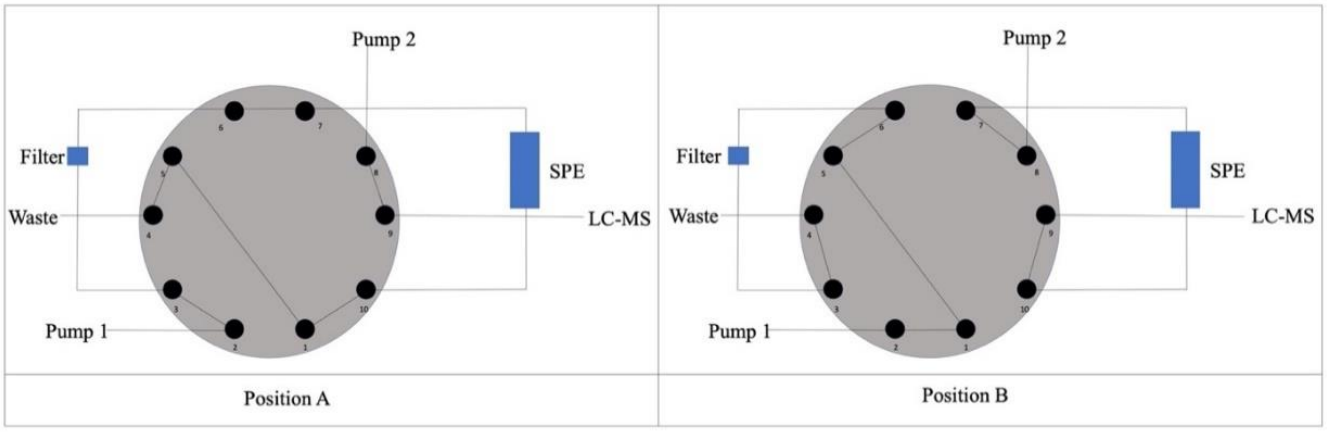

Figure 15. The figure illustrates the 10-port valve used in the automated filtration and filter flush solid phase extraction in position A and B. In position A, the sample is pumped by Pump 1 through the filter and the SPE. In position B, the filter is backflushed by Pump 1, while Pump 2 transports the mobile phase with the eluting analytes through the SPE and to the LC-MS. Adapted from [61].

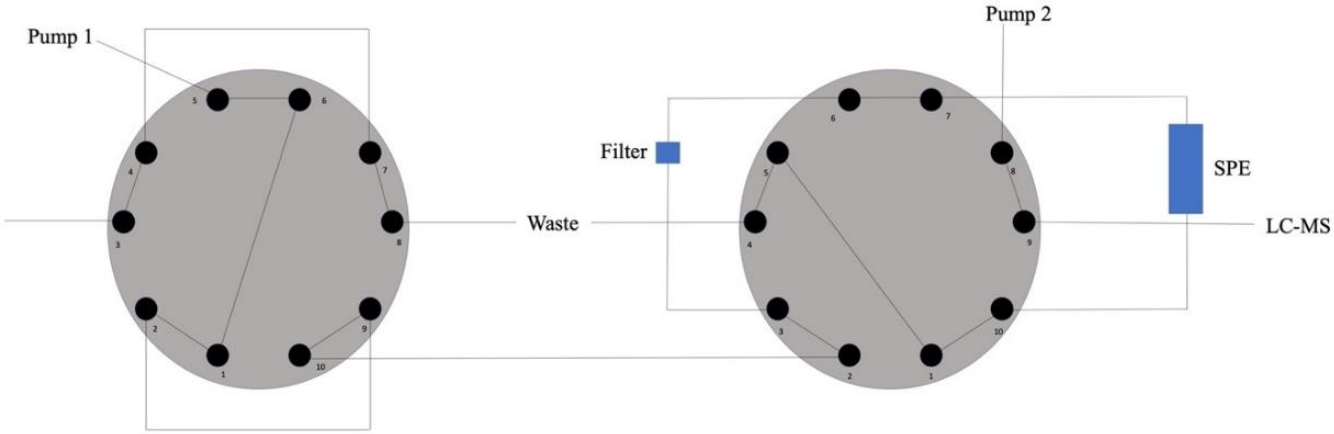

Figure 16. The figure illustrates how two 10-port valves can be used to connect organ-in-a-column (left) to the AFFL system (right). Adapted from [61].

2 Aim of study

Non-alcoholic fatty liver disease (NAFLD) is a global health problem with increasing prevalence [18, 19, 23]. Detecting the disease at an early stage is crucial as the disease can be reversed in the early stages. However, there is a lack of non-invasive diagnostic methods [29]. To overcome this, organoids, which mimic human physiology better than animal models, are being explored for studying the disease [11]. Research suggests that oxysterols, metabolites of cholesterol, could serve as markers for the disease progression in NAFLD [26, 36].

The study aimed to develop a method for detecting oxysterols without derivatization. To improve the sensitivity for poorly ionizable native oxysterols, various acids and organic modifiers were examined. Coelution of isomers were explored to enhance sensitivity and address the issue of high detection limits. Different stationary phases were examined for this purpose.

The analytes of interest can be divided into two groups: dihydroxycholesterol (diHC) and hydroxycholesterol (HC). The diHC group includes oxysterols with two hydroxyl-groups, while the HC group consists of oxysterols with one hydroxyl-group. The diHC-analytes were 7α,25-dihydroxycholesterol, 7β,25-dihydroxycholesterol, 7α,26-dihydroxycholesterol, 7β,26-dihydroxycholesterol, and 7α,24(*S*)-dihydroxycholesterol. The HC-analytes were 24(*S*)-hydroxycholesterol, 25-hydroxycholesterol, and 26-hydroxycholesterol (often referred to as 27-HC [62]).

The ultimate objective was to use an organ-in-a-column system as a disease modeling platform for NAFLD and monitor oxysterols in relation to disease development. NAFLD can be induced in liver organoids by exposing them to fatty acids. As a proof-of-concept, the aim of this study was to establish oxysterol fingerprints from healthy and steatotic liver organoids using organ-in-a-column technology.

3 Experimental

3.1 Chemicals

LC-MS grade acetonitrile (ACN), LC-MS grade water, LC-MS grade methanol (MeOH), LC-MS grade 2-propanol (isopropanol, IPA), LC-MS grade formic acid (FA, ≥ 99 %), 2-propanol (isopropanol, IPA) and chloroform were purchased from VWR Chemicals (Radnor, PA, USA). Difluoroacetic acid (DFA, 96 %) was purchased from Sigma Aldrich (St. Louis, MO, USA). Type 1 water was produced with a Milli-Q ultrapure water purification system from Millipore (Burlington, MA, USA). Nitrogen gas (5.0 quality (99.999 %)) and Argon gas (5.0 quality (99.999 %)) was purchased from Nippon Gases Norge AS (Oslo, Norway).

3.1.1 Standards of oxysterols

7α,24(*S*)-diHC, 7α,25-diHC, 7β,25-diHC, 7α,26-diHC, 7β, 26-diHC, 24(*S*)-HC and 26-HC were purchased from Avanti Polar Lipids (Alabaster, AL, USA). 25-HC was purchased from Sigma-Aldrich (St. Louis, MA, USA). The stock solutions were prepared in 2-propanol (IPA, LC-MS-grade, Rathburn Chemicals Ltd., Walkerburn, Scotland, UK).

The stock solutions of diHC standards with concentrations of 40 μg/mL were prepared in 2-propanol and stored at – 20℃. The stock solutions of HC standards were stored at 4 ℃ and prepared in different concentrations. The standard of 24(*S*)-HC was prepared in IPA with a concentration of 100 μg/mL. The standard of 25-HC was prepared in IPA with a concentration of 188 μg/mL. The standard of 26-HC was prepared in IPA with a concentration of 500 μg/mL and 60 μg/mL.

3.1.2 Cell medium

Neat cell medium for spiking with analytes was provided by Aleksandra Aizenshtadt (HTH). She also supplied samples of cell medium from organoids in a 96-well plate, both control and steatotic.

3.2 Materials and equipment

Eppendorf Safe-Lock Tubes (1.5 mL) were purchased from Eppendorf AG (Hamburg, Germany). FinnTip pipette tips were purchased from VWR. Autosampler vials were purchased from VWR. A 25 μL syringe used was purchased from Hamilton (Reno, NV, USA). SPE cartridges Oasis Prime 1 cc was purchased from Waters (Milford, MA, USA)

Two Avantor ACE chromatographic columns (2.1 mm x 5 cm) packed with respectively UltraCore 2.5 SuperPhenyl Hexyl (2.5 μm) and UltraCore 2.5 SuperC18 (2.5 μm) were purchased from VWR. A CORTECS^{TM} Premier chromatographic column (2.1 mm x 5 cm) packed with C18 (2.7 μm) was purchased from Waters. A HotSep® column (1.00 x 5.0 mm) packed with C18 Kromasil (5 μm) was from G&T Septech (Ski, Norway).

A Concentrator plus (SPEED VAC) was from Eppendorf. The mixer used was a Hula Dancer digital from IKA (Staufen, Germany). The syringe pump used for direct injection was a Fusion 100T model from Chemyx Inc. (Stafford, TX, USA).

Stainless steel (SS) unions, SS ferrules and nuts (for 1/16" tubing), SS reducing unions (1/16" to 1/32"), SS tubing (1/32" OD, 0.12 mm, 0.25 mm and 0.50 mm ID), 1/32" SS screens (1 μm pores), internal reducers (1/16" to 1/32"), a tubing cutter and two 2-position 10-port valves (for 1/32", C82X-6670ED) were purchased from VICI Valco (Schenkon, Switzerland).

Viper™ and nanoViper™ Fingertight Fitting Systems in SS from Thermo Fisher Scientific (Waltman, MS, USA) were used in the following sizes: 0.18 x 750 mm, 0.18 x 450 mm, and 0.15 x 550 mm.

3.3 Solutions

All samples of oxysterol standards were prepared and stored in Eppendorf tubes. If not stated otherwise, LC-MS quality water is hereafter referred to as water. This was used in all dilutions of the standard solutions with water.

3.3.1 Dilution of standard solutions of oxysterols

The different standard solutions prepared are listed in **Table 1**. The details are given in the appendix.

Table 1. Overview of the standard solutions prepared for method development.

Analyte(s) present in the standard solution	**Total concentration of analytes in the standard solution (*μ*g/mL)**	**Solvent**	**Procedure described in appendix**
24(*S*)-HC, 25-HC and 26-HC	0.12	Water	**Table 14**
7a, 24(*S*)-diHC, 7a, 25-diHC, 7b, 25-diHC, 7a, 26-diHC and 7b, 26-diHC	0.21	Water	**Table 15**
24(*S*)-HC	10	50:50 MeOH:Water (+ 0.1 % FA)	**Table 16**
25-HC	10	50:50 MeOH:Water (+ 0.1 % FA)	**Table 16**
26-HC	10	50:50 MeOH:Water (+ 0.1 % FA)	**Table 16**
24(*S*)-HC, 25-HC and 26-HC	10	50:50 MeOH:Water (+ 0.1 % FA)	**Table 17**
7a, 24(*S*)-diHC	10	50:50 MeOH:Water (+ 0.1 % FA)	**Table 18**
7a, 25-diHC	10	50:50 MeOH:Water (+ 0.1 % FA)	**Table 18**
7b, 25-diHC	10	50:50 MeOH:Water (+ 0.1 % FA)	**Table 18**
7a, 26-diHC	10	50:50 MeOH:Water (+ 0.1 % FA)	**Table 18**
7b, 26-diHC	10	50:50 MeOH:Water (+ 0.1 % FA)	**Table 18**
7a, 24(*S*)-diHC, 7a, 25-diHC, 7b, 25-diHC, 7a, 26-diHC and 7b, 26-diHC	10	50:50 MeOH:Water (+ 0.1 % FA)	**Table 19**

24(*S*)-HC, 25-HC, 26-HC, 7a, 24(S)-diHC, 7a, 25-diHC, 7b, 25-diHC, 7a, 26-diHC and 7b, 26-diHC	10	50:50 MeOH:Water (+ 0.1 % FA)	**Table 20**
24(*S*)-HC, 25-HC and 26-HC	1.2	50:50 MeOH:Water (+ 0.1 % FA)	**Table 21**
7a, 24(*S*)-diHC	1	50:50 IPA:Water (+ 0.1 % FA)	**Table 22**
7a, 25-diHC	1	50:50 IPA:Water (+ 0.1 % FA)	**Table 22**
7b, 25-diHC	1	50:50 IPA:Water (+ 0.1 % FA)	**Table 22**
7a, 26-diHC	1	50:50 IPA:Water (+ 0.1 % FA)	**Table 22**
7b, 26-diHC	1	50:50 IPA:Water (+ 0.1 % FA)	**Table 22**
24(*S*)-HC, 25-HC, 26-HC, 7a, 24(S)-diHC, 7a, 25-diHC, 7b, 25-diHC, 7a, 26-diHC and 7b, 26-diHC	1	50:50 IPA:Water (+ 0.1 % FA)	**Table 23**
24(*S*)-HC, 25-HC, 26-HC, 7a, 24(S)-diHC, 7a, 25-diHC, 7b, 25-diHC, 7a, 26-diHC and 7b, 26-diHC	0.1	50:50 IPA:Water (+ 0.1 % FA)	**Table 23**
24(*S*)-HC, 25-HC, 26-HC, 7a, 24(S)-diHC, 7a, 25-diHC, 7b, 25-diHC, 7a, 26-diHC and 7b, 26-diHC	0.09	50:50 IPA:Water (+ 0.1 % FA)	**Table 23**
24(*S*)-HC, 25-HC, 26-HC, 7a, 24(S)-diHC, 7a, 25-diHC, 7b, 25-diHC, 7a, 26-diHC and 7b, 26-diHC	0.01	50:50 IPA:Water (+ 0.1 % FA)	**Table 24**
25-HC	10	50:50 IPA:Water (+ 0.05 % DFA)	**Table 25**
24(*S*)-HC, 25-HC, 26-HC, 7a, 24(S)-diHC, 7a, 25-diHC, 7b, 25-diHC, 7a, 26-diHC and 7b, 26-diHC	0.1	10:90 IPA:Water (+ 0.1 % FA)	**Table 26**
7a, 24(*S*)-diHC	1	Cell medium	**Table 27**
7a, 25-diHC	1	Cell medium	**Table 27**
7b, 25-diHC	1	Cell medium	**Table 27**
7a, 26-diHC	1	Cell medium	**Table 27**
7b, 26-diHC	1	Cell medium	**Table 27**
7a, 24(*S*)-diHC	0.1	Cell medium	**Table 27**

7a, 25-diHC	0.1	Cell medium	**Table 27**
7b, 25-diHC	0.1	Cell medium	**Table 27**
7a, 26-diHC	0.1	Cell medium	**Table 27**
7b, 26-diHC	0.1	Cell medium	**Table 27**
24(*S*)-HC, 25-HC, 26-HC, 7a, 24(S)-diHC, 7a, 25-diHC, 7b, 25-diHC, 7a, 26-diHC and 7b, 26-diHC	1	Cell medium	**Table 28**
24(*S*)-HC, 25-HC, 26-HC, 7a, 24(S)-diHC, 7a, 25-diHC, 7b, 25-diHC, 7a, 26-diHC and 7b, 26-diHC	0.1	Cell medium	**Table 28**
7a, 24(*S*)-diHC	1	50:50 IPA:Cell medium	Table **29**
7a, 25-diHC	1	50:50 IPA:Cell medium	Table **29**
7b, 25-diHC	1	50:50 IPA:Cell medium	Table **29**
7a, 26-diHC	1	50:50 IPA:Cell medium	Table **29**
7b, 26-diHC	1	50:50 IPA:Cell medium	Table **29**
7a, 24(*S*)-diHC	0.1	50:50 IPA:Cell medium	Table **29**
7a, 25-diHC	0.1	50:50 IPA:Cell medium	Table **29**
7b, 25-diHC	0.1	50:50 IPA:Cell medium	Table **29**
7a, 26-diHC	0.1	50:50 IPA:Cell medium	Table **29**
7b, 26-diHC	0.1	50:50 IPA:Cell medium	Table **29**
24(*S*)-HC, 25-HC, 26-HC, 7a, 24(S)-diHC, 7a, 25-diHC, 7b, 25-diHC, 7a, 26-diHC and 7b, 26-diHC	1	50:50 IPA:Cell medium	**Table 30**

24(*S*)-HC, 25-HC, 26-HC, 7a, 24(S)-diHC, 7a, 25-diHC, 7b, 25-diHC, 7a, 26-diHC and 7b, 26-diHC	0.1	50:50 IPA:Cell medium	**Table 30**
24(*S*)-HC, 25-HC, 26-HC, 7a, 24(S)-diHC, 7a, 25-diHC, 7b, 25-diHC, 7a, 26-diHC and 7b, 26-diHC	1	IPA	**Table 31**
24(*S*)-HC, 25-HC, 26-HC, 7a, 24(S)-diHC, 7a, 25-diHC, 7b, 25-diHC, 7a, 26-diHC and 7b, 26-diHC	0.1	10:90 IPA:Cell medium	**Table 32**

3.3.2 Preparation of medium samples

Neat medium was spiked with standard solutions of oxysterols, see **Table 1** above. The medium samples from control and steatotic liver organoids were diluted in 10 % and 50 % IPA by pipetting the ratio of sample and IPA into an Eppendorf vial.

3.4 Off-line sample preparation using solid phase extraction

Five different approaches of off-line sample preparation using SPE was performed using Oasis prime SPE cartridges.

3.4.1 Solid phase extraction of spiked cell medium

The general procedure using Oasis prime is performed by first loading the sample, then washing the sorbent with a solvent with proper elution strength, and finally eluting the analytes with a stronger solvent. There is no need for conditioning of the sorbent before loading the sample when using Oasis prime.

SPE was utilized in three different ways to extract diHC from cell medium spiked with a concentration of 0.1 μg/mL, as described in **Table 2**. Procedure 1 and 3 was also performed on standard solutions of diHC in IPA:Water, without cell medium. The washing solution was subsequently analyzed to ensure that the analytes did not elute during this step. Additionally, Procedure 3 was employed for two different solutions containing 0.1 μg/mL diHC dissolved in 50:50 IPA:Cell medium and 10:90 IPA:Cell medium, referred to as Procedure 4 and 5 in **Table 2**. The eluate obtained from the procedures underwent LC-MS analysis in both MRM mode and full scan.

Table 2. Overview of the different steps in the five SPE procedures, 1-5. The different steps are defined as sample loading, washing, elution, evaporation of solvent and resolvation.

Procedure	**#1**	**#2**	**#3**	**#4**	**#5**
Sample loading	200 μL of a solution of 0.1 μg/mL diHC in cell medium			200 μL of a solution of 0.1 μg/mL diHC (in 50:50 IPA:Cell medium)	200 μL of a solution of 0.1 μg/mL diHC (in 10:90 IPA:Cell medium)
Washing	500 μL water *				
Elution	200 μL 50:50 IPA:Water	200 μL 100 % IPA	200 μL 100 % IPA	200 μL 100 % IPA	200 μL 100 % IPA
Evaporation of solvent	÷	2 hours	÷	÷	÷
Resolvation	÷	200 μL water	÷	÷	÷

* Water at the tip of the SPE was removed before elution to avoid dilution of the sample

3.4.2 Preparation of standard solutions of oxysterols after solid phase extraction

The eluate obtained from procedure 4 and 5 (**Table 2**) was dissolved in 100 % IPA. Subsequently, to achieve further dilution, additional IPA was added. This process is described in **Table 33** and

Table 34 in appendix.

3.5 Adsorption of analyte to surface examination

Standards of diHC were diluted in cell medium to a total volume of 200 μL. After one hour, the solution was removed from the tube. Subsequently, 200 μL of IPA was added to the Eppendorf tube. After another hour, the solution was diluted by adding 200 μL of water. LC-MS analysis was performed on both the cell medium collected after one hour and the solution of IPA:Water obtained. This procedure is illustrated in **Figure 17** and was conducted for solutions with diHC concentrations of 1.0 and 0.1 μg/mL.

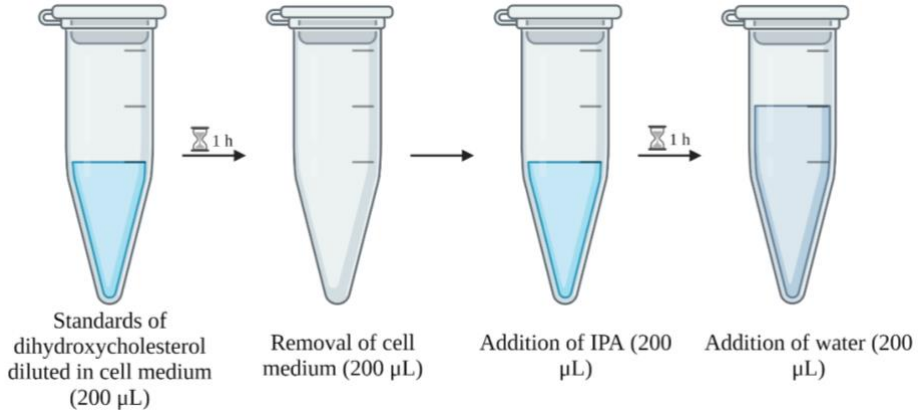

Figure 17. Illustration of the procedure conducted to examine adsorption of analytes to the surface of vials and Eppendorf tubes. Created in BioRender.

3.6 Optimization of mass spectrometer parameters

The optimization of mass spectrometer (MS) parameters was performed by performing direct injection on a TSQ Vantage triple quadrupole MS with a Heated ESI (HESI) source from Thermo Fisher Scientific (Waltman, MS, USA).

Diluted standard solutions with a concentration of 10 μg/mL in 50:50 MeOH:Water (+ 0.1 % FA) were injected directly into the ESI-MS for all the analytes. A 250 μL syringe was filled with 150 μL of a diluted standard solution. To connect the syringe to the ESI source, a PEEK tubing with inner diameter (ID) 0.005 “ and outer diameter (OD) 1/16 “ of 30 cm was used. A syringe pump was used to empty the syringe through the tubing and into the ESI source, and

the flow rate was set to 10 μL/min. The syringe and tubing were rinsed with 50:50 MeOH:Water between each direct injection of a new analyte.

The MS was operated in full scan mode, scanning over *m/z* range 300-450. After finding the most abundant ions in full scan mode, the MS was set to MRM mode to study the fragmentation. The software reported optimized values for collision energy and S-lens values for the chosen parent ions.

3.7 Instruments

Two different instrument setups, namely setup 1 and setup 2, were utilized throughout the project. Both setups involved the use of a Dionex UltiMate 3000 UHPLC system and a TSQ Vantage triple quadrupole MS with a HESI-II ion source from Thermo Fisher Scientific (Waltman, MS, USA). Setup 1 is illustrated in **Figure 18**.

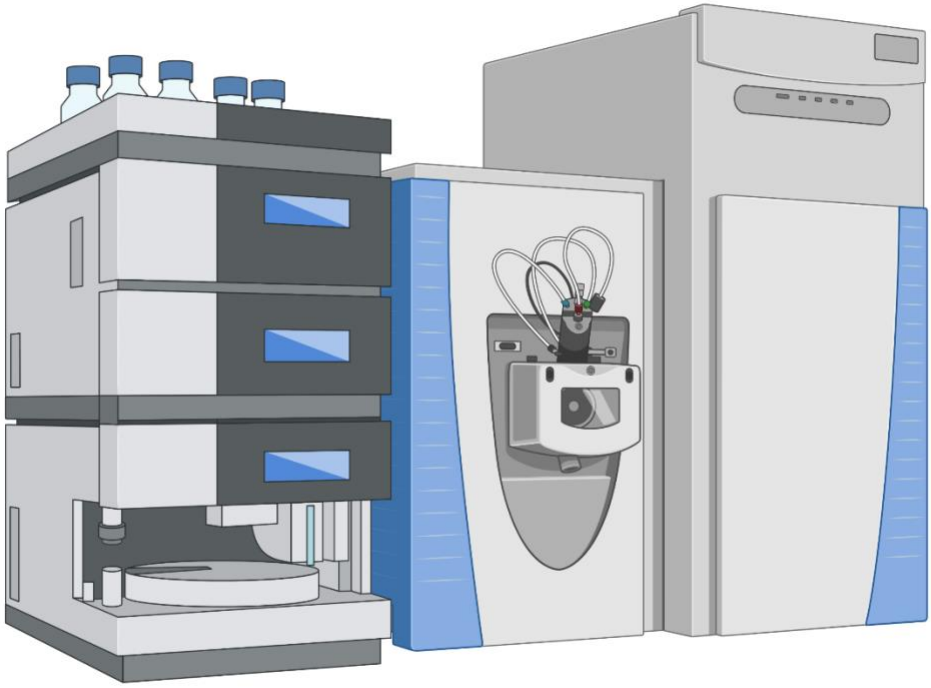

Figure 18. Illustration of setup 1: A Dionex Ultimate 3000 UHPLC system coupled to the ESI-MS. Created in BioRender.

Setup 2 incorporated an AFFL-system prior to the HPLC-MS, as illustrated in **Figure 19**. A Hitatchi L-7100 pump model (Tokyo, Japan) was used for this purpose. The setup also included two 2-position 10-port valves (for 1/32", C82X-6670ED) from VICI Valco.

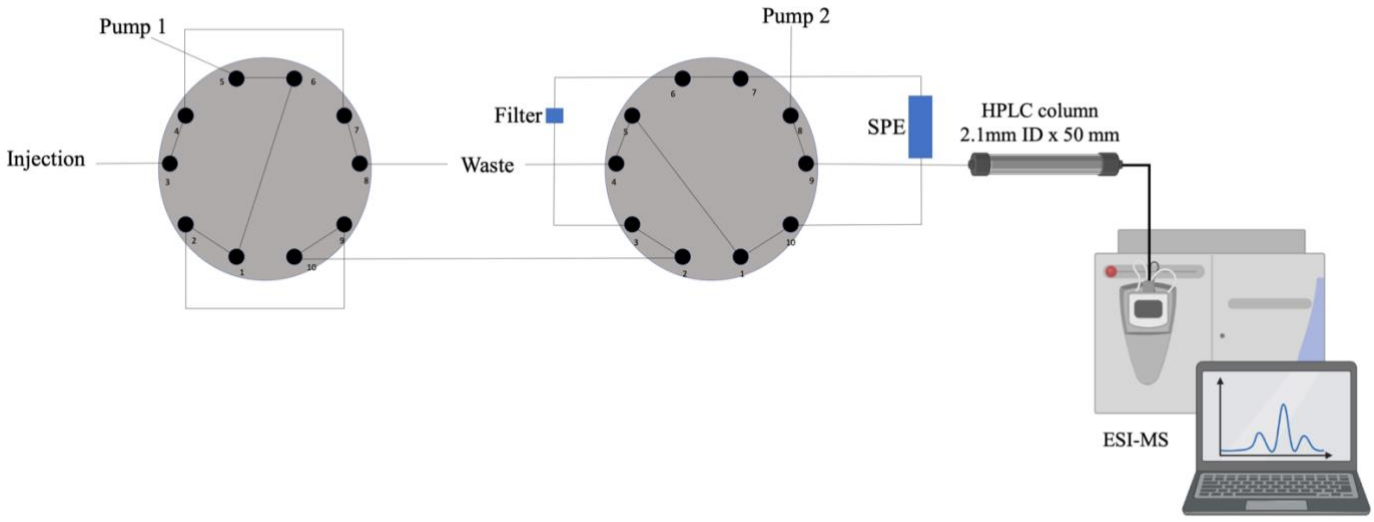

Figure 19. Illustration of setup 2: An AFFL-system prior to the HPLC-MS. Created in BioRender.

3.8 Setup 1: Liquid chromatography – mass spectrometry

The analytes were separated using different columns, with the column temperature maintained at 40 ℃. The Dionex UltiMate 3000 UHPLC-system used for the chromatographic analysis provided a flow rate of 400 μL/min. MS-analysis was performed using a TSQ Vantage triple quadrupole mass spectrometer operating in MRM mode. The injection volume ranged from 1-5 μL. Details about the different mobile phases examined are provided below.

3.8.1 Mobile phases

Isocratic elution was employed to examine four different mobile phase compositions, which are listed in **Table 3**. Additionally, two mobile phase compositions were examined utilizing multi-isocratic steps, as presented in **Table 4** and **Table 5**.

Table 3. The different mobile phase compositions examined utilizing isocratic elution.

Mobile phase	**Water**	**ACN**	**MeOH**	**IPA**	**pH control**
1	0-65 %	30-85 %	5-50 %		0.1 % FA
2	10-80 %			20-90 %	0.1 % FA
3	5-80 %		20-95 %		0.1 % FA
4	60-70 %			30-40 %	0.05 % DFA

Table 4. The first mobile phase composition examined by utilizing multi-isocratic steps. Mobile phase A is water added 0.1 % FA, mobile phase B is IPA added 0.1 % FA.

Time	**% B**	**Purpose**
0 min	20	Dwell time
3 min	20	
3 min	42	Elution
7 min	42	
7 min	95	Wash
9.5 min	95	
9.5 min	20	Re-equilibration
12 min	20	

Table 5. The second mobile phase composition examined by utilizing multi-isocratic steps. Mobile phase A is water added 0.1 % FA, mobile phase B is IPA added 0.1 % FA.

Time	**% B**	**Purpose**
0 min	20	Dwell time
2 min	20	
2 min	45	Elution
5 min	45	
5 min	95	Wash
7.5 min	95	
7.5 min	20	Re-equilibration
10 min	20	

3.8.2 MS settings

The mass spectrometer settings can be found in **Table 6** and **Table 7**.

Table 6. The mass spectrometer settings for capillary temperature, vaporizer temperature, sheath gas pressure, auxiliary gas flow and spray voltage.

Parameter	**Value**
Capillary temperature	350 °C
Vaporizer temperature	300 °C
Sheath gas pressure	35 psi
Auxiliary gas flow	10 arbitrary units
Spray voltage	+ 3000 V

Table 7. The mass spectrometer settings for MRM mode, listing the parent ions, product ions, collision energy, S-lens values, and polarity.

Name of observed ion	**Parent ion** (*m/z*)	**Product ion** (*m/z*)	**SRM Collision Energy, eV**	**S-Lens value**	**Polarity**
DiHC -3H_2O	365	90.9	46	84	+
DiHC - 3H_2O	365	104.9	38	84	+
HC - 2H_2O	367.2	90.93	49	85	+
HC - 2H_2O	367.2	104.9	40	85	+
DiHC - 2H_2O	383	90.9	52	85	+
DiHC - 2H_2O	383	104.9	41	85	+
HC - H_2O	385.2	90.93	49	92	+
HC - H_2O	385.2	104.9	43	92	+

3.9 Setup 2: Automated filtration and filter flush solid phase extraction liquid chromatography – mass spectrometry

Setup 2 closely resembles setup 1, with the notable inclusion of AFFL-SPE in the LC-MS system. The separation of analytes was performed on a superphenyl hexyl column, with the column temperature set to 40 ℃. The Dionex UltiMate 3000 UHPLC-system with a flow rate of 400 μL/min. The injection volume was set to 5 μL. Pump 1, connected to the AFFL-system, utilized a loading solution consisting of 3 % MeOH in water with 0.1 % FA added. The flow rate was set to 100 μL/min. MS-analysis was performed on a TSQ Vantage triple quadrupole

mass spectrometer operating in MRM mode. The MS settings for this setup are similar to those of setup 1. Details about the different mobile phases examined are provided below.

3.9.1 Mobile phases

The mobile phase composition investigated using multi-isocratic steps is presented in **Table 8**. Additionally, gradient elution was examined using a gradient ranging from 20 to 50-90 % IPA, with water serving as the other component of the mobile phase.

Table 8. The mobile phase composition examined by utilizing multi-isocratic steps with AFFL-SPE-LC-MS. Mobile phase A is water added 0.1 % FA, mobile phase B is IPA added 0.1 % FA.

Time	**% B**	**Purpose**
0 min	20	Dwell time
3 min	20	
3 min	60	Elution
7 min	60	
7 min	95	Wash
9.5 min	95	
9.5 min	20	Re-equilibration
12 min	20	

3.10 Data processing

Xcalibur™ and Freestyle™ from Thermo Scientific was used for processing of the chromatograms and mass spectra. Smoothing Gaussian 7 were used for all chromatograms.

4 Results and discussion

Developing a method for detection of underivatized oxysterols using LC-MS involves optimizing different experimental parameters, starting with the MS parameters. The sections below describe the choices made for mobile phase composition, elution mode, stationary phase, pH control, and injection volume. Additionally, difficulties encountered during the process will be discussed, such as poor signals from one of the analyte groups, the absence of signals in cell medium, and issues related to carry-over. Furthermore, challenges were faced when applying the LC-MS method to the system including AFFL-SPE prior to LC-MS.

The intended use of organoids in OiC connected to the AFFL-SPE-LC-MS system was to study the secretion of oxysterols from both healthy and steatotic organoids. Unfortunately, the organoids did not arrive on time. Therefore, the developed method could not be tested with the OiC. Nevertheless, the method was employed to analyze medium that had been in contact with both healthy and steatotic organoids.

4.1 Optimization of MS parameters

Oxysterols are neutral molecules that do not easily ionize in ESI. In order to detect oxysterols in medium samples, the MS parameters were optimized through direct infusion of standard solutions. Each analyte was dissolved in MeOH:Water + 0.1 % FA at a concentration of 10 μg/mL. The MS was operated in full scan mode, scanning over the *m/z* range 300-450, as the ionized analytes were expected to appear within this range. The monoisotopic mass for HC-analytes is 402.35 and 418.34 for diHC-analytes. The difference in mass is due to one extra hydroxygroups added to the diHC-analytes.

During the analysis, it was observed that the oxysterols were indeed ionized with ESI, but with the loss of one, two or three water molecules, resulting in $[M+H-xH_2O]^+$ ions. The HC-analytes lost one and two water molecules, while the diHC-analytes lost two and three water molecules (**Table 9**). This phenomenon can be attributed to the presence of different numbers of hydroxygroups in the analytes, which can be lost during adduct formation in ESI. The observation of the MS signal exhibiting water loss aligns with previous findings, such as the study by Røberg-Larsen et al. [44], where the same water loss was observed for 25-HC. Hence,

the MS proved to be effective in detecting underivatized oxysterols, considering the observed ionization patterns and water loss characteristics.

Upon identifying the most abundant ions in full scan mode, the MS was switched to MRM mode to study the fragmentation patterns. The software provided optimized collision energy and S-lens values for the selected parent ions, ensuring efficient fragmentation during the analysis. To ensure reliable identification of the analytes, two product ions were chosen for each parent ion, enabling accurate and robust characterization of the analytes. The product ions selected for analysis were the ones common to the analytes within each group and that exhibited the highest signal intensity, listed in **Table 9**.

Table 9. Overview of the observed ions using ESI-MS, the m/z values for the parent ions and the product ions chosen for MRM.

Observed ion using ESI-MS	**Parent ion** (*m/z*)	**Product ion** (*m/z*)
DiHC -3H_2O	365	90.9
DiHC - 3H_2O	365	104.9
HC - 2H_2O	367.2	90.93
HC - 2H_2O	367.2	104.9
DiHC - 2H_2O	383	90.9
DiHC - 2H_2O	383	104.9
HC - H_2O	385.2	90.93
HC - H_2O	385.2	104.9

The MS parameters were optimized for the detection of underivatized oxysterols, successfully ionizing the analytes with ESI and exhibiting characteristic water loss patterns.

4.2 Mobile phase optimization for enhanced signal

In the process method development, different mobile phase compositions were examined using a superphenyl hexyl stationary phase. The objective of the optimization was to identify the most suitable organic modifier that would facilitate optimal ionization of the oxysterols. This step was crucial as underivatized oxysterols exhibit poor ionization, resulting in high detection limits. Additionally, it was a specific objective to achieve coelution of the isomeric oxysterols to enhance the sensitivity. Coelution leads to higher signal intensity, dealing with the high limits of detection issue.

4.2.1 Evaluation of ACN and MeOH as organic modifier

The initial mobile phase examined consisted of a mixture of ACN, MeOH and water with 0.1 % FA. This particular mobile phase composition was found to be effective for derivatized oxysterols, as demonstrated by Kømurcu et al. (56-62 % Water, 38-44 % Organic modifier) [36] . However, the same composition did not yield satisfactory results for underivatized oxysterols. When the organic modifier content was below 70 % (60 % ACN, 10 % MeOH), the HC-analytes were too well retained on the phenyl hexyl stationary phase. Conversely, when the organic modifier content exceeded 75 % (65 % ACN, 10 % MeOH), the analytes showed minimal to no retention. Consequently, a small range between 71-74 % organic modifier was left for further optimization. This is illustrated in **Figure 20**.

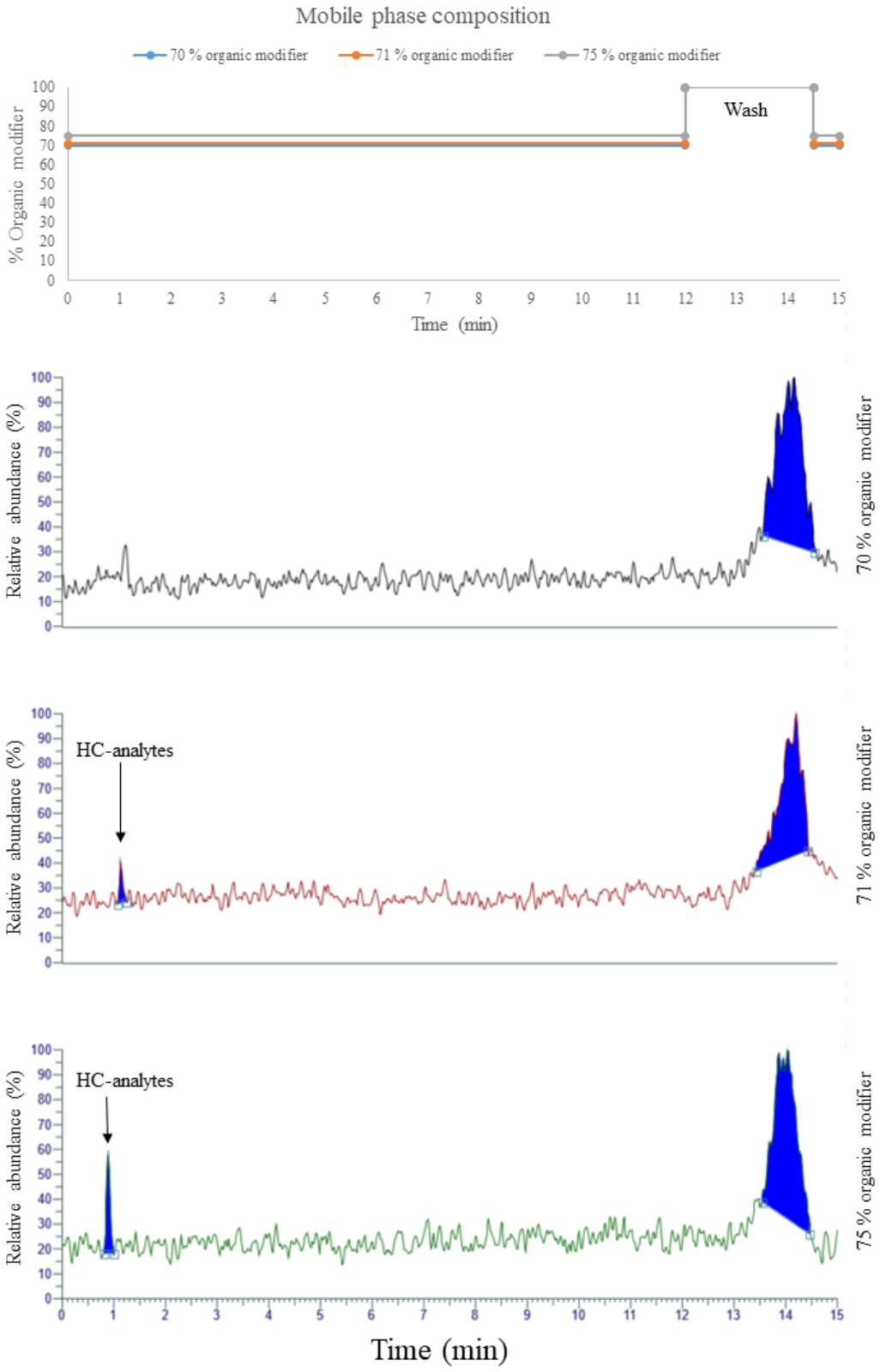

Figure 20. An overview of the mobile phase composition with isocratic elution, accompanied by chromatograms demonstrating the influence of the organic modifier on the retention time of HC-analytes solved in water. The chromatograms show the relative abundance of the analytes m/z in percentage (y-axis) and the retention time in minutes (x-axis). The chromatograms were obtained through the analysis of a HC-standard solution containing all HC-analytes with a total concentration of 0.040 μg/mL in MRM mode (m/z 385.2 → 90.9, 385.2 → 104.9).

The top chromatogram illustrates that the HC-analytes are too well retained and do not elute before the washing step (14 min) when the mobile phase contains 70 % organic modifier. From the middle chromatogram, with 71 % organic modifier in the mobile phase, it is illustrated that the analytes exhibit some retention and elute after one minute. Lastly, the bottom chromatogram demonstrates that the analytes have minimal to no retention when the mobile phase contains 75 % organic modifier.

A mobile phase composition containing 71-74 % organic modifier resulted in some retention of the analytes. The HC-analytes are less hydrophobic compared to the diHC-analytes and should therefore have the highest degree of retention. The chromatogram in **Figure 20** illustrates that the HC-analytes eluted at a retention time of 1.1 minute with 71 % organic modifier. Meaning that this composition of the mobile phase would make the diHC-analytes elute too early. In addition to inadequate retention of the analytes, the provided signals were low in intensity.

Different mobile phase compositions of ACN, MeOH and water were examined using low concentrations of HC-analytes (0.040 μg/mL). In retrospect, it was realized that the concentration of the standard solutions should have been higher. During the method development process, it became apparent that working with higher concentrations of the standard solutions would facilitate easier optimization. Consequently, higher concentration standards were used to examine the other mobile phase compositions. In hindsight, conducting the examination of mobile phases under the same conditions, including standardized concentrations, would have provided a better basis for comparison.

4.2.2 Evaluation of MeOH as organic modifier

A mobile phase composition of MeOH and Water (+ 0.1 % FA) was examined as an attempt to enhance the signal intensity from the analytes. Proper retention of the analytes and coelution was an issue when using MeOH and water as the mobile phase constituents. This problem is illustrated in **Figure 21**.

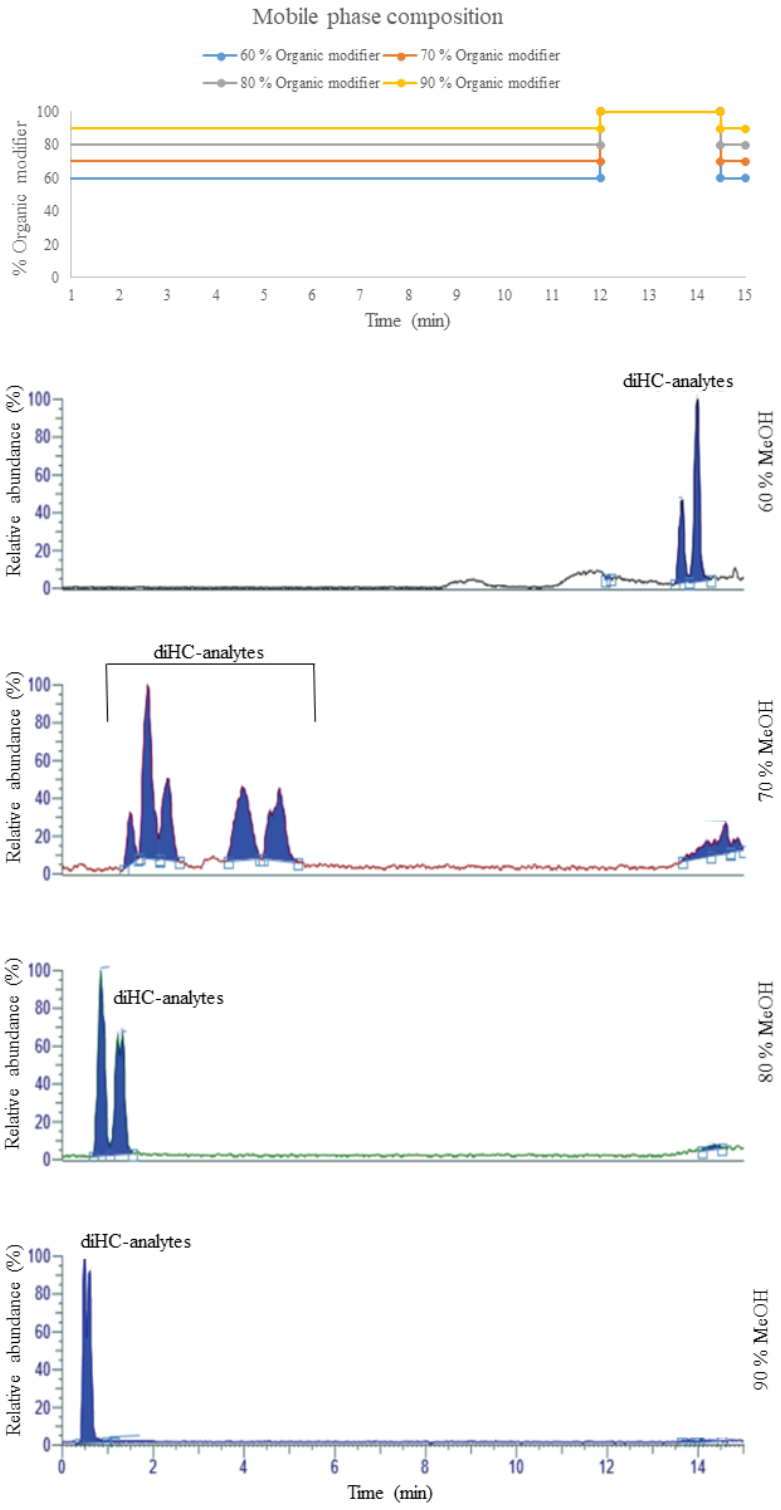

Figure 21. An overview of the mobile phase composition with isocratic elution using MeOH as organic modifier, accompanied by chromatograms that demonstrate the influence of the organic modifier on the retention time of diHC-analytes. The chromatograms show the relative abundance of the analytes m/z in percentage (y-axis) and the retention time in minutes (x-axis). The chromatograms were obtained through the analysis of a diHC-standard solution solved in 50:50 MeOH:Water + 0.1 % FA, containing all diHC-analytes with a total concentration of 5 μg/mL in MRM mode (m/z 383 → 90.9, 383 → 104.9).

The top chromatogram shows that the diHC-analytes are too retained and fail to elute before the washing step of 100 % MeOH, when using 60 % MeOH in the mobile phase. In the second chromatogram, the analytes demonstrate some retention with 70 % MeOH in the mobile phase. However, they elute within a range of 1.9 to 4 minutes, indicating that the desired coelution was not achieved. The two bottom chromatograms shows how the analytes have minimal to no retention when the mobile phase contains 80-90 % MeOH.

Since the achievement of coelution was considered crucial to deal with the high limits of detection, the use of MeOH as organic modifier in the mobile phase had to be ruled out. When attempting to achieve coelution with MeOH concentrations higher than 90 %, the analytes showed no retention. On the other hand, MeOH concentrations lower than 60 % resulted in too high retention of the analytes. 70 % MeOH led to separation of the diHC-analytes and did not provide sufficient signal strength from the HC-analytes.

4.2.3 Evaluation of IPA as organic modifier

The third mobile phase composition examined was a combination of isopropanol (IPA) and water (+ 0.1 % FA). IPA was chosen as organic modifier as previous students had observed that the native oxysterols needed to be dissolved in an alcohol for signal enhancement. This combination provided higher signal intensity compared to the other mobile phases and it was possible to achieve both coelution and proper retention of the analytes. The optimization of the ratio between IPA and water are described in section 4.5.

IPA gave the highest signal intensity of the analytes and was chosen as organic modifier.

4.2.4 General considerations of organic modifier optimization and column choice

The optimization of the mobile phase composition could have been approached differently by examining the three combinations of mobile phases on the three available columns. The selection of the mobile phase was based on utilizing phenyl hexyl as the stationary phase. However, it is possible that one of the mobile phases would have been better suited for the C18 stationary phases. Since the other mobile phases, MeOH + Water and ACN + MeOH + Water, did not offer sufficient retention on phenyl hexyl, employing a more hydrophobic stationary

phase like C18 could potentially result in improved retention of the hydrophobic analytes. This is because C18 exhibits a greater extent of hydrophobic interactions compared to phenyl hexyl.

The standard solutions used for evaluation of the mobile phases had different concentrations (0.040 and 5 μg/mL), and were also dissolved in different solvents (Water and 50:50 Water:MeOH + 0.1 % FA). Preferably, the results used for comparison should have had the same experimental conditions and concentration as of the standard solutions used. The difference in concentration can be explained by starting too low in the early stage of the method development. The decision to increase the concentration was not made until later. Experiments performed with lower concentrations were not repeated due to limited time.

4.2.5 Formic acid provides better chromatographic performance and signal for MS detection than difluoroacetic acid

In the process of method development, obtaining adequate signals from the analyte group of HCs was a challenge. To address this issue, different acids were tested for pH control in the mobile phase. The acids functions depends on factors such as the analytes, the experimental conditions and the MS being used [59].

Initially, the experiments were conducted using formic acid (FA) as the pH control. FA was chosen due to its availability and low toxicity. However, the potential of difluoroacetic acid (DFA) as an alternative to FA was explored. DFA was selected as it is known to provide good chromatographic behavior and causing less suppression of the MS signal compared to trifluoroacetic acid (TFA) [58]. The exploration of alternative acids was motivated by the aim to enhance ionization efficiency, considering the oxysterols poor ionizability. It was important to examine different acids in order to improve the performance of the method.

To compare the use of FA and DFA as pH control, an analysis was conducted using a standard solution containing all analytes at a concentration of 10 µg/mL. The mobile phase consisted of 40 % IPA and 60 % water, either with 0.1 % FA or 0.05 % DFA. The different percentages of organic acid added to the mobile phase were based on difference in acid strength. As a result, both mobile phases had a final pH of approximately 3. The average area and standard deviation provided for the analytes are shown in **Figure 22** and **Figure 23** respectively.

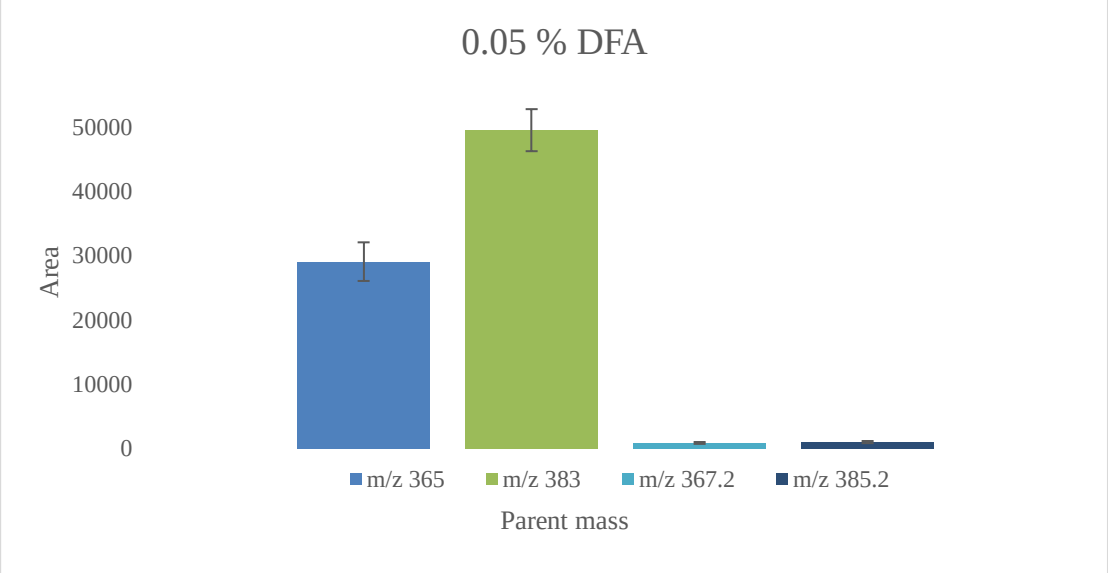

Figure 22. Bar chart displaying the average area and standard deviation resulting from the injection of a standard solution containing all analytes at a total concentration of 10 µg/mL dissolved in 50:50 MeOH:Water + 0.1 % FA. The analysis was performed in MRM mode using 0.05 % DFA in the mobile phase as pH control. The data presented in the chart is based on three replicates (n = 3).

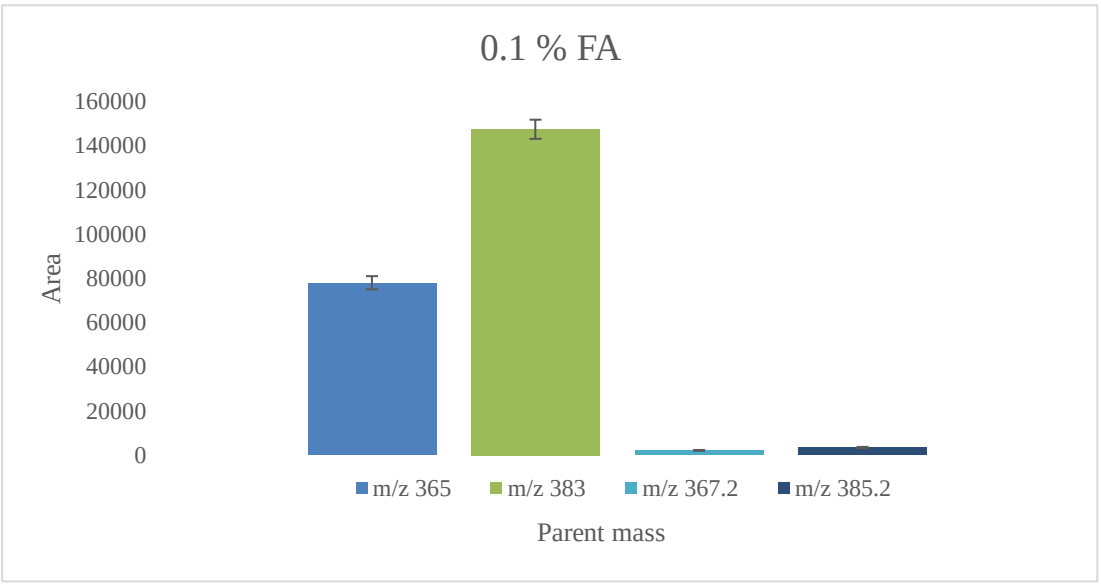

Figure 23. Bar chart displaying the average area and standard deviation resulting from the injection of a standard solution containing all analytes at a total concentration of 10 µg/mL dissolved in 50:50 MeOH:Water + 0.1 % FA. The analysis was performed in MRM mode using 0.1 % FA in the mobile phase as pH control. The data presented in the chart is based on three replicates (n =3).

Based on the observations from both figures (**Figure 22** and **Figure 23**), it can be noted that the signal intensity for the HC-analytes with parent masses *m/z* 367.2 and 385.2 is relatively low when using both DFA and FA as pH control. However, the signals detected using FA are up to 42 % higher compared to DFA. Additionally, the relative standard deviation is 16 % when using DFA, whereas it ranges between 9-10 % using FA.

In the case of the diHC-analytes with parent masses *m/z* 365 and 383, it is evident that the signal intensity obtained using both acids is significantly stronger compared to the HC-analytes. Nevertheless, the signals are up to 37 % higher when FA is used instead of DFA. Moreover, FA demonstrates better repeatability, with a relative standard deviation below 4 %, while DFA shows a range between 6 % and 10 %.

Comparing the areas and relative standard deviation, FA clearly provides better ionization than DFA. However, neither acid contributed to an enhanced signal from the HC-analytes. Ultimately, under the given experimental conditions, FA emerges as the preferred choice for pH control in the analysis of underivatized oxysterols.

The observed variability between the runs was notably high. Consequently, conducting more than three replicates would have been beneficial, as it would have facilitated a clearer decision regarding the choice of pH control. Nevertheless, the results obtained clearly demonstrate a significant difference between using DFA and FA as pH control.

Formic acid yielded superior signals for MS detection compared to DFA, leading to the selection of FA as the pH control for further method development.

4.3 Excluding the hydroxycholesterols as analytes

Both hydroxycholesterols (HCs) and dihydroxycholesterols (diHCs) were studied in the introductory phase of the method development. When studying both analyte groups simultaneously it became clear that the HCs were harder to ionize. The signals were low compared to diHC. A selection of chromatograms comparing signals provided from HC-analytes with the three different columns (Avantor C18, Cortecs C18, and Avantor SuperPhenyl hexyl) are presented in **Figure 24**. **Figure 25** compares the signals provided from the three columns for HC- and diHC-analytes by average area of the peaks and standard deviations. The phenyl hexyl column was also examined using 70 % MeOH as organic modifier, this provided no signal for HC (see Appendix **Figure 42** for chromatogram).

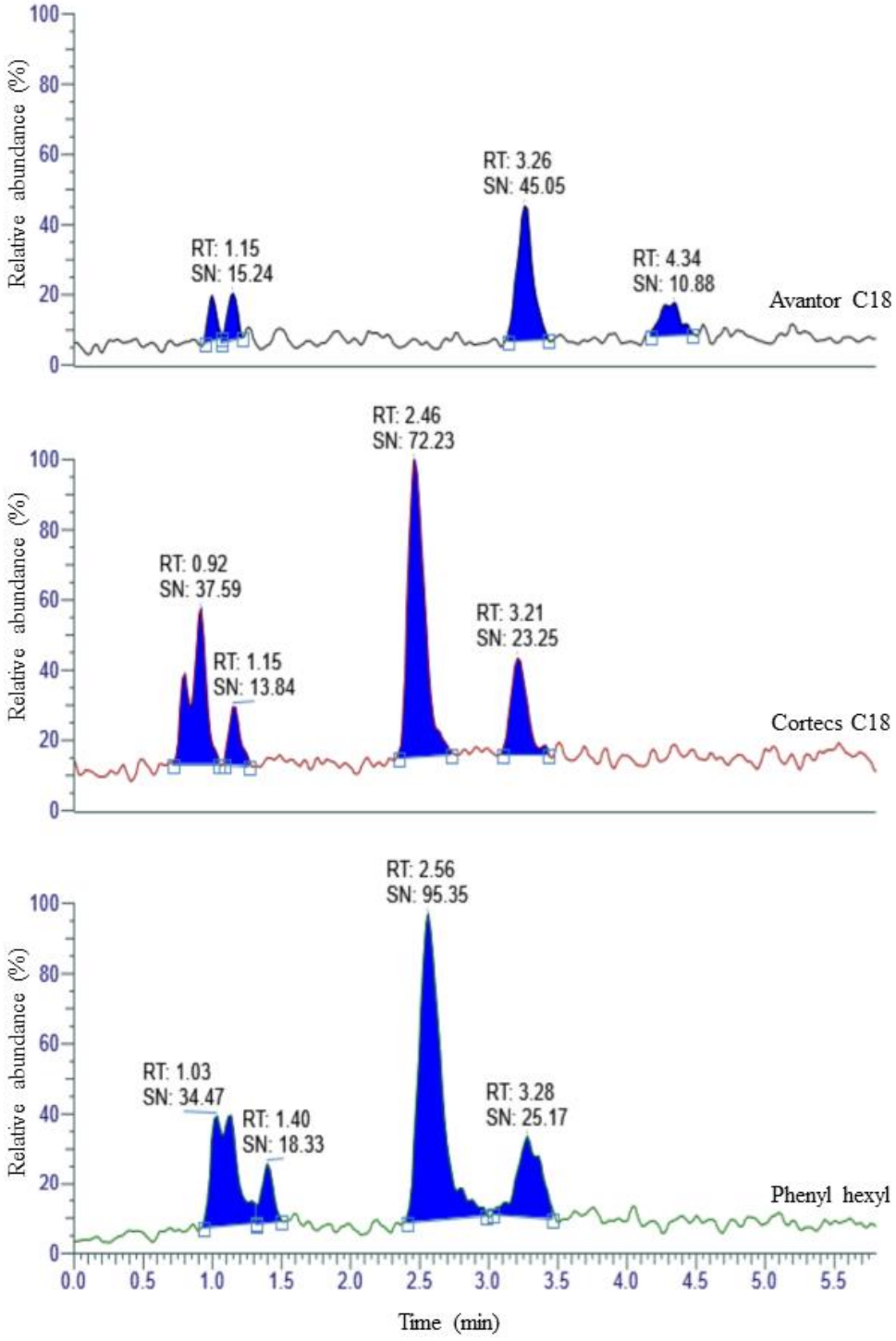

Figure 24. Chromatograms that demonstrate the influence of the stationary phase on the retention of HC-analytes. The chromatograms show the relative abundance of the analytes *m/z* in percentage (*y*-axis) as a function of retention time in minutes (*x*-axis). The chromatograms were obtained through the analysis of a HC-standard solution containing all HC-analytes with a total concentration of 5 μg/mL dissolved in 50:50 MeOH:Water + 0.1 % FA in MRM mode (*m/z* 367.2 → 90.9, *m/z* 367.2 → 104.9) on an Avantor C18 column, a Cortecs C18 column and an Avantor SuperPhenyl hexyl column. The analysis was conducted using isocratic elution of a mobile phase consisting of 40 % IPA and 60 % water + 0.1 % FA. The chromatograms are normalized (fixed scale).

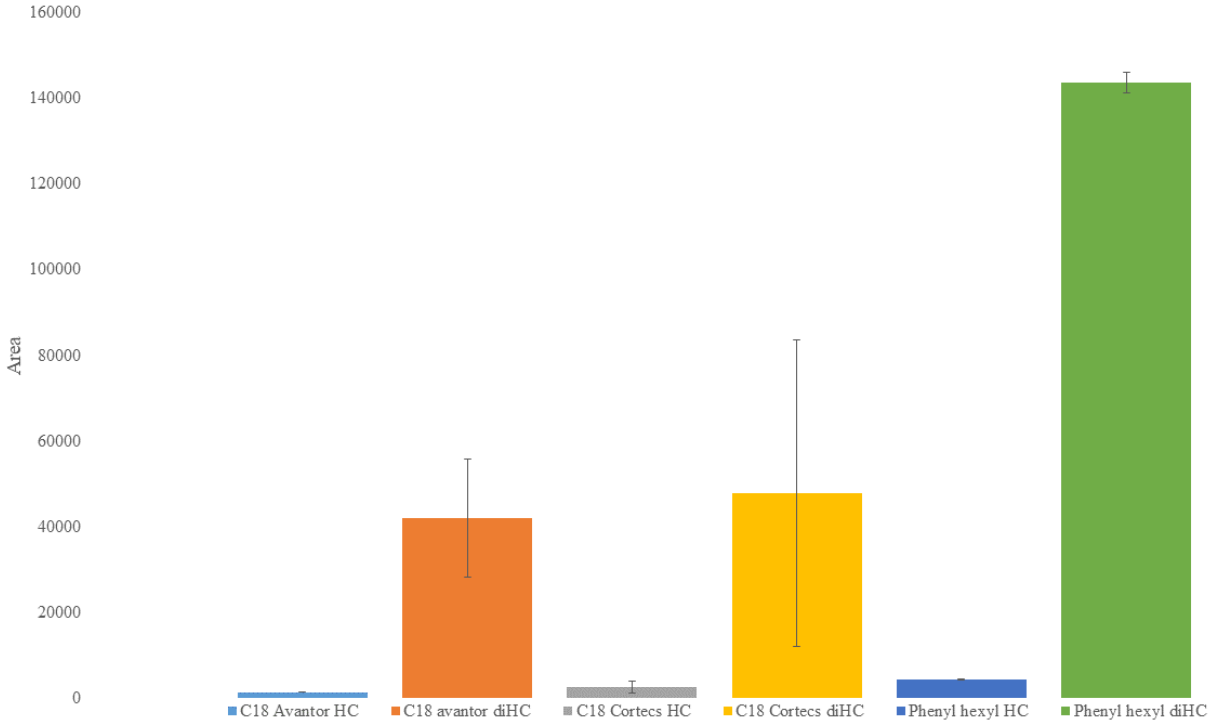

Figure 25. The bar chart displays the average area and standard deviation resulting from the injection of a standard solution containing all analytes at a total concentration of 10 µg/mL dissolved in 50:50 MeOH:Water + 0.1 % FA in MRM mode (*m/z* 367.2 → 90.9, *m/z* 367.2 → 104.9 for HC and *m/z* 383 → 90.9, *m/z* 383 → 104.9 for diHC) on an Avantor C18 column, a Cortecs C18 column and an Avantor SuperPhenyl hexyl column. The analysis was performed using isocratic elution of a mobile phase consisting of 40 % IPA and 60 % water + 0.1 % FA. The data presented in the chart is based on three replicates (n = 3).

The figures above shows that the HC-analytes provided little to no signal compared to the diHC-analytes. This may be due to HCs having one less hydroxy-group, thus being harder to ionize than the group of diHC. This problem has not been discussed in existing literature, as oxysterols often are derivatized in advance of analysis. Previous research has focused on the secretion of HC from organoids, as it has been more difficult to obtain good signals from diHC with derivatization [36]. Contrarily, underivatized diHCs provided better signals than HCs. After this realization the study would continue focusing on diHCs as analytes.

The analyte group of HCs were excluded from the rest of the studies as they were hard to ionize. Thus, the method development continued focusing on the analyte group of diHCs.

4.4 Stationary phase optimization for enhanced signal

Three different stationary phases were examined to achieve the best possible coelution of the analytes. The columns were two Avantor ACE columns (2.1 mm x 5 cm) packed with respectively UltraCore 2.5 SuperPhenyl Hexyl (2.5 μm) and UltraCore 2.5 SuperC18 (2.5 μm), and a Cortecs Premier column (2.1 mm x 5 cm) packed with C18 (2.7 μm). The analytes are relatively hydrophobic with four characteristic cholesterol ring-structures. The C18 packing uses hydrophobic interactions to retain the analytes [49, p. 71], while the phenyl hexyl is less hydrophobic and retains analytes based on other interactions like pi-pi. Therefore, it was expected that the C18 packing better retained the analytes than phenyl hexyl. **Figure 26** compares the three stationary phases examined.

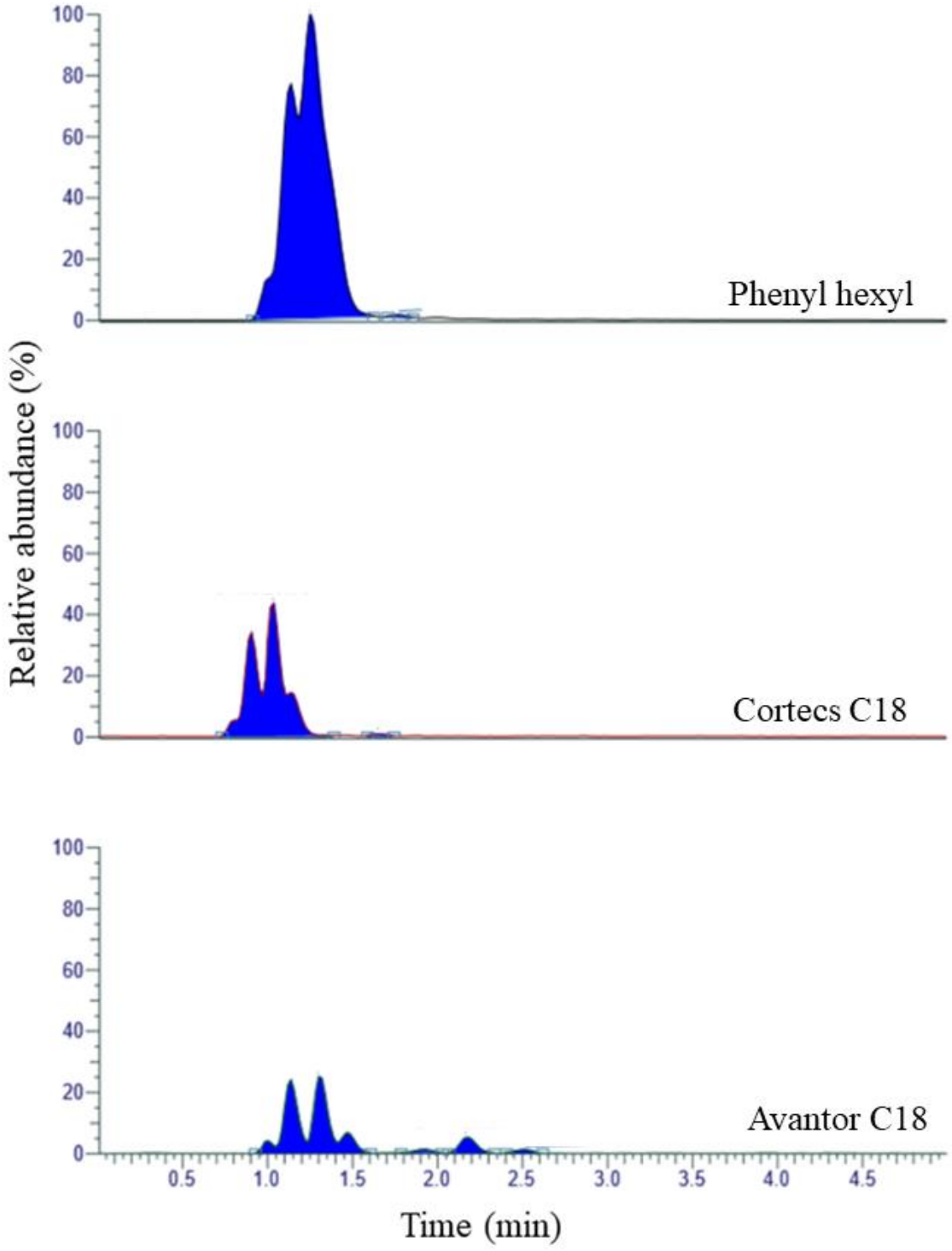

Figure 26. Chromatograms that demonstrate the influence of the stationary phase on the signal intensity of diHC-analytes. The chromatograms show the relative abundance of the analytes *m/z* in percentage (*y*-axis) as a function of retention time in minutes (*x*-axis). The chromatograms were obtained through the analysis of a diHC-standard solution containing all diHC-analytes with a total concentration of 5 μg/mL dissolved in 50:50 MeOH:Water + 0.1 % FA in MRM mode (*m/z* 383 → 90.9, *m/z* 383 → 104.9) on an Avantor C18 column, a Cortecs C18 column and an Avantor SuperPhenyl hexyl column. The analysis was conducted using isocratic elution of a mobile phase consisting of 40 % IPA and 60 % water + 0.1 % FA. The chromatograms are normalized (fixed scale) for comparison.

The chromatograms above suggest that greater coelution equals higher signal intensity. The signal provided by phenyl hexyl is 3 times higher than the Cortecs C18, and almost 5 times higher than the super C18. None of the two C18 columns led to sufficient coelution which could explain the low signal intensity.

Having access to more data would have helped deciding the best suited stationary phase. For example, testing the different columns with alternative mobile phase compositions. Different ratios of IPA:Water were the only mobile phase composition tested for all three stationary phases. The results for the C18 columns could have been better using other mobile phases. Unfortunately, there was not enough time to further research the alternative stationary phases. Phenyl hexyl provided better signals and less noise than C18 and was for this reason the best alternative, based on the available results.

Phenyl hexyl proved to be the stationary phase best suited for detection of underivatized oxysterols providing highest signal intensity and coelution of the analytes.

4.5 Optimizing the retention time of the analytes using IPA as organic modifier and phenyl hexyl as stationary phase

To optimize the retention time of the analytes, it is essential to determine the appropriate amount of organic modifier to achieve coelution, along with selecting the suitable elution mode for proper retention time. Additionally, it is important to select the mobile phase composition that yields the highest signal intensity, given the high detection limits associated with underivatized oxysterols. This is discussed in the following sections.

4.5.1 Retention time and coelution of dihydroxycholesterol are dependent on the percentage of isopropanol in mobile phase

The optimization of different parameters was crucial to enhance the signal intensity of underivatized oxysterols, which are poorly ionizable. Coeluting the analytes to enhance the signal offered a potential solution to overcome the high limits of detection. By achieving coelution in an on-line system, it would be possible to obtain fingerprints from the steatotic organoids. It is worth mentioning that this approach cannot be employed to investigate the

biological aspects of NAFLD. The coelution of the analytes depends on the retention time, which is influenced by the composition of the mobile phase.

The combination of IPA and Water (+ 0.1 % FA) provided the greatest signal intensities and was therefore the natural choice as mobile phase. The ratio of IPA and Water had to be optimized to achieve coelution of the analytes. **Figure 27** illustrates how the retention time of one of the analytes (7b, 25-diHC) is dependent of the percentage of organic modifier in the mobile phase, in this case IPA. **Figure 28** shows how the different percentages of IPA in the mobile phase affects the retention time by chromatograms obtained by analysis of diHC-analytes. **Figure 29** displays how the average area increases with the increasing amount of IPA in the mobile phase.

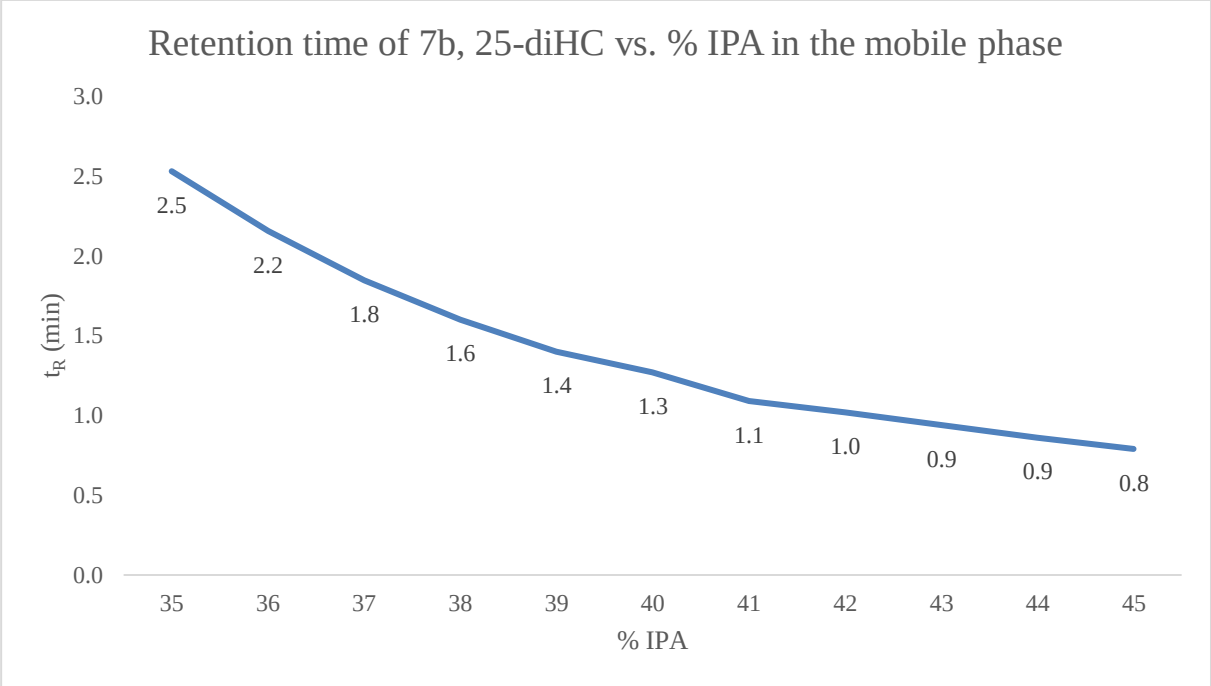

Figure 27. Illustration of how the retention time of 7b, 25-diHC (y-axis) is dependent on the % IPA in the mobile phase (x-axis). The results are obtained by analysis of a standard solution containing all diHC-analytes at a total concentration of 5 µg/mL dissolved in 50:50 MeOH:Water + 0.1 % FA in MRM mode (m/z 383 → 90.9, m/z 383 → 104.9) on a phenyl hexyl stationary phase. The analysis was performed using isocratic elution of the mobile phase consisting of different percentages of IPA with water and 0.1 % FA. The data presented is based on two replicates (n = 2).

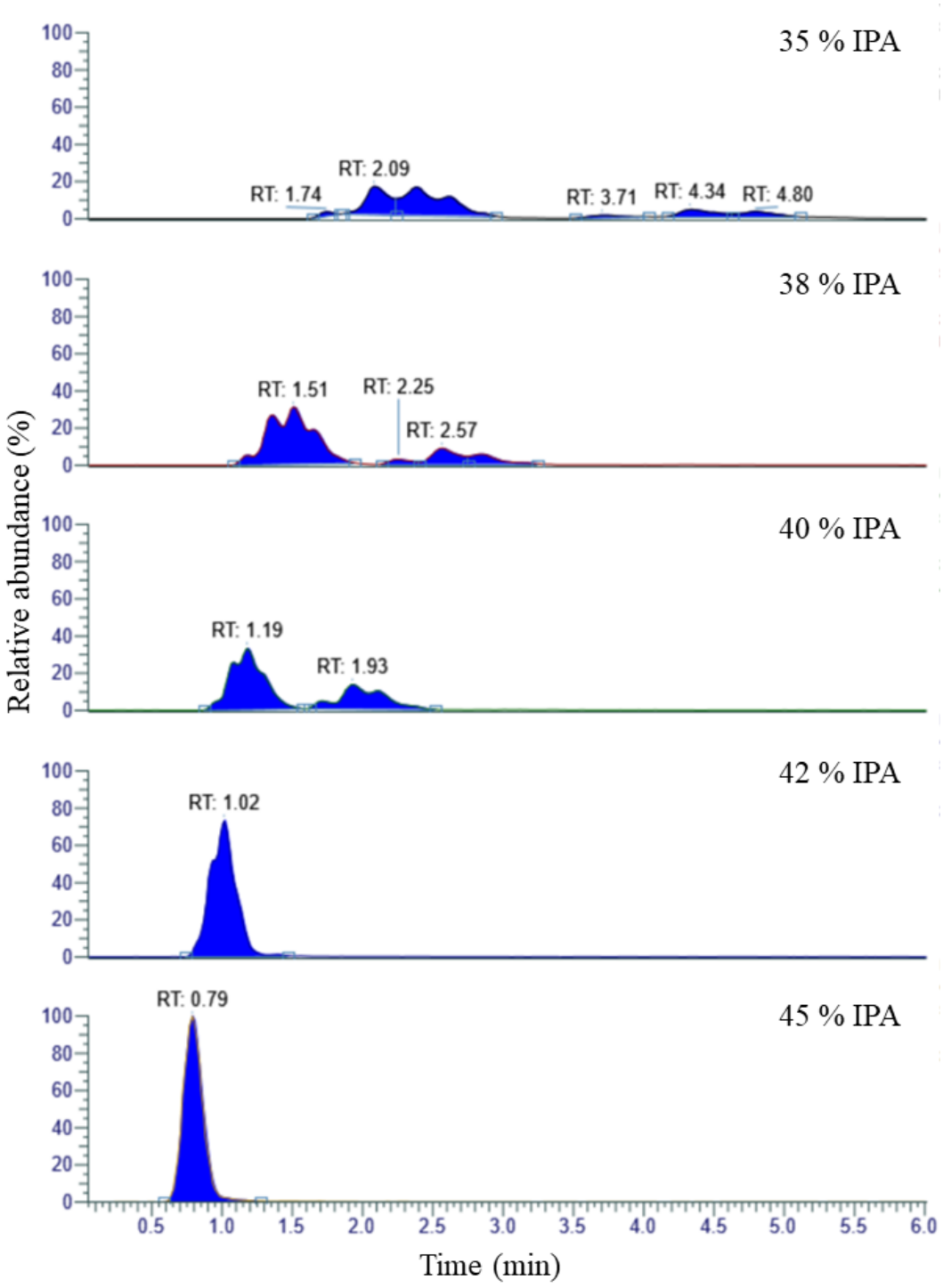

Figure 28. Representative chromatograms that demonstrate the influence of the amount of organic modifier on the retention time of the diHC-analytes. The chromatograms show the relative abundance of the analytes *m/z* in percentage (*y*-axis) as a function of retention time in minutes (*x*-axis). The chromatograms were obtained through the analysis of a standard solution containing all diHC-analytes with a total concentration of 5 μg/mL dissolved in 50:50 MeOH:Water + 0.1 % FA in MRM mode (*m/z* 383 → 90.9, *m/z* 383 → 104.9).

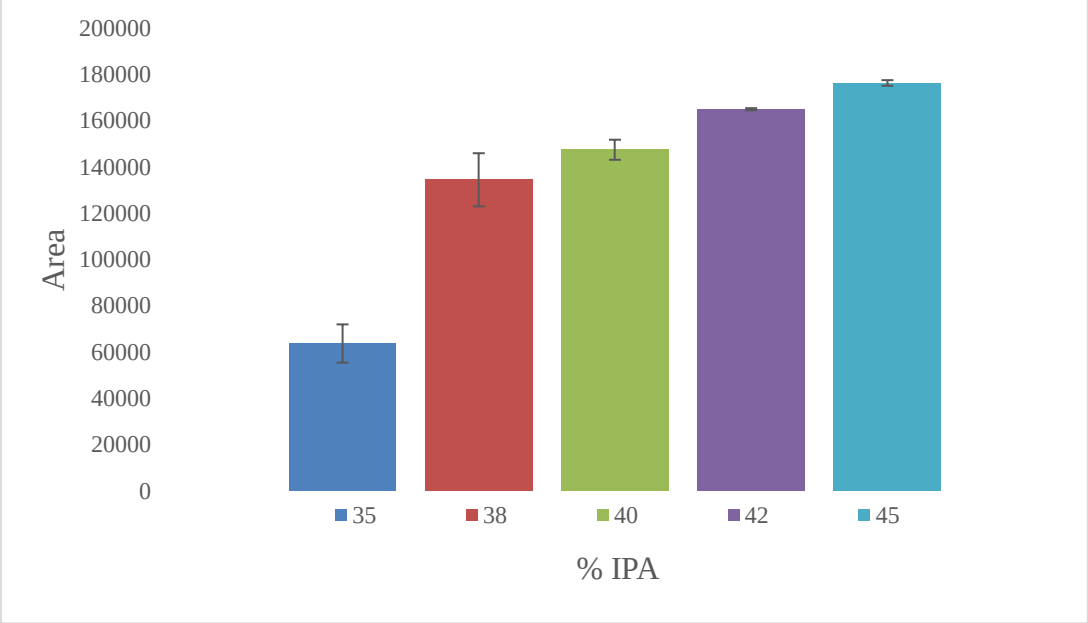

Figure 29. Bar chart displaying the average area and standard deviation resulting from the injection of a standard solution containing all diHC-analytes at a total concentration of 5 µg/mL dissolved in 50:50 MeOH:Water + 0.1 % FA with different percentages of IPA in the mobile phase. The analysis was performed in MRM mode using 0.1 % FA in the mobile phase as pH control. The data presented in the chart is based on three replicates for 35, 38 and 40 % IPA (n = 3), and two replicates for 42 and 45 % IPA (n = 2).

Figure 28 demonstrates that achieving coelution required a mobile phase containing more than 40 %. However, this composition failed to provide adequate retention of the analytes. On the other hand, mobile phase compositions that provided sufficient retention of the analytes, such as 35 % IPA, resulted in separation of the analytes. **Figure 29** illustrates how the signal intensity increased with the increasing percentage of IPA in the mobile phase. It was crucial to both retain the analytes adequately and achieve coelution, which appeared to be unattainable using isocratic elution. Consequently, the challenge prompted the exploration of isocratic segments as a potential solution.

4.5.2 Isocratic segments provide both coelution and retention of the analytes

Coelution and retention of the analytes proved to be a challenge with the use of isocratic elution. The combination of 45 % IPA and 55 % water led to the sharpest peaks and coelution of all diHC-analytes. However, with this mobile phase composition the analytes had close to no retention – eluting in less than a minute (0.8 min).

By utilizing isocratic segments, the retention time of the analytes could be adjusted while maintaining sharp peaks [57]. **Figure 30** illustrates the optimized isocratic steps for proper retention of the analytes and the functions of the different steps: dwell time, elution, wash, and re-equilibration. **Figure 31** shows how the use of isocratic steps enabled both coelution and retention of the analytes, unlike isocratic elution which did not give proper retention.

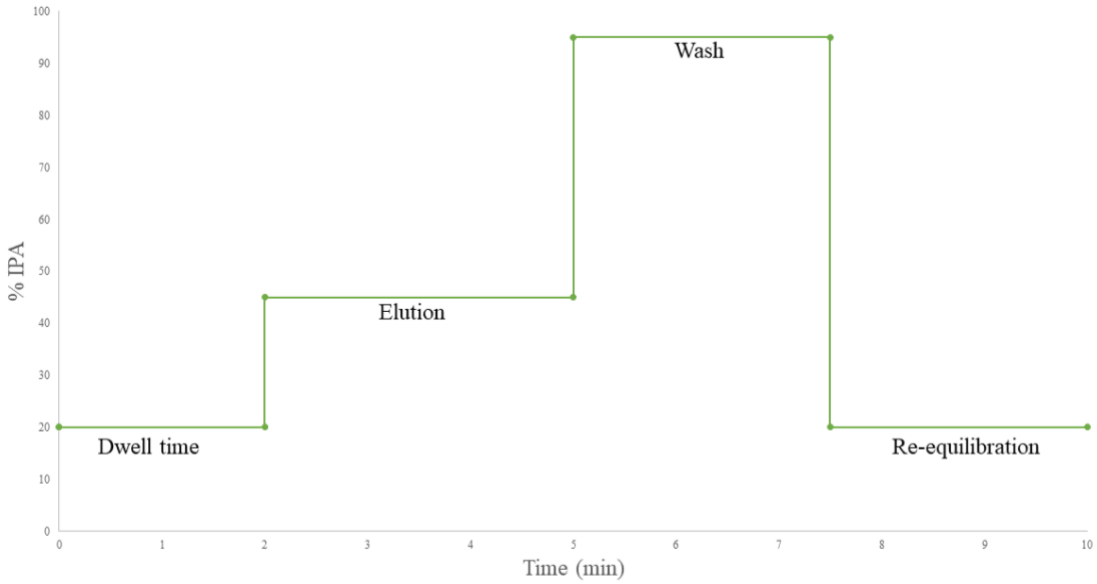

Figure 30. Illustration of the mobile phase composition in the isocratic steps that yielded both coelution and appropriate retention of the analytes. The isocratic steps are defined by dwell time (20 % IPA), elution (45 % IPA), wash (95 % IPA) and re-equilibration (20 % IPA).

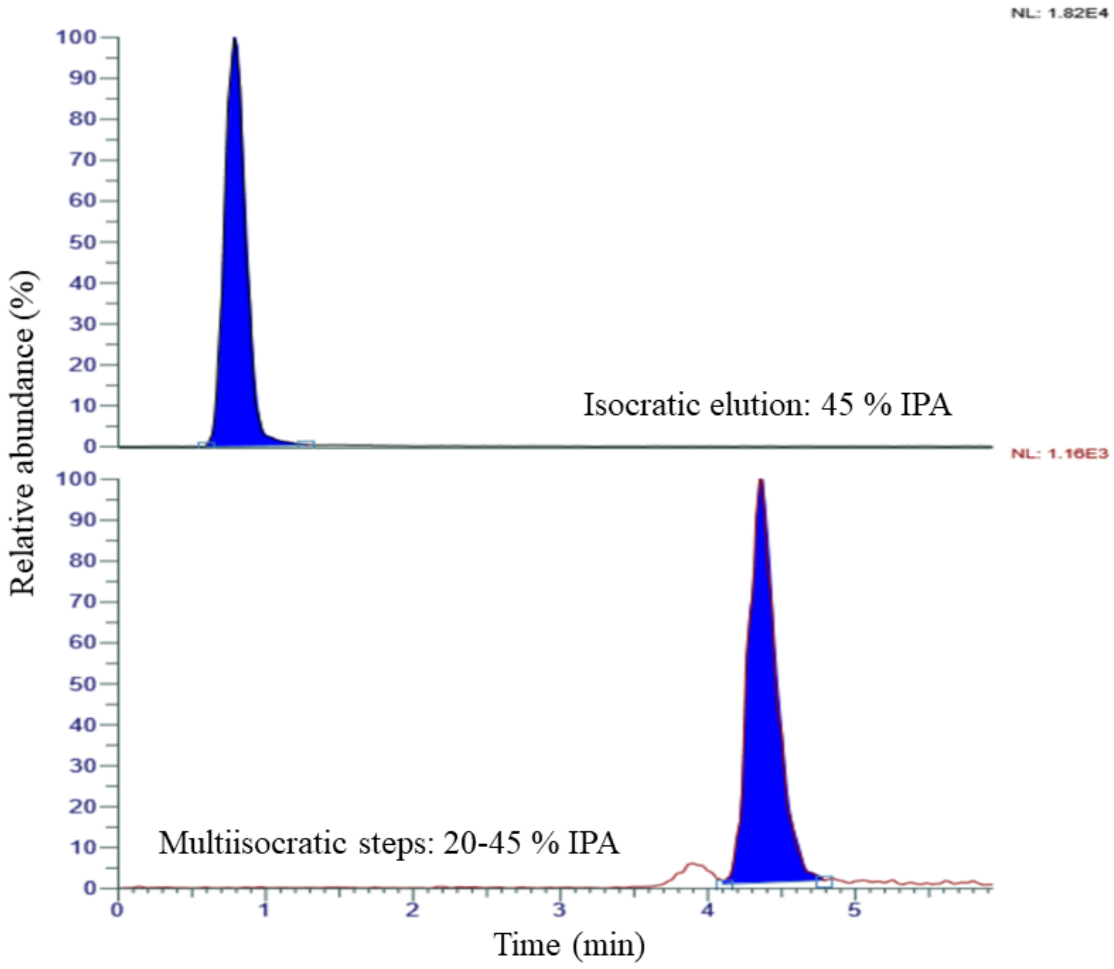

Figure 31. Chromatograms representative for the diHC-analytes dissolved in 50:50 IPA:Water + 0.1 % FA (m/z 383 → 90.9, 383 → 104.9) performing isocratic elution and multi-isocratic elution respectively, illustrating how the peak is moved and the retention time is changed using multi-isocratic steps. The difference in signal intensity is caused by different concentrations of the standard solutions used, 10 μg/mL and 0.1 μg/mL.

As seen in **Figure 31**, the use of multi-isocratic steps with 20-45 % IPA instead of isocratic elution with 45 % IPA, elongated the retention time of the diHC analytes from 0.79 min to 3.92 min. The use of multi-isocratic steps with a mobile phase consisting of 20-45-95-20 % IPA was determined to be a good fit for the analytes considering retention time and coelution. The use of multi-isocratic steps was optimized using LC-MS.

The highest signal intensity, as well as the optimal retention time and coelution of the analytes, were attained by employing multi-isocratic steps with a mobile phase composition of 45 % IPA.

4.6 Linearity between signal and injection volume

During the method development, different injection volumes of standard solutions were examined. The injection volume of the sample has a linear impact on the peak height [60]. Increasing the sample volume for injection could assist in addressing the high limits of detection of the underivatized oxysterols. Injection volumes ranging from 1 μL to 5 μL were examined. The use of OiC imposes limitations on the injection volume due to a flow rate of 15 μL/hour. Employing larger volumes would result in excessively long injection time. **Figure 32** demonstrates the linear relationship between the increase in injection volume and the corresponding peak area.

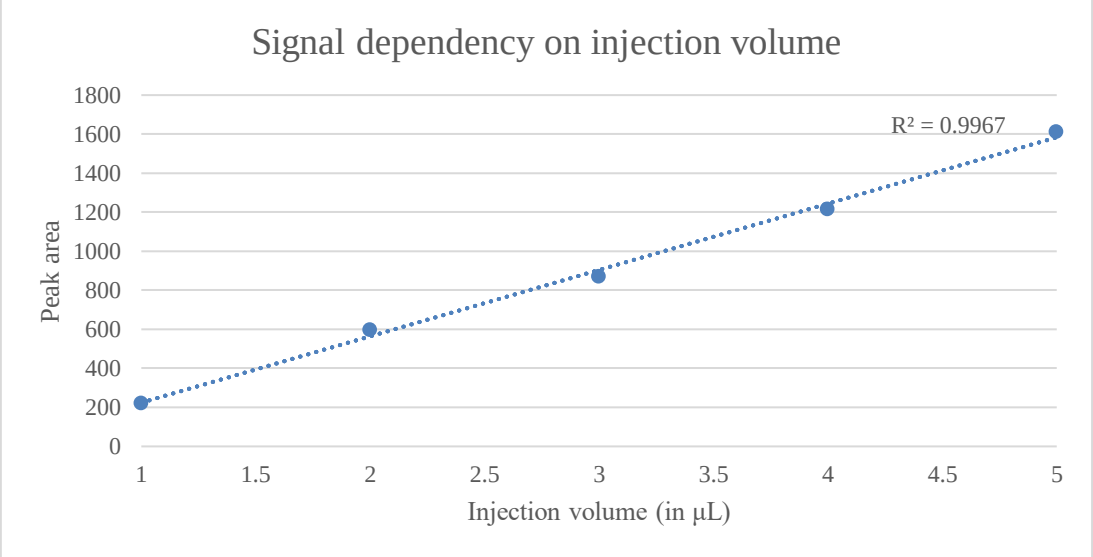

Figure 32. Illustrates how the increase in injection volume (x-axis) leads to a linear increase in the peak area (y-axis). The average peak area of the different injection volumes are obtained by analysis of a standard solution of all diHC-analytes at a total concentration of 0.01 μg/mL dissolved in 50:50 IPA:Water + 0.1 % FA. The analysis was performed in MRM mode (m/z 383 → 90.9, 383 → 104.9). The stationary phase used was phenyl hexyl, the mobile phase was consisting of 40 % IPA and 60 % water added 0.1 % FA performing isocratic elution with a flow of 0.400 mL/min. The data presented is based on three replicates (n = 3).

As illustrated in **Figure 32**, the highest injection volume (5 μL) provided the signal of highest intensity. The analysis of the standards injecting different volumes confirmed the fact that the relationship between the injection volume and peak area is linear. It is worth mentioning that the standards were solved in 50:50 IPA:Water, meaning that the content of organic modifier was higher in the injected sample than in the mobile phase. This is not ideal as it leads to dilution of the sample [49, p. 52]. However, this was chosen to be sure the hydrophobic oxysterols were dissolved in the solution.

The injection volume of 5 µL was selected as it offered the highest signal intensity while remaining compatible with the OiC-system.

4.7 Analysis of diHC in cell medium: loss of signal intensity

The experimental parameters of the method was optimized with the use of standard solutions of oxysterols dissolved in 50:50 IPA:Water with 0.1 % FA. The sample matrix when using the OiC-system with liver organoids is cell medium. To ensure that the method would work using OiC, cell medium was spiked with the diHC-analytes and analyzed by the method developed. Surprisingly, no signal was observed in the spiked samples. This may have been caused by an interference from the matrix. To solve this, attempts to remove the matrix interferences was examined in the off-line approach.

4.7.1 SPE of diHC from cell medium

SPE was conducted following the procedures outlined in section 3.4.1 to investigate whether the absence of signal from standards in cell medium was due to interferences in the matrix. Additionally, Procedure 1 and 3 were performed on standard solutions of diHC in IPA:Water, without cell medium, to verify the effectiveness of the SPE method for extracting the analytes. The standards in cell medium did not yield any detectable signal. However, it was confirmed that the different SPE procedures were successful, as evidenced by the eluate from the standard solutions in IPA:Water producing signals. Further examination revealed that when the diHC-analytes were dissolved in 50:50 IPA:Cell medium and 10:90 IPA:Cell medium, the eluate yielded signals. The average peak area and relative standard deviation resulting from these analyses are presented in **Table 10**.

Table 10. Overview of the average area and relative standard deviation obtained through analysis of 0.1 µg/mL diHC-analytes dissolved in 50:50 IPA:Cell medium and 10:90 IPA:Cell medium after SPE in MRM mode (m/z 383 → 90.9, 383 → 104.9).

0.1 ug/mL diHC-analytes dissolved in	**Average area**	**RSD (%)**
50:50 IPA:Cell medium	24553,4	11,7
10:90 IPA:Cell medium	14526,1	18,5

The SPE procedures did not work in enhancing the signal from diHC-analytes in cell medium. None of the SPE procedures from cell medium provided signal of diHC-analytes. The SPE procedure was successful when the diHC-analytes were solved in either 50:50 IPA:Cell medium or 10:90 IPA:Cell medium. The addition of IPA to cell medium was important, leading to the question of whether the analytes were being solved in the cell medium or if they got adsorbed to the wall of the vials and Eppendorf tubes.

4.7.2 DiHC adsorbs to the wall of the vial when dissolved in cell medium

Due to the lack of signal from analyte in cell medium, it was hypothesized that the hydrophobic analytes adsorbed to the surface of the Eppendorf tubes and vials. To examine this, standards of diHC were first diluted in cell medium to a total volume of 200 μL. After one hour, the solution was removed from the tube. Subsequently, 200 μL of IPA was added to the Eppendorf tube. After another hour, the solution was diluted by adding 200 μL of water. LC-MS analysis was performed on both the cell medium collected after one hour and the solution of IPA:Water. This procedure was conducted for solutions with diHC concentrations of 1.0 and 0.1 μg/mL, results presented in **Figure 33** and **Figure 34**.

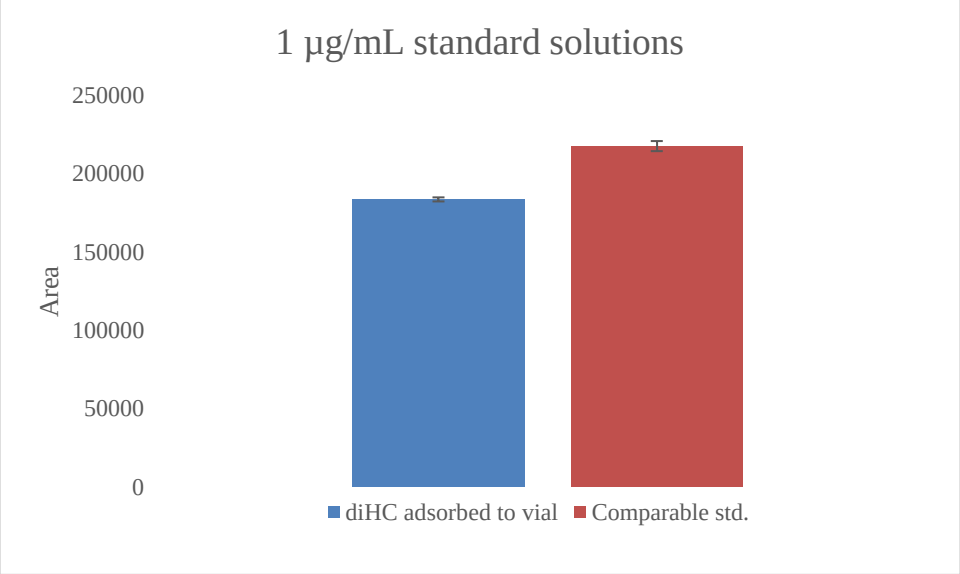

Figure 33. The average area and standard deviation resulting from the injection of a standard solution of 1 µg/mL diHC from the vial-procedure compared to the signals from a standard solution of 1 µg/mL diHC dissolved in 50:50 IPA:Cell medium. The analysis was performed in MRM mode (m/z 383 → 90.9, 383 → 104.9). The data presented in the chart are based on three replicates (n=3).

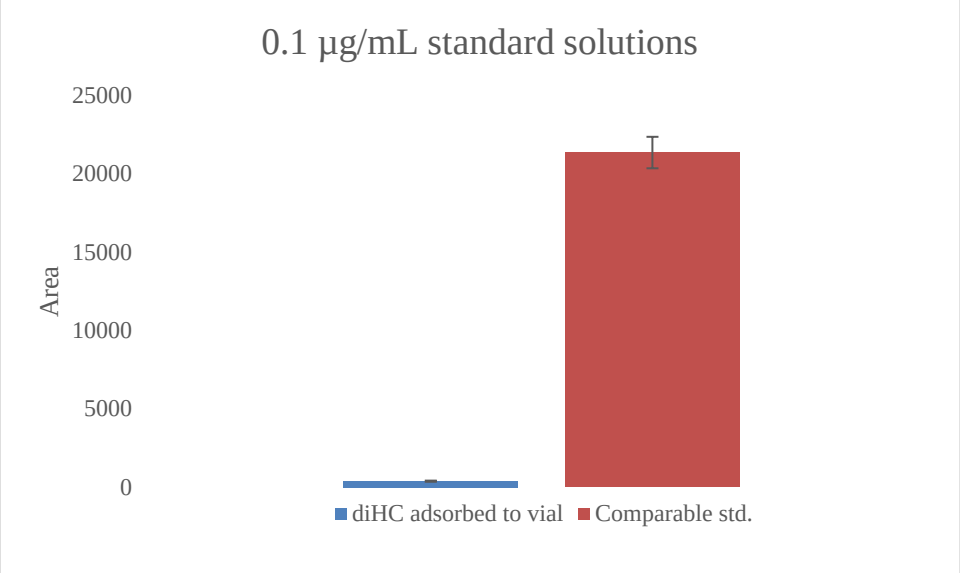

Figure 34. The average area and standard deviation resulting from the injection of a standard solution of 0.1 µg/mL diHC from the vial-procedure compared to the signals from a standard solution of 0.1 µg/mL diHC dissolved in 50:50 IPA:Cell medium. The analysis was performed in MRM mode (m/z 383 → 90.9, 383 → 104.9). The data presented in the chart are based on three replicates (n = 3).

The solution from the vial examination provided signals up to 84 % compared to the standard solution in IPA:Cell medium with the same concentration. The procedure was also performed on a solution of a lower concentration (0.1 μg/mL), as seen in **Figure 34**. This solution did only provide signal up to 2.5 % compared to the standard solution in IPA:Cell medium with the same concentration. Yet, it was clear that a significant amount of the analytes would adsorb to the wall of the Eppendorf tube and vials reading the signals provided from the solutions.

The solubility of the analytes in different matrices could be an explanation to why they would adsorb to the wall of the vials and Eppendorf tubes. The analytes are hydrophobic and easily solved in a nonpolar organic solvent like IPA, thus providing proper signals from LC-MS analysis. In contrast, cell medium is a relatively polar solvent, consisting mainly of water. The vials and Eppendorf tubes used for the solutions are made of polypropylene, a plastic polymer. As the analytes are hydrophobic, they will not have the same solubility in cell medium as in an organic solvent. The analytes attraction to the hydrophobic container of polypropylene could be an explanation to the lack of signal when analyzing diHC dissolved in cell medium.

Sample clean-up using off-line SPE had no effect on the signals provided from the spiked cell medium. Adding IPA to the sample ahead of analysis, thus solving the analytes in a nonpolar solvent, could be a possible solution to achieve proper signals from diHC in cell medium.

However, when the OiC-system is introduced the use of vials or Eppendorf tubes will not be necessary, as the sample generation occurs on-line in the OiC.

The lack of signal from the analytes in cell medium was caused by the analytes adsorbing to the wall of the Eppendorf tube and vials.

4.8 Overview of the method developed with LC-MS

A method for detection of underivatized oxysterols was developed using LC-MS. The experimental conditions of the optimized method are included in **Table 11**. This method uses isocratic segments as described in section 4.5.2.

Table 11. Overview of the parameters in the method developed for detection of underivatized oxysterols with LC-MS.

Parameter	
Injection volume	5 μL
Flow	400 μL/min
Elution mode	Multi-isocratic steps
Mobile phase composition	20-45-95-20 % IPA, 80-55-5-80 % Water
pH control	0.1 % FA
Column	UltraCore 2.5 SuperPhenyl Hexyl (2.5 μm) (2.1 mm x 5 cm)
Column temperature	40 ℃

The method was optimized using standard solutions with concentrations of 10 μg/mL diHC. It was eventually tested with standard solutions of lower concentrations. **Figure 35** illustrates how the signal intensity relates to the concentration of standard solutions.

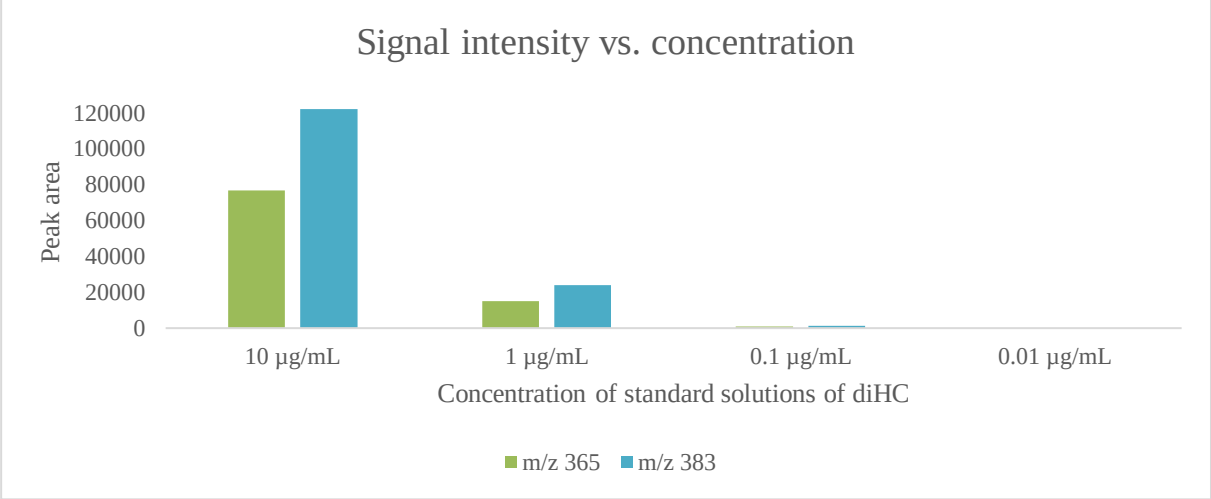

Figure 35. Illustration of how the peak area of the signals relate to the concentration of the standard solutions from 10 µg/mL down to 0.01 µg/mL with an injection volume of 1 µL.

As illustrated by **Figure 35**, the detection limit (LOD) was approximately 0.01 μg/mL. This concentration provided a weak signal when injecting 1 μL. This was better illustrated in section 4.6, where an injection volume of 5 μL of a standard solution of 0.01 μg/mL provided sufficient signal from the analytes.

4.9 Introducing sample clean up by AFFL-SPE-LC-MS

As the matrix of cell medium could contain potential interferences, salts and proteins, an automated filtration and filter flush solid phase extraction (AFFL-SPE) was included in the instrumentation. AFFL-SPE prior to LC-MS secures robust analysis through the removal of particles by filtration [61]. This added complexity to the system, and the use of isocratic steps did not work as indented concerning retention time, signal from the analytes, carry-over, and unwanted signals. The amount of IPA in the elution step was increased to 60 %, as an attempt to achieve coelution and proper signals, illustrated in **Figure 36**. Using isocratic segments with AFFL-SPE-LC-MS, unwanted signals in the blank runs became an issue. This was assumed to be carry-over from the previous injection and several blanks was injected, illustrated in **Figure 37** and **Figure 38**.

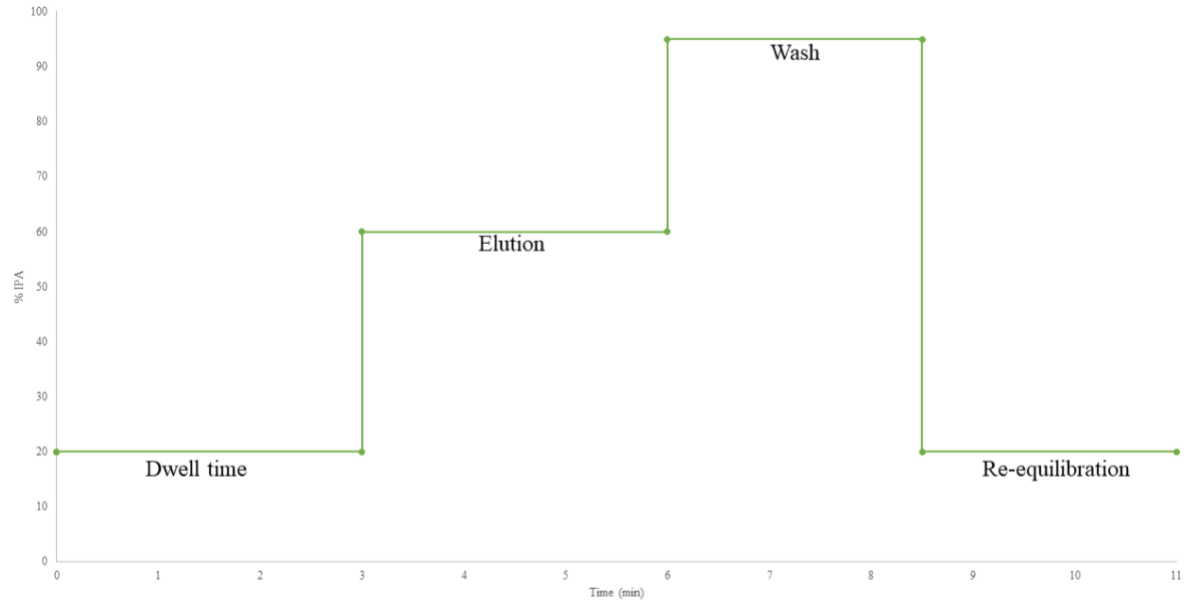

Figure 36. Illustration of the mobile phase composition in the isocratic steps used with LC-MS in combination with AFFL-SPE. The isocratic steps are defined by dwell time (20 % IPA), elution (60 % IPA), wash (95 % IPA) and re-equilibration (20 % IPA).

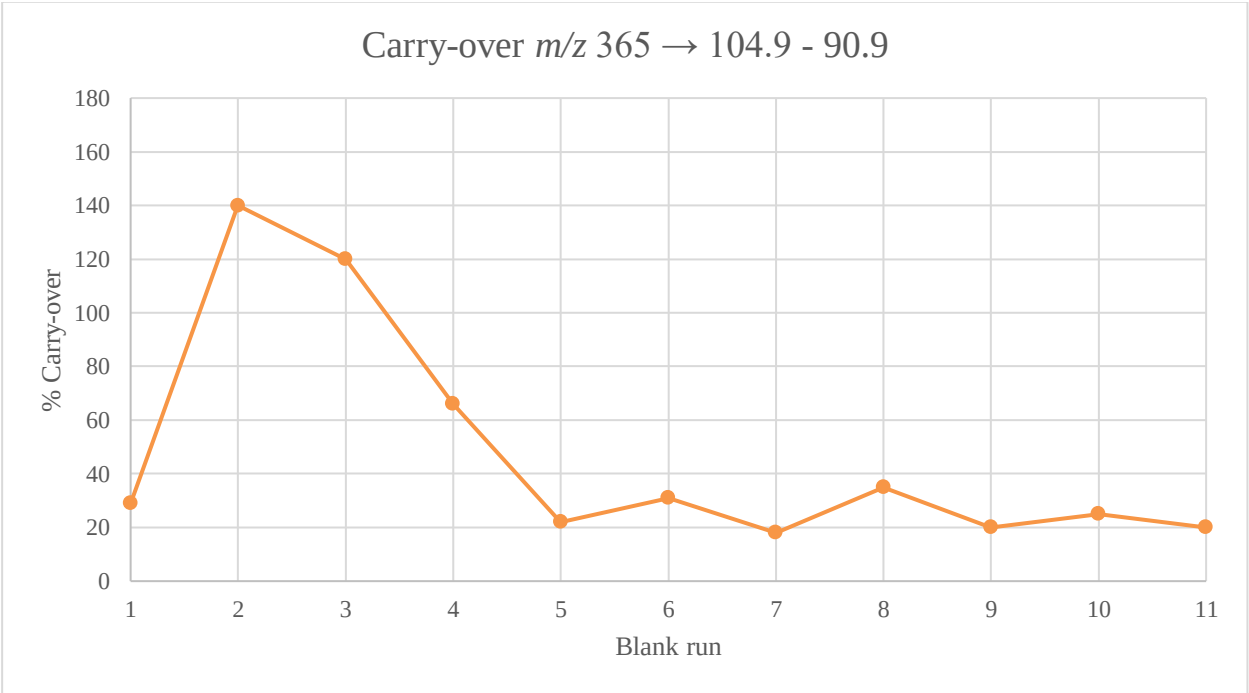

Figure 37. The carry-over in % of m/z 365 → 104.9 and 365 → 90.9 after 1 to 11 blank runs.

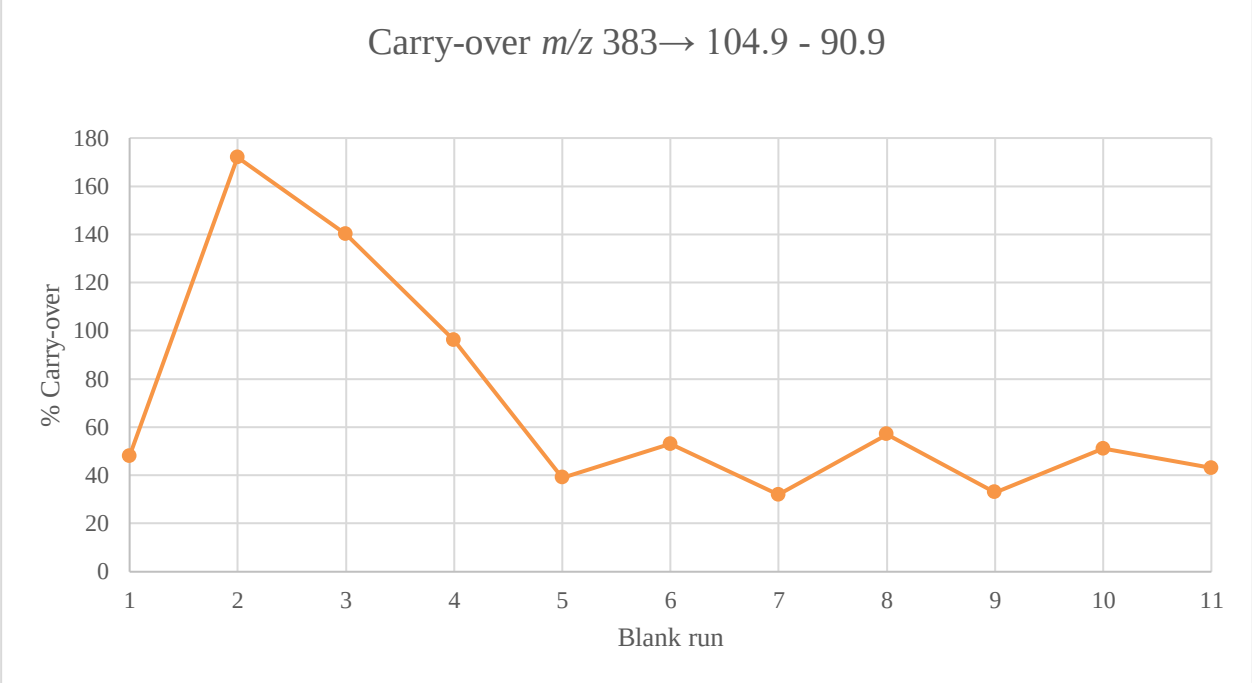

Figure 38. The carry-over in % of m/z 383 → 104.9 and 383 → 90.9 after 1 to 11 blank runs.

As seen in **Figure 37** and **Figure 38**, the signals from blank 2 and 3 were even higher than from the previously injected standard solution of 0.1 μg/mL diHC. The intensity did not decrease as expected in the case of carry-over. As the signals in the blanks did not disappear after numerous runs and extensive washing, different approaches were carried out to localize the root of the unwanted signals. This included washing for twice as long, changing columns, washing the column and system with chloroform, changing the tubing, and preparing new mobile phases. The signals did not change. The AFFL-system was disconnected from the system without affecting the signals. The MS was set in full scan mode to examine if the signals could be caused by other compounds eluting within the retention window, shown in **Figure 39**.

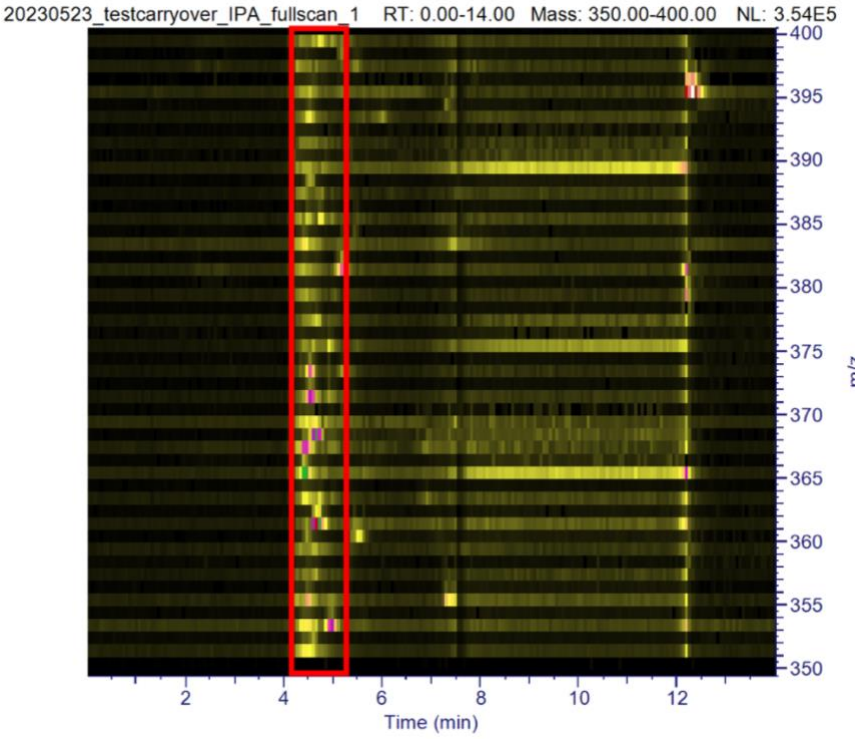

Figure 39. Map view from a full scan from m/z 350 to 400 of a blank injection with time in minutes at the x-axis and m/z at the y-axis, the retention window is marked with a red square. The abundance in percent is illustrated by colors: black = 0 %, yellow = 20 %, pink = 40 %, green = 60 %, red = 80 % and white = 100 %.

The map view of the full scan reveals that multiple ions elute within the same retention window as the analytes, indicating that the detected signals may originate from the matrix and wash step rather than the standard solutions. Isocratic steps were not feasible due to the inability to eliminate these signals. Sudden changes in the organic modifier level could potentially impact the ionization and result in undesired signals. Therefore, alternative elution modes needed to be explored as the next course of action.

4.9.1 Optimizing the method on AFFL-SPE-LC-MS using gradient elution

Gradient elution was examined as solution to avoid unwanted signals when using multi-isocratic steps. As the unwanted signals had the same retention time as the analytes, it was important to make them elute at a different time than the analytes. Different gradients were examined, all starting at 20 % going up to 50-90 % IPA over 4-5 minutes. The gradient illustrated in **Figure 40** yielded sufficient retention of the analytes and moved the unwanted signals from the analyte's retention time. **Figure 40** illustrates the effect of the gradient on the analysis of a standard solution of diHC.

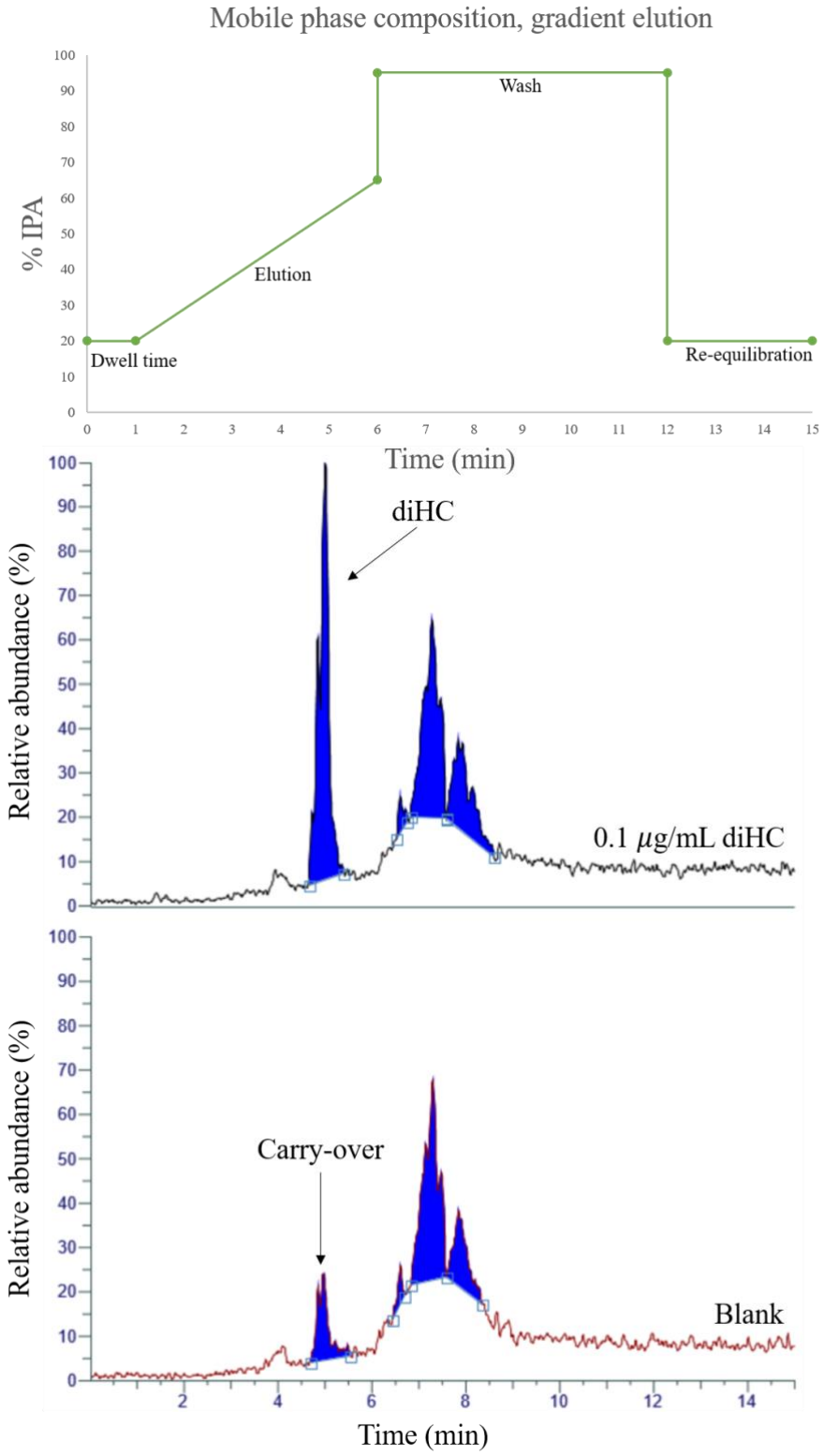

Figure 40. An overview of the mobile phase composition in gradient elution using 20-65 % IPA, accompanied by chromatograms obtained by analysis of a standard solution of 0.1 µg/mL diHC dissolved in 50:50 IPA:Water + 0.1 % FA and the following blank injection. The chromatograms show the relative abundance of the m/z in percentage (y-axis and the retention time in minutes (x-axis). The signals were obtained in MRM mode (m/z 383 → 90.9, 383 → 104.9). The chromatograms are normalized (fixed scale).

The considerable amount of carry-over questions the quality of the gradient, as shown in **Figure 40**. Even a washing time twice as long had no effect on this. The carry-over would only be removed by injecting 2-3 blanks. Using this gradient also created more noise leading to a higher limit of detection. Still, it was the only way to remove the unwanted signals described in the previous section.

The use of gradient elution with 20-60 % IPA removed the unwanted signals from the analytes retention time.

4.10 Overview of the method developed with AFFL-SPE-LC-MS

The method described in section 4.8 had to be modified after introducing an on-line automated filtration and filter flush solid phase extraction (AFFL-SPE) to the system. The optimization of the mobile phase composition is described in the previous section (4.9.1). The experimental conditions of the optimized method for detection of underivatized oxysterols are described in **Table 12**.

Table 12. Overview of the parameters in the method developed for detection of underivatized oxysterols with AFFL-SPE-LC-MS.

Parameter	
Injection volume	5 μL
Flow	400 μL/min
Elution mode	Gradient
Mobile phase composition	20-65-95-20 % IPA, 80-35-5-80 % Water
pH control	0.1 % FA
Column	UltraCore 2.5 SuperPhenyl Hexyl (2.5 μm) (2.1 mm x 5 cm)
Column temperature	40 ℃

The method was optimized using standard solutions with concentrations of 0.1 μg/mL diHC. It was eventually tested with standard solutions of lower concentrations. **Figure 41** illustrates how the signal intensity relates to the concentration of standard solutions.

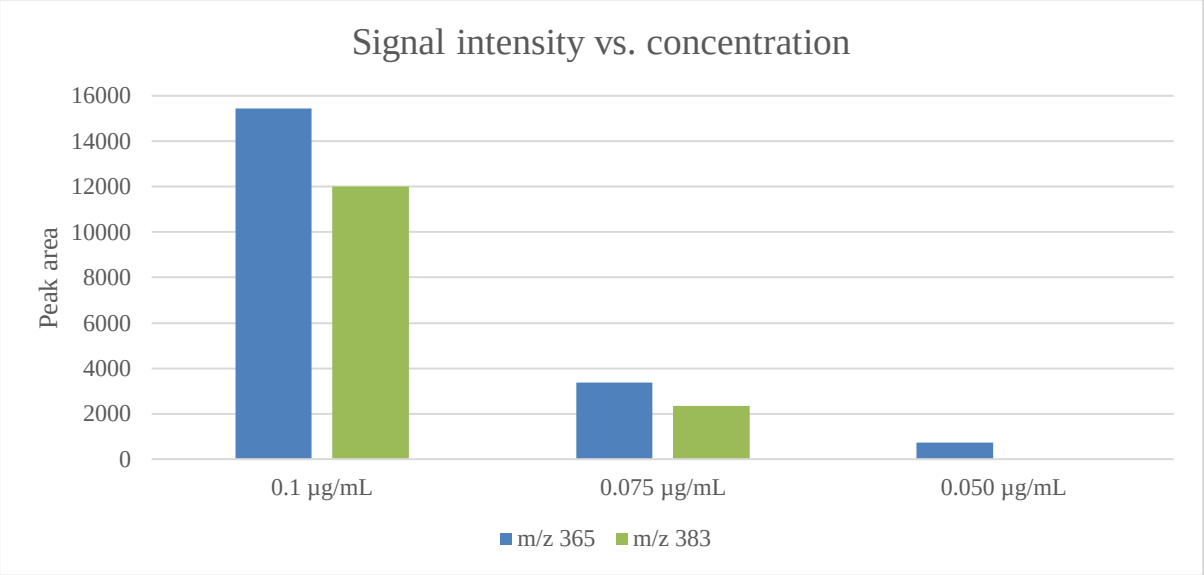

Figure 41. Illustration of how the peak area of the signals relate to the concentration of the standard solutions from 0.1 µg/mL down to 0.050 µg/mL with an injection volume of 5 µL.

The detection limit of the method was 0.050 μg/mL. However, as illustrated in **Figure 41**, only one of two parent ions (*m/z* 383) provided signal. For parent mass *m/z* 383 the detection limit was somewhere between 0.050 μg/mL and 0.075 μg/mL. One concern with this method is the amount of carry-over. An example of the amount of carry-over is shown in **Table 13**.

Table 13. Overview of the average area yielded by injection of a standard solution of 0.075 µg/mL analyzed in MRM mode (m/z 383 → 90.9, 383 → 104.9, m/z 365 → 90.9, 365 → 104.9) and the average carry-over of the signal in percentage.

	m/z 365	*m/z* 383
Average area of 0.075 µg/mL solved in 10:90 IPA:Water	3380	2335
Average carry-over (%)	7	26

As seen in **Table 13**, the carry-over for *m/z* 383 can be rather high as the average value is 26 %. The carry-over was removed after two to three blank runs. As this amount of carry-over is suboptimal, there is a need to develop the method further.

4.11 Analysis of medium from liver organoids

The AFFL-SPE-LC-MS method was used to analyze medium samples obtained from an on-chip experiment conducted by Aleksandra Aizenshtadt (HTH). In order to address the issue of the analytes adsorbing to the container wall, the medium samples were diluted with different amounts of IPA (0, 10 and 50 %) before analysis. As anticipated, none of these samples exhibited any signals for diHC.

The method's detection limit was established as 0.05 μg/mL (equivalent to 120 000 pM), while the estimated concentration of oxysterols in the samples was estimated to be 500 pM. With the discussed method, the sample volume injected was 5 μL. To detect oxysterol levels as low as 500 pM, a sample volume of 1.2 mL would be required (as calculated in Appendix 6.4). However, considering that the OiC-system operates at a flow rate of 15 μL/hour, it would take 80 hours to fill a loop of 1.2 mL. This indicates that the detection limits achieved with the developed method are not compatible with the OiC-system.

The developed method utilizing AFFL-SPE-LC-MS was unable to detect diHC in the medium samples. The method's detection limits were found to be incompatible with the OiC-system due to the time required to fill the necessary sample volume for detecting low levels of oxysterols.

5 Conclusion

The aim of this study was to develop a method for detection of underivatized oxysterols using LC-MS. The end goal was to utilize an organ-in-a-column system as a disease modeling platform for NAFLD and monitor the secretion of oxysterols in relation to disease development. This study aimed to establish a "proof-of-concept" by generating distinct fingerprints of oxysterol secretion from both control and steatotic liver organoids, employing the organ-in-a-column technology.

The method development process presented several challenges, particularly in terms of achieving adequate sensitivity. Overcoming these challenges involved addressing issues such as coelution, optimization of the mobile phase composition and elution mode, mitigation of unwanted signals in blanks, carry-over, and the loss of signal in cell medium. Additionally, the group of hydroxycholesterols was excluded from the method development due to insufficient signal from the standard solutions. The implementation of an automated filtration and filter flush solid phase extraction (AFFL-SPE) prior to LC-MS ensured robust analysis by eliminating particles from the matrix, although it added complexity to the system.

Nevertheless, a method for detecting underivatized oxysterols was successfully developed, enabling their quantification at concentrations as low as 0.050 μg/mL in cell medium added 10 % IPA. The optimized experimental parameters included a 5 μL injection volume, a gradient elution utilizing IPA as the organic modifier (20-65 %), 0.1 % formic acid for pH control in the mobile phase, and the use of an SuperPhenyl hexyl (2.1 mm x 5 cm) column at a temperature of 40 ℃.

At its current stage, the developed method still possesses a detection limit that is insufficient for the detection of native oxysterols secreted from liver organoids. Further refinement and advancement of the method are necessary before implementing the organ-in-a-column approach for disease monitoring. Specifically, it is crucial to address the carry-over issues and optimize the method to ensure reliable and accurate results.

Bibliography

1. Lin, A., F. Sved Skottvoll, S. Rayner, S. Pedersen-Bjergaard, G. Sullivan, S. Krauss, S. Ray Wilson, and S. Harrison, *3D cell culture models and organ-on-a-chip: meet separation science and mass spectrometry.* Electrophoresis, 2020. **41**(1-2): p. 56-64.
2. Materne, E.-M., A.G. Tonevitsky, and U. Marx, *Chip-based liver equivalents for toxicity testing–organotypicalness versus cost-efficient high throughput.* Lab on a Chip, 2013. **13**(18): p. 3481-3495.
3. Skardal, A., T. Shupe, and A. Atala, *Organoid-on-a-chip and body-on-a-chip systems for drug screening and disease modeling.* Drug discovery today, 2016. **21**(9): p. 1399-1411.
4. Passier, R., V. Orlova, and C. Mummery, *Complex tissue and disease modeling using hiPSCs.* Cell stem cell, 2016. **18**(3): p. 309-321.
5. Van der Worp, H.B., D.W. Howells, E.S. Sena, M.J. Porritt, S. Rewell, V. O'Collins, and M.R. Macleod, *Can animal models of disease reliably inform human studies?* PLoS medicine, 2010. **7**(3): p. e1000245.
6. Oliveira, J.M. and R.L. Reis, *Biomaterials- and Microfluidics-Based Tissue Engineered 3D Models*. 2020, Springer International Publishing : Imprint: Springer: Cham.
7. Schutgens, F. and H. Clevers, *Human organoids: tools for understanding biology and treating diseases.* Annual Review of Pathology: Mechanisms of Disease, 2020. **15**: p. 211-234.
8. *Method of the Year 2017: Organoids.* Nature Methods, 2018. **15**(1): p. 1-1.
9. Lancaster, M.A. and J.A. Knoblich, *Organogenesis in a dish: modeling development and disease using organoid technologies.* Science, 2014. **345**(6194): p. 1247125.
10. Mittal, R., F.W. Woo, C.S. Castro, M.A. Cohen, J. Karanxha, J. Mittal, T. Chhibber, and V.M. Jhaveri, *Organ-on-chip models: implications in drug discovery and clinical applications.* Journal of cellular physiology, 2019. **234**(6): p. 8352-8380.
11. Beckwitt, C.H., A.M. Clark, S. Wheeler, D.L. Taylor, D.B. Stolz, L. Griffith, and A. Wells, *Liver 'organ on a chip'.* Experimental cell research, 2018. **363**(1): p. 15-25.
12. Bellin, M., M.C. Marchetto, F.H. Gage, and C.L. Mummery, *Induced pluripotent stem cells: the new patient?* Nature reviews Molecular cell biology, 2012. **13**(11): p. 713-726.
13. Kogler, S., K.S. Kømurcu, C. Olsen, J.-y. Shoji, F.S. Skottvoll, S. Krauss, S.R. Wilson, and H. Røberg-Larsen, *Organoids, organ-on-a-chip, separation science and mass spectrometry: An update.* TrAC Trends in Analytical Chemistry, 2023: p. 116996.
14. Bhatia, S.N. and D.E. Ingber, *Microfluidic organs-on-chips.* Nature biotechnology, 2014. **32**(8): p. 760-772.
15. Tian, C., Q. Tu, W. Liu, and J. Wang, *Recent advances in microfluidic technologies for organ-on-a-chip.* TrAC Trends in Analytical Chemistry, 2019. **117**: p. 146-156.
16. Huh, D., B.D. Matthews, A. Mammoto, M. Montoya-Zavala, H.Y. Hsin, and D.E. Ingber, *Reconstituting organ-level lung functions on a chip.* Science, 2010. **328**(5986): p. 1662-1668.
17. Kogler, S., A. Aizenshtadt, S. Harrison, F.S. Skottvoll, H.E. Berg, S. Abadpour, H. Scholz, G. Sullivan, B. Thiede, and E. Lundanes, *"Organ-in-a-Column" Coupled On-line with Liquid Chromatography-Mass Spectrometry.* Analytical Chemistry, 2022.

18. Stefan, N., H.-U. Häring, and K. Cusi, *Non-alcoholic fatty liver disease: causes, diagnosis, cardiometabolic consequences, and treatment strategies.* The lancet Diabetes & endocrinology, 2019. **7**(4): p. 313-324.
19. Pydyn, N., K. Miękus, J. Jura, and J. Kotlinowski, *New therapeutic strategies in nonalcoholic fatty liver disease: A focus on promising drugs for nonalcoholic steatohepatitis.* Pharmacological Reports, 2020. **72**: p. 1-12.
20. Singh, S., A.M. Allen, Z. Wang, L.J. Prokop, M.H. Murad, and R. Loomba, *Fibrosis progression in nonalcoholic fatty liver vs nonalcoholic steatohepatitis: a systematic review and meta-analysis of paired-biopsy studies.* Clinical gastroenterology and hepatology, 2015. **13**(4): p. 643-654. e9.
21. de Alwis, N.M.W. and C.P. Day, *Non-alcoholic fatty liver disease: the mist gradually clears.* Journal of hepatology, 2008. **48**: p. S104-S112.
22. Sanyal, A.J., *AGA technical review on nonalcoholic fatty liver disease.* Gastroenterology, 2002. **123**(5): p. 1705-1725.
23. Le, M.H., Y.H. Yeo, X. Li, J. Li, B. Zou, Y. Wu, Q. Ye, D.Q. Huang, C. Zhao, and J. Zhang, *2019 global NAFLD prevalence-A systematic review and meta-analysis.* Clinical Gastroenterology and Hepatology, 2021.
24. Goodrich, J.A., D. Walker, X. Lin, H. Wang, T. Lim, R. McConnell, D.V. Conti, L. Chatzi, and V.W. Setiawan, *Exposure to perfluoroalkyl substances and risk of hepatocellular carcinoma in a multiethnic cohort.* Journal of Hepatology 2022. **4**(10): p. 100550.
25. Ratziu, V., S. Bellentani, H. Cortez-Pinto, C. Day, and G. Marchesini, *A position statement on NAFLD/NASH based on the EASL 2009 special conference.* Journal of hepatology, 2010. **53**(2): p. 372-384.
26. Raselli, T., T. Hearn, A. Wyss, K. Atrott, A. Peter, I. Frey-Wagner, M.R. Spalinger, E.M. Maggio, A.W. Sailer, and J. Schmitt, *Elevated oxysterol levels in human and mouse livers reflect nonalcoholic steatohepatitis [S].* Journal of lipid research, 2019. **60**(7): p. 1270-1283.
27. Noureddin, M., A. Vipani, C. Bresee, T. Todo, I.K. Kim, N. Alkhouri, V.W. Setiawan, T. Tran, W.S. Ayoub, and S.C. Lu, *NASH leading cause of liver transplant in women: updated analysis of indications for liver transplant and ethnic and gender variances.* The American journal of gastroenterology, 2018. **113**(11): p. 1649.
28. Wang, J., W. He, P.-J. Tsai, P.-H. Chen, M. Ye, J. Guo, and Z. Su, *Mutual interaction between endoplasmic reticulum and mitochondria in nonalcoholic fatty liver disease.* Lipids in Health and Disease, 2020. **19**(1): p. 1-19.
29. Fitzpatrick, E. and A. Dhawan, *Noninvasive biomarkers in non-alcoholic fatty liver disease: current status and a glimpse of the future.* World journal of gastroenterology: WJG, 2014. **20**(31): p. 10851.
30. Bril, F., C. Ortiz-Lopez, R. Lomonaco, B. Orsak, M. Freckleton, K. Chintapalli, J. Hardies, S. Lai, F. Solano, and F. Tio, *Clinical value of liver ultrasound for the diagnosis of nonalcoholic fatty liver disease in overweight and obese patients.* Liver International, 2015. **35**(9): p. 2139-2146.
31. Anstee, Q.M., G. Targher, and C.P. Day, *Progression of NAFLD to diabetes mellitus, cardiovascular disease or cirrhosis.* Nature reviews Gastroenterology & hepatology, 2013. **10**(6): p. 330-344.
32. Ratziu, V., F. Charlotte, A. Heurtier, S. Gombert, P. Giral, E. Bruckert, A. Grimaldi, F. Capron, T. Poynard, and L.S. Group, *Sampling variability of liver biopsy in nonalcoholic fatty liver disease.* Gastroenterology, 2005. **128**(7): p. 1898-1906.
33. Argo, C.K. and S.H. Caldwell, *Epidemiology and natural history of non-alcoholic steatohepatitis.* Clinics in liver disease, 2009. **13**(4): p. 511-531.

34. Lee, S.S., S.H. Park, H.J. Kim, S.Y. Kim, M.-Y. Kim, D.Y. Kim, D.J. Suh, K.M. Kim, M.H. Bae, and J.Y. Lee, *Non-invasive assessment of hepatic steatosis: prospective comparison of the accuracy of imaging examinations.* Journal of hepatology, 2010. **52**(4): p. 579-585.
35. Van Herck, M.A., L. Vonghia, and S.M. Francque, *Animal models of nonalcoholic fatty liver disease—a starter's guide.* Nutrients, 2017. **9**(10): p. 1072.
36. Kømurcu, K.S., I. Wilhelmsen, J.L. Thorne, S.J. Karl Krauss, S.R. Haakon Wilson, A. Aizenshtadt, and H. Røberg-Larsen, *Mass Spectrometry Reveals that Oxysterols are Secreted from Non-Alcoholic Fatty Liver Disease Induced Organoids.* bioRxiv, 2023: p. 2023.02. 22.529551.
37. Uehara, K. and P.M. Titchenell, *Curing Fatty Liver with Oxysterols?* Cellular and Molecular Gastroenterology and Hepatology, 2022. **13**(4): p. 1265-1266.
38. Borah, K., O.J. Rickman, N. Voutsina, I. Ampong, D. Gao, E.L. Baple, I.H. Dias, A.H. Crosby, and H.R. Griffiths, *A quantitative LC-MS/MS method for analysis of mitochondrial-specific oxysterol metabolism.* Redox biology, 2020. **36**: p. 101595.
39. Gill, S., R. Chow, and A.J. Brown, *Sterol regulators of cholesterol homeostasis and beyond: the oxysterol hypothesis revisited and revised.* Progress in lipid research, 2008. **47**(6): p. 391-404.
40. Ikegami, T., H. Hyogo, A. Honda, T. Miyazaki, K. Tokushige, E. Hashimoto, K. Inui, Y. Matsuzaki, and S. Tazuma, *Increased serum liver X receptor ligand oxysterols in patients with non-alcoholic fatty liver disease.* Journal of gastroenterology, 2012. **47**(11): p. 1257-1266.
41. Pandak, W.M. and G. Kakiyama, *The acidic pathway of bile acid synthesis: Not just an alternative pathway.* Liver research, 2019. **3**(2): p. 88-98.
42. Roberg-Larsen, H., K. Lund, T. Vehus, N. Solberg, C. Vesterdal, D. Misaghian, P.A. Olsen, S. Krauss, S.R. Wilson, and E. Lundanes, *Highly automated nano-LC/MS-based approach for thousand cell-scale quantification of side chain-hydroxylated oxysterols [S].* Journal of lipid research, 2014. **55**(7): p. 1531-1536.
43. Dias, I.H., S.R. Wilson, and H. Roberg-Larsen, *Chromatography of oxysterols.* Biochimie, 2018. **153**: p. 3-12.
44. Roberg-Larsen, H., C. Vesterdal, S.R. Wilson, and E. Lundanes, *Underivatized oxysterols and nanoLC–ESI-MS: A mismatch.* Steroids, 2015. **99**: p. 125-130.
45. Solheim, S., S.A. Hutchinson, E. Lundanes, S.R. Wilson, J.L. Thorne, and H. Roberg-Larsen, *Fast liquid chromatography-mass spectrometry reveals side chain oxysterol heterogeneity in breast cancer tumour samples.* The Journal of steroid biochemistry and molecular biology, 2019. **192**: p. 105309.
46. McDonald, J.G., D.D. Smith, A.R. Stiles, and D.W. Russell, *A comprehensive method for extraction and quantitative analysis of sterols and secosteroids from human plasma.* Journal of lipid research, 2012. **53**(7): p. 1399-1409.
47. Ahonen, L., F.B. Maire, M. Savolainen, J. Kopra, R.J. Vreeken, T. Hankemeier, T. Myöhänen, P. Kylli, and R. Kostiainen, *Analysis of oxysterols and vitamin D metabolites in mouse brain and cell line samples by ultra-high-performance liquid chromatography-atmospheric pressure photoionization–mass spectrometry.* Journal of Chromatography A, 2014. **1364**: p. 214-222.
48. Sugimoto, H., M. Kakehi, Y. Satomi, H. Kamiguchi, and F. Jinno, *Method development for the determination of 24S-hydroxycholesterol in human plasma without derivatization by high-performance liquid chromatography with tandem mass spectrometry in atmospheric pressure chemical ionization mode.* Journal of Separation Science, 2015. **38**(20): p. 3516-3524.

49. Lundanes, E., L. Reubsaet, and T. Greibrokk, *Chromatography : basic principles, sample preparations and related methods*. 2014, Weinheim: Wiley-VCH.
50. Greaves, J. and J. Roboz, *Mass spectrometry for the novice*. 2014, Boca Raton: CRC Press.
51. Harris, D.C. and C.A. Lucy, *Quantitative chemical analysis*. 9th ed. 2016, New York: Freeman.
52. Hansen, S.H. and S. Pedersen-Bjergaard, *Bioanalysis of pharmaceuticals : sample preparation, separation techniques, and mass spectrometry*. 2015, Wiley: West Sussex, England.
53. Gross, J.H., *Mass Spectrometry : A Textbook*. 2017, Springer International Publishing : Imprint: Springer: Cham.
54. Poole, C.F., *The essence of chromatography*. 2003, Amsterdam: Elsevier.
55. Cole, R.B., *Electrospray ionization mass spectrometry : fundamentals, instrumentation, and applications*. 1997, New York: Wiley.
56. Nakamura, K., S. Saito, and M. Shibukawa, *Intrinsic difference between phenyl hexyl- and octadecyl-bonded silicas in the solute retention selectivity in reversed-phase liquid chromatography with aqueous mobile phase.* Journal of Chromatography A, 2020. **1628**: p. 461450.
57. Fekete, S., A. Beck, J.-L. Veuthey, and D. Guillarme, *Proof of concept to achieve infinite selectivity for the chromatographic separation of therapeutic proteins.* Analytical chemistry, 2019. **91**(20): p. 12954-12961.
58. Lardeux, H., B.L. Duivelshof, O. Colas, A. Beck, D.V. McCalley, D. Guillarme, and V. D'Atri, *Alternative mobile phase additives for the characterization of protein biopharmaceuticals in liquid chromatography–Mass spectrometry.* Analytica Chimica Acta, 2021. **1156**: p. 338347.
59. Garcia, M., *The effect of the mobile phase additives on sensitivity in the analysis of peptides and proteins by high-performance liquid chromatography–electrospray mass spectrometry.* Journal of Chromatography B, 2005. **825**(2): p. 111-123.
60. Groskreutz, S.R. and S.G. Weber, *Quantitative evaluation of models for solvent-based, on-column focusing in liquid chromatography.* Journal of Chromatography A, 2015. **1409**: p. 116-124.
61. Svendsen, K.O., H.R. Larsen, S.A. Pedersen, I. Brenna, E. Lundanes, and S.R. Wilson, *Automatic filtration and filter flush for robust online solid-phase extraction liquid chromatography.* Journal of separation science, 2011. **34**(21): p. 3020-3022.
62. Fakheri, R.J. and N.B. Javitt, *27-Hydroxycholesterol, does it exist? On the nomenclature and stereochemistry of 26-hydroxylated sterols.* Steroids, 2012. **77**(6): p. 575-577.

6 Appendix

The volumes and concentrations used for dilution of standard solutions of oxysterols are summarized in tables, from

Table 14 to **Table 34** provide a summary of the volumes and concentrations employed for diluting standard solutions of oxysterols. **Table 35** and **Table 36** present a comparison of oxysterol signals obtained using DFA and FA as pH control in the mobile phase. **Figure 42** demonstrates the difference in signal intensity between the two analyte groups when MeOH is utilized as the organic modifier. Section 6.4 includes a calculation outlining the required sample volume for detecting oxysterols secreted from liver organoids.

6.1 Dilution of standard solutions

Table 14. Preparation of a mixture of diluted standard solutions of HC-analytes in water with a total concentration of 0.12 μg/mL.

	Analyte concentration in μg/mL, solved in 100 % IPA	**Volume standard solution (μL)**	**Volume water added (μL)**	**Analyte concentration after dilution with water (μg/mL)**	**Total concentration of analytes in the mixture (μg/mL)**
24S-HC	100	40	99 931	0.040	0.12
25-HC	188	21		0.040	
26-HC	500	8		0.040	

Table 15. Preparation of a mixture of diluted standard solutions of diHC-analytes in water with a total concentration of 0.21 μg/mL.

	Analyte concentration in μg/mL, solved in 100 % IPA	**Volume standard solution (μL)**	**Volume water added (μL)**	**Analyte concentration in μg/mL, after dilution with water**	**Total concentration of analytes in the mixture (μg/mL)**
7α, 24*S*-HC	40	105	99 475	0.042	0.21
7α, 25-HC	40	105		0.042	
7β, 25-HC	40	105		0.042	
7α, 26-HC	40	105		0.042	
7β, 26-HC	40	105		0.042	

Table 16. Preparation of diluted standard solutions of HC-analytes in 50:50 MeOH:Water + 0.1 % FA to an end concentration of 10 μg/mL.

	Analyte concentration in μg/mL, solved in 100 % IPA	**Volume added of standard solution (analyte) (in μL)**	**Volume added of 50:50 Water:MeOH (in μL)**	**Volume added of formic acid (in μL)**	**Analyte concentration in μg/mL, after dilution (μg/mL)**
24S-HC	100	50	450	0.5	10
25-HC	188	26.5	472	0.5	10
26-HC	500	10	490	0.5	10

Table 17. Preparation of a mixture of diluted standard solutions of HC-analytes in 50:50 MeOH:Water + 0.1 % FA to a total concentration of 10 μg/mL.

	Analyte concentration in μg/mL, solved in 50:50 Water:MeoH	**Volume added of diluted standard solution (in μL)**	**Analyte concentration after dilution (μg/mL)**	**Total analyte concentration after dilution (μg/mL)**
24S-HC	10	20	3.33	10
25-HC	10	20	3.33	
26-HC	10	20	3.33	

Table 18. Preparation of diluted standard solutions of diHC-analytes in 50:50 MeOH:Water + 0.1 % FA to an end concentration of 10 μg/mL.

	Analyte concentration in μg/mL, solved in 100 % IPA	**Volume added of standard solution (analyte) (in μL)**	**Volume added of 50:50 Water:MeOH (in μL)**	**Volume added of formic acid (in μL)**	**Analyte concentration in μg/mL, after dilution**
7a, 24S-diHC	40	126	374	0.5	10
7a, 25-diHC	40	126	374	0.5	10
7b, 25-diHC	40	126	374	0.5	10
7a, 26-diHC	40	126	374	0.5	10
7b, 26-diHC	40	126	374	0.5	10

Table 19. Preparation of a mixture of diluted standard solutions of diHC-analytes in 50:50 MeOH:Water + 0.1 % FA to a total concentration of 10 μg/mL.

	Analyte concentration in μg/mL, solved in 50:50 Water:MeOH	**Volume added of diluted standard solution (in μL)**	**Analyte concentration after dilution (μg/mL)**	**Total analyte concentration after dilution (μg/mL)**
7a, 24S-diHC	10	20	2	10
7a, 25-diHC	10	20	2	
7b, 25-diHC	10	20	2	
7a, 26-diHC	10	20	2	
7b, 26-diHC	10	20	2	

Table 20. Preparation of a mixture of diluted standard solutions of HC- and diHC-analytes in 50:50 MeOH:Water + 0.1 % FA to a total concentration of 10 μg/mL.

Solution	**Volume added (in μL)**	**Concentration of analyte group in mix (μg/mL)**	**Total concentration of oxysterols in mixture (μg/mL)**
10 μg/mL HC in 50:50 MeOH:Water	20	5	10
10 μg/mL diHC in 50:50 MeOH:Water	20	5	

Table 21. Preparation of a mixture of diluted standard solutions of HC-analytes in 50:50 MeOH:Water + 0.1 % FA to a total concentration of 1.2 μg/mL.

	Analyte concentration in μg/mL, solved in 100 % IPA	**Volume added of standard solution (analyte) (in μL)**	**Volume added of 50:50 Water:MeOH (in μL)**	**Analyte concentration after dilution (μg/mL)**	**Total concentration of analytes (μg/mL)**
24S-HC	100	403	98 716	0.4	1.2
25-HC	188	214		0.4	
26-HC	60	667		0.4	

Table 22. Preparation of diluted standard solutions of diHC-analytes in 50:50 IPA:Water + 0.1 % FA to a total concentration of 1 μg/mL.

	Analyte concentration in μg/mL, solved in 100 % IPA	**Volume standard solution (μL)**	**Volume added of 50:50 IPA:Water (μL)**	**Volume added of formic acid (μL)**	**Analyte concentration after dilution (μg/mL)**
7α, 24*S*-HC	40	12.5	487	0.5	1
7α, 25-HC	40	12.5		0.5	1
7β, 25-HC	40	12.5		0.5	1
7α, 26-HC	40	12.5		0.5	1
7β, 26-HC	40	12.5		0.5	1

Table 23. Preparation of a mixtures of diluted standard solutions of HC and diHC-analytes in 50:50 IPA:Water + 0.1 % FA to a total concentrations of 1, 0.1 and 0.091 μg/mL.

Concentration of each diHC-analyte standard before dilution (in μg/mL)	**Volume of each diHC-standard *added to mixture…* (in μL)**	**Volume added of 50:50 Water:IPA (in μL)**	**Total volume (in μL)**	**Concentration of each diHC-analyte after dilution in 50:50 Water:IPA (in μg/mL)**	**Total concentration of diHC-analytes after dilution in 50:50 Water:IPA (in μg/mL)**
1	20	0	100	0.2	1
1	20	900	1000	0.02	0.1
1	20	1000	1100	0.018	0.091

Table 24. Preparation of a mixture of diluted standard solutions of HC and diHC-analytes in 50:50 IPA:Water + 0.1 % FA to a total concentration of 0.01 μg/mL.

Total analyte concentration in 50:50 IPA:Water (μg/mL)	**Volume added of standard solution (μL)**	**Volume added of 50:50 IPA:Water (μL)**	**Total analyte concentration in diluted standard in 50:50 IPA:Water (μg/mL)**
0.1	10	90	0.01

Table 25. Preparation of a mixture of a diluted standard solution of 25-HC in 50:50 IPA:Water + 0.05 % DFA to a concentration of 10 μg/mL.

	Analyte concentration in μg/mL, solved in 100 % IPA	**Volume added of standard solution (analyte) (in μL)**	**Volume added of 50:50 IPA:Water (in μL)**	**Volume added of DFA (in μL)**	**Analyte concentration in μg/mL, after dilution**
25-HC	188	53	946	0.5	10

Table 26. Preparation of a mixture of diluted standard solutions of HC and diHC-analytes in 10:90 IPA:Water + 0.1 % FA to a total concentration of 0.1 μg/mL.

Concentration of analyte in 100 % IPA before dilution (in μg/mL)	**Volume standard solution of analyte added (in μL)**	**Volume added of IPA (in μL)**	**Volume added of water (in μL)**	**Concentration of analyte diluted in 10:90 IPA:Water (in μg/mL)**
40	0.5	97.5	900	0.1

Table 27. Preparation of diHC-analytes diluted in cell medium to the total concentrations of 1 and 0.1 μg/mL.

Concentration of each analyte in 100 % IPA before dilution (in μg/mL)	**Volume of each standard solution added (in μL)**	**Volume cell medium added (in μL)**	**Total concentration of the analytes diluted separately in cell medium (in μg/mL)**
40	25	975	1
40	2.5	997.5	0.1

Table 28. Preparation of mixtures of standard solutions of diHC-analytes in cell medium to the total concentrations of 1 and 0.1 μg/mL.

Concentration of each diHC-analyte standard diluted in cell medium (in μg/mL)	**Volume of each diHC-standard added to mixture (in μL)**	**Total volume (in μL)**	**Concentration of each diHC-analyte after dilution in cell medium (in μg/mL)**	**Total concentration of diHC-analytes after dilution in cell medium (in μg/mL)**
1	200	1000	0.2	1
0.1	200	1000	0.02	0.1

Table 29. Preparation of diHC-analytes diluted in 50:50 IPA:Cell medium to the total concentrations of 1 and 0.1 μg/mL.

Concentration of each analyte in 100 % IPA before dilution (in μg/mL)	**Volume standard solution of analyte added (in μL)**	**Volume added of 50:50 IPA:Cell medium (in μL)**	**Concentration of analyte diluted in 50:50 IPA:Cell medium (in μg/mL)**
40	25	975	1
40	2.5	997.5	0.1

Table 30. Preparation of mixtures of standard solutions of diHC-analytes in 50:50 IPA:Cell medium to the total concentrations of 1 and 0.1 μg/mL.

Concentration of each diHC-analyte standard diluted in 50:50 Cell medium:IPA (in μg/mL)	**Volume of each diHC-standard *added to mixture* (in μL)**	**Total volume (in μL)**	**Concentration of each diHC-analyte after dilution in 50:50 IPA:Cell medium (in μg/mL)**	**Total concentration of diHC-analytes after dilution in 50:50 IPA:Cell medium (in μg/mL)**
1	200	1000	0.2	1
0.1	200	1000	0.02	0.1

Table 31. Preparation of standard solutions of diHC-analytes in 100 % IPA to the total concentration of 1 μg/mL.

Concentration of each analyte in 100 % IPA before dilution (μg/mL)	**Volume standard solution of each analyte added (in μL)**	**Volume added of IPA (in μL)**	**Total concentration of the analytes diluted in IPA (μg/mL)**
40	5	975	1

Table 32. Preparation of standard solutions of diHC-analytes in 100 % IPA to the total concentration of 0.1 μg/mL.

Concentration of analyte in 100 % IPA before dilution (μg/mL)	**Volume diluted standard solution added (in μL)**	**Volume added of Cell medium (in μL)**	**Concentration of analyte diluted in IPA (μg/mL)**
1	100	900	0.1

Table 33. Dilution of eluate of standard solutions originally solved in 50:50 IPA:Cell medium of the analytes after SPE to the total concentrations of 0.05 and 0.01 μg/mL.

Concentration of eluate with analytes after SPE in 100 % IPA (μg/mL)	**Volume of eluate (μL)**	**Volume added of 100 % IPA (μL)**	**Concentration of analyte in diluted solution (μg/mL)**
0.1	50	50	0.05
0.1	10	90	0.01

Table 34. Dilution of eluate of standard solutions originally solved in 10:90 IPA:Cell medium of the analytes after SPE to the total concentrations of 0.05 and 0.01 μg/mL.

Concentration of eluate with analytes after SPE in 100 % IPA (μg/mL)	**Volume of eluate (in μL)**	**Volume added of 100 % IPA (in μL)**	**Concentration of analyte in diluted solution (μg/mL)**
0.1	50	50	0.05
0.1	10	90	0.01

6.2 Comparison of DFA and FA as pH control

Table 35. Overview of the average area, standard deviation and relative standard deviation obtained from a mixture of HC- and diHC-analytes with a concentration of 10 μg/mL dissolved in 50:50 MeOH:Water + 0.1 % FA using 0.05 % DFA in a mobile phase consisting of 40 % IPA and 60 % Water. The analysis was conducted in MRM mode (m/z 367.2 → 90.9, 367.2 → 104.9, 385.2 → 90.9, 385.2 → 104.9, 365 → 90.9, 365 → 104.9, 383 → 90.9, 383 → 104.9).

	HC-analytes		**diHC-analytes**	
Parent mass (*m/z*)	367.2	385.2	365	383
Average area	880.46	1016.8	29087.95	49541.8
Standard deviation	145.08	168.30	3003.57	3270.67
Relative standard deviation (%)	16.48	16.55	10.33	6.60

Table 36. Overview of the average area, standard deviation and relative standard deviation obtained from a mixture of HC- and diHC-analytes with a concentration of 10 μg/mL dissolved in 50:50 MeOH:Water + 0.1 % FA using 0.1 % FA in a mobile phase consisting of 40 % IPA and 60 % Water. The analysis was conducted in MRM mode (m/z 367.2 → 90.9, 367.2 → 104.9, 385.2 → 90.9, 385.2 → 104.9, 365 → 90.9, 365 → 104.9, 383 → 90.9, 383 → 104.9).

	HC-analytes		**diHC-analytes**	
Parent mass (*m/z*)	367.2	385.2	365	383
Average area	2085.93	3366.13	77970.71	147437.25
Standard deviation	200.81	312.05	2987.19	4339.82
Relative standard deviation (%)	9.63	9.27	3.83	2.94

6.3 Comparison of signals from HC and diHC-analytes using methanol as organic modifier

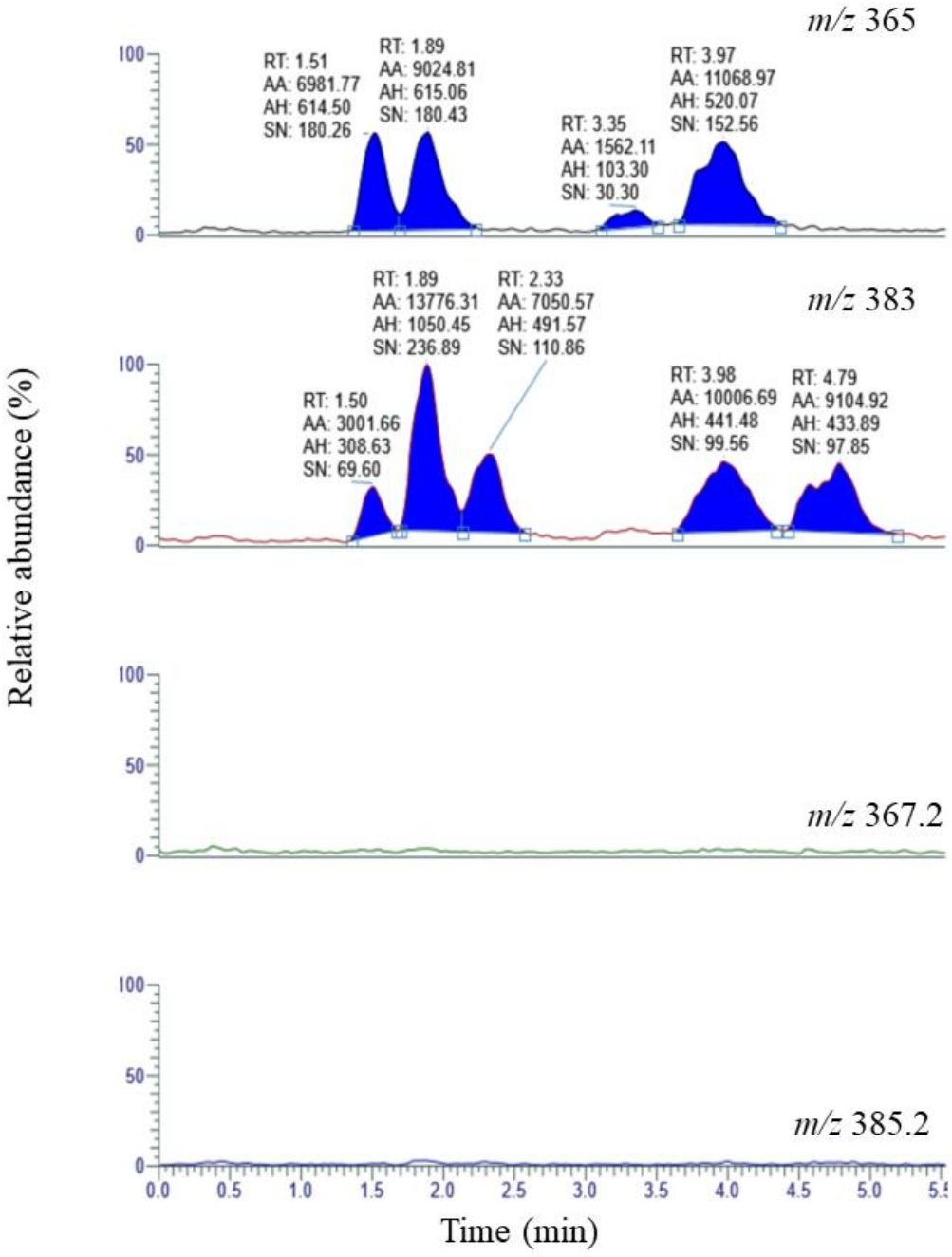

Figure 42. Chromatograms from the injection of 1 µL of a solution of 10 µg/mL HC and diHC-mix on a phenyl hexyl stationary phase with a mobile phase consisting of 70 % MeOH + 30 % Water (+ 0.1 % FA). The analysis was conducted in MRM mode (m/z 367.2 → 90.9, 367.2 → 104.9, 385.2 → 90.9, 385.2 → 104.9, 365 → 90.9, 365 → 104.9, 383 → 90.9, 383 → 104.9). To illustrate the difference in signal intensity, the chromatograms are normalized (fixed scale).

6.4 Calculation of the sample volume needed for detection of oxysterols secreted from liver organoids

The sample volume necessary to detect levels of oxysterols down to 500 pM with detection limits of 120 000 pM using a 5 μL loop:

$$v_2 = \frac{120\ 000\ pM * 5\ \mu L}{500\ pM} = 1200\ \mu L = 1.2\ mL$$